SYNTHESIS OF ANTIBACTERIAL SILVER NANOPARTICLES FROM ACTINOMYCETES ISOLATED FROM THIKA INDUSTRIAL WASTE DUMP SITES SOIL AND MOLECULAR IDENTIFICATION OF POTENTIAL ACTINOMYCETES

ABEBE BIZUYE KASSAHUN

DOCTOR OF PHILOSOPHY IN MOLECULAR BIOLOGY AND BIOTECHNOLOGY

PAN AFRICAN UNIVERSITY INSTITUTE FOR BASIC SCIENCES, TECHNOLOGY AND INNOVATION

2018

SYNTHESIS OF ANTIBACTERIAL SILVER NANOPARTICLES FROM ACTINOMYCETES ISOLATED FROM THIKA INDUSTRIAL WASTE DUMP SITES SOIL AND MOLECULAR IDENTIFICATION OF POTENTIAL ACTINOMYCETES

Abebe Bizuye Kassahun

MB400-0005/15

A Thesis submitted to Pan African University Institute for Basic Sciences, Technology and Innovation in partial fulfillment of the requirements for the degree of Doctor of Philosophy in Molecular Biology and Biotechnology

2018

DECLARATION

Statement by the student

I, declare that this thesis submitted to the Pan African University Institute of Basic Sciences, Technology and Innovation in partial fulfillment of the requirements for the degree of doctor of philosophy in Molecular Biology and Biotechnology, is original research work done by me under the supervision and guidance of my supervisors, except where due acknowledgement is made in the text; to the best of my knowledge it has not been submitted to in this institution or other institutions seeking for similar degree or other purposes.

Student name: Abebe Bizuye Kassahun Signature----------Date----------

ID: MB400-0005/2015

This thesis has been submitted with our approval as university supervisors.

1. Professor Naomi Maina Signature----------Date----------

   JKUAT, Nairobi, Kenya

2. Professor Erastus Gatebe Signature----------Date----------

   KIRDI, Nairobi, Kenya

3. Doctor Christine Bii Signature----------Date----------

   KEMRI, Nairobi, Kenya

DEDICATION

I dedicated this work to my parents and family for their support and encouragement throughout my studies. May God bless you!

ACKNOLEDGEMENTS

It is a privilege to acknowledge my supervisors Professor Naomi Maina, Professor Erastus Gatebe and Doctor Christine Bii for their supervision, guidance and support by facilitating and connecting me with research and laboratory institutions.

My acknowledgement goes to KIRDI, KEMRI, PAUSTI and JKUAT allowing me to use their laboratories. I thank African Union Commission (ADF/BD/WP/2013/68 to CNM) and Japanese International Co-operation Agency (JICA) (00025 to CNM) for funding this research work and University of Gondar, Department of Biology for giving me supportive materials and study leave.

My acknowledgement goes to Mark Mongaka, Godfrey Mwangi, Evangelen Mathiu, Kamathi Muchuna and Taoheed Abddulkareem for their assistance during soil sampling, isolation of actinomycetes, bioassay, FTIR and PCR activities, respectively.

My special thanks go to my family and colleagues who directly or indirectly supported and encouraged me towards the accomplishment of this work.

Finally, thank you GOD for giving me wisdom, mental and physical health and strength to undertake and finish this work.

LIST OF ABBREVIATIONS AND ACRONYMS

AgNPs	Silver Nanoparticles
ANOVA	Analysis of Variance
ATCC	American type culture collection
BLAST	Basic Local Alignment Search Tool
CFU/g	Colony forming unit per gram
ESBL	Extended spectrum beta-lactamase
FTIR	Fourier Transform Infrared spectroscopy
GPS	Global Positioning System
HTUs	Hypothetical Taxonomic Units
JKUAT	Jomo Kenyata University of Agriculture and Technology
KEMRI	Kenya Medical Research Institute
KRDI	Kenya Research and Development Institute
LCA	Last Common Ancestor
MEGA	Molecular Evolutionary Genetics Analysis
ML	Maximum Likelihood
MRSA	Methicillin resistance *Staphylococcus aureus*
MUSCLE	Multiple Sequence Comparison by Log- Expectation
NCBI	National Center for Biotechnology Information
NJ	Neighbor Joining
MSA	Multiple Sequence Alignment
OTUs	Operational Taxonomic Units
SPSS	Statistical Package for Social Sciences
PHYLIP	PHYLogeny interference Package
RDP	Ribosomal Database Project

rRNA gene	ribosomal RiboNucleic Acid gene
RNA	Ribonucleic Acid
UPGMA	Unweighted Pair Group Method with Arithmetic Mean
UV-vis spectroscopy	Ultra Violet visible Spectroscopy

TABLE OF CONTENTS

LIST OF TABLES

LIST OF FIGURES

LIST OF APPENDICES

ABSTRACT

Infectious diseases caused by antibiotic resistant bacteria lead to considerable increase in human morbidity and mortality globally. This requires searching for potential actinomycetes isolates from undiscovered habitats as source of effective bioactive metabolites. The purpose of the present study was to identify actinomycetes isolates from waste dump sites that produce bioactive metabolites capable of synthesizing antibacterial silver nanoparticles. Soil samples were collected from selected waste dump sites and composite soil samples prepared. Composite soil samples were pre-treated with heat and $CaCO_3$. Soil suspension (0.1 ml) from 10^{-5} serially diluted composite soil sample was spread on selective media for selective growth and isolation of actinomycetes. The primary and secondary screenings of antibacterial active isolates were done by streak plate and well diffusion assay, respectively. The metabolites produced by the KDT32 and KGT32 isolates were harvested and mixed with 10 mM $AgNO_3$ solution for silver nanoparticle synthesis. The synthesis of nanoparticle was confirmed by visual detection and UV-vis spectrophotometer analysis whereas functional groups involved for synthesis was identified by FTIR spectrophotometer. The antibacterial activity of silver nanoparticle was tested *in vitro* by well diffusion assay. The identification of the potential isolates was done based on 16s rRNA gene sequence analysis using databases from NCBI and EzTaxon-e. The bioassay guided primary screening result showed that from 125 isolates, 29 (23.2%) isolates showed antibacterial activity. From these, isolate KGT22 showed 30±0 mm, 31.3±0.6 mm, 30±0 mm and 36±1 mm inhibition zone against *E. coli ATCC 25922*, *S. boydii*, *S. typhi* and *V. cholerea*, respectively. Isolate KDO24 showed antibacterial activity against both MRSA (16.25±0.5 mm) and *E. coli* (26.5±0.58 mm). From 29 isolates, supernatants from 11(37.93%) isolates showed antibacterial activity during secondary screening. Supernatant from BML45, KGT31 and PLS34 showed 17±1 mm inhibition

zone against *E. coli ATCC25922, S. boydii* and *S. typhi,* respectively. The visual detection showed that dark salmon and pale golden rod color change was observed due to the formation of KDT32-AgNP and KGT32-AgNP, respectively. The synthesis was confirmed by a characteristic UV-spectra peak at 415.5 nm for KDT32-AgNP and 416 nm for KGT32-AgNP. The FTIR spectra revealed that OH, C=C and S-S functional groups were involved for the synthesis of KDT32-AgNP whereas OH, C=C and C-H were involved for the formation of KGT32-AgNP. The inhibition zone results revealed that KDT32-AgNP showed 22.0±1.4 mm and 19.0±1.4 mm against *E. coli* and *S. typhi* whereas KGT32-AgNP showed 21.5±0.7 mm and 17.0±0.0 mm, respectively. The sequence similarity search result revealed that KDT32 isolate showed 99.8 % sequence similarity with *S. lavenduligriseus* NRRL ISP-5487 whereas KGT32 isolate showed 99.79 % similarity with *S. albidoflavus* DSM40455, *S. koyangensis* strain VK-A60, *S. hydrogenans strain* NBRC 13475, *S. daghestanicus* strain NRRL B-5418 and *S. violascens* strain ISP 5183. The NJ and ML tree revealed that KDT32 isolate formed monophyletic clade with *S. nodosus* strain ATCC 14899 that showed 99.7% sequence similarity. However, KGT32 formed a distinct clade with *S. fabae* T66 and *S. cinerochromogenes* NBRC13822 that showed 99.68 % and 99.58 % sequence similarity, respectively. Isolates produce bioactive metabolites capable of synthesize antibacterial silver nanoparticles, were identified as genus *Streptomyces* and deposited in GenBank as *S. pausti* KDT32 (MH301089) and *S. pausti* KGT32 (MH301090). The synthesis of antibacterial nanoparticle using the bioactive metabolites from such isolates is the first report in this area. Due to its bactericidal activity of the synthesized silver nanoparticles can be used for antibacterial activity in different biomedical applications.

CHAPTER ONE: INTRODUCTION

1.1. Background

Bacteria are one of the common causative agents of infectious diseases that can be managed, prevented and treated via antibacterial agents. However, bacteria can be either intrinsically or acquired resistant to antibacterial agents. Acquired resistance to antibacterial agents can occur either by chromosomal gene mutation or by horizontal resistance gene transfer via transduction, conjugation and transformation. The spread of antibiotic resistant bacteria is a challenge in the treatment of infectious diseases. These can be by decreasing the entry of antibacterial agents, changes the antibacteria targets and metabolic inactivation of antibacterial agents (Blair, Webber, Baylay, Ogbolu, & Piddock, 2014). These increase human morbidity and mortality (Kaye & Pogue, 2015) that bring considerable impact on clinical and economic issues globally (Giske, Monnet, Cars, & Carmeli, 2008; Sabtu, Enoch, & Brown, 2015).

Escherichia coli and *Kellebsela pneumonia* are some of the most frequently occurring drug resistant gram-negative bacteria worldwide. While, *E. coli*, *Salmonella species*, *Shigella species*, *Vibrio species* are frequently occurring drug resistant gram-negative bacteria in East Africa region (Omulo, Thumbi, Njenga, & Call, 2015). Resistance to Amoxicillin, trimethoprim-sulfamethoxazole, tetracycline, nalidixic acid, ceftriaxone, ciprofloxacin and ofloxacin has been reported among *E. coli* isolates (ME, NE, & ME, 2012). *Salmonella* sp showed resistance against fluoroquinolone, ceftriaxone, ciprofloxacin and azithromycin (Lin, Chen, Wai-Chi Chan, & Chen, 2015). Moreover, most *Shigella spp* isolated from children in hospital showed resistant to tetracycline and trimethoprim-sulfamethoxazole (Jafari et al., 2009). These indicate the need for effective antibacterial agents.

Actinomycetes (Actinobacteria) are unicellular gram positive prokaryotes, filamentous, aerobic bacteria having DNA with high G+C composition that produce diverse groups of antibiotics (Barka et al., 2016). They are found everywhere in natural environments in both terrestrial and aquatic bodies. However, they are widely and commonly distributed groups of soil microorganisms (Sharma, 2014). Garden rhizosphere soil and composite soil (Bizuye, Moges, & Andualem, 2013), mangrove forest soil (Zainal Abidin, Abdul Malek, Zainuddin, & Chowdhury, 2016), virgin soil (Rotich, Magiri, Bii, & Maina, 2017), agriculture field soil (P. S. Kumar, Duraipandiyan, & Ignacimuthu, 2014), acidic soil (Busti et al., 2006) are just list of a few terrestrial places where bioactive metabolite producing actinomycetes has been isolated. They are major sources of effective antibiotics for the treatment of infectious human pathogens. Actinomycetes isolated from Ethiopia and Kenya soil showed antibacterial activity against *E. coli* (Bizuye, Bii, Erastus, & Maina, 2017; Bizuye et al., 2013; Kibret et al., 2018; Rotich et al., 2017). The *Streptomyces* species isolated from Ethiopian and Iran soil produce bioactive metabolite against *S. typhi* (Kibret et al., 2018; Tabrizi, Hamedi, & Mohammadipanah, 2013). Additionally, the bioactive compound produced by *Streptomyces* species isolated from Ethiopia soil also showed antibacterial activity against *S. bodii* (Kibret et al., 2018).

In addition to searching for effective bioactive metabolites from actinomycetes isolated from undiscovered sites, bioactive metabolite-based synthesis of silver nanoparticles has provided an alternative for potential antibacterial agents. Previous reports showed that actinomycetes can accumulate and detoxify metals due to various reductase enzymes that are capable of reducing silver salts to silver nanoparticles (P. Singh, Kim, Zhang, & Yang, 2016). Synthesis of silver nanoparticle by metabolite from *Streptomyces* isolated from soil in Egypt and India showed antibacterial activity against *E. coli* (Abd-Elnaby, Abo-Elala,

Abdel-Raouf, & Hamed, 2016; Chauhan, Kumar, & Abraham, 2013). Bioactive metabolites produced by *Streptomyces species* isolated from soil were able to synthesize silver nanoparticles that was active against *S. typhi* (Abd-Elnaby et al., 2016; Prakasham, Kumar, Kumar, & Kumar, 2014). Infectious bacteria are unlikely to develop resistance against metabolite mediated antibacterial silver nanoparticles compared to narrow spectrum antibiotics, because the silver attacks a broad range of targets in the bacterial pathogens (Dhanasekaran, Latha, Saha, Thajuddin, & Panneerselvam, 2013).

However, the status of synthesis of antibacterial silver nanoparticle using bioactive metabolites produced by actinomycetes isolated from East African region is limited. Majority of the ecological niches in this region have been unexplored. Waste dump habitat, in this region, is one of the potential unexplored areas. It may be exposed to diverse groups of nutrients (carbon source, nitrogen source, minerals, and metals such as silver) so that diverse bioactive metabolite producing potential actinomycetes may be found. In addition, the probability of getting antibacterial metabolite producing actinomycetes that involve the bio-reduction of metals such as silver is high. Thus, the main purpose of this study was to identify potential actinomycetes isolates from Thika waste dump sites that produce antibacterial metabolites capable of synthesizing antibacterial silver nanoparticles.

1.2. Statement of problem

Drug resistant infectious pathogens are the major challenges for human kind across the world. The Africa continent is one of the victims that is frequently affected drug resistant pathogens such as *Salmonella sp, Shigella sp, Vibrio sp* and *E. coli* (Omulo et al., 2015). Antibiotic resistant pathogens have enormous clinical and economic effects across the continent.

Thus, searching effective antibacterial agents from microorganisms isolated from undiscovered habitat should be given high priority. Actinomycetes isolated from different habitat are the first among successful antibiotics producing microorganisms.

Synthesis of actinobacteria bioactive metabolite mediated antibacterial silver nanoparticles is also vital to tackle the challenge of drug resistant pathogens. Biological methods of silver nanoparticle synthesis provide particles with good control over the size distribution that promotes the efficacy of nanoparticles against resistant bacteria (Lakshmi & Roshmi, 2014).

1.3. Justification

Human health is supported by antibacterial compounds. Most of antibacterial compounds used in clinic are derived from actinomycetes. However, some of these antibacterial agents are failed for the treatment of infection due to the emergence of resistance bacteria. Antibacterial compounds from actinomycetes and silver nanoparticles synthesized by actinomycetes reduce human infectious disease caused by resistance bacteria. Actinomycetes are potential source of antibacteria agents and an excellent nanofactories. Studies showed that antibacterial silver nanoparticles synthesized by actinomycetes metabolites (extracellular) are environmentally friendly, cost effective, attacks a broad range of targets in bacteria and easily scale up for downstream application (Zhang, Liu, Shen, & Gurunathan, 2016).

Silver nanoparticles synthesized by actinomycetes metabolites apply significant effect on bacterial pathogens. It can be exploited as effective antibacterial agent against bacterial pathogens in clinical application and could complement or replace antibacterial compounds failed in treatment of bacterial infections.

1.4. Research questions

Question 1: What is the antibacterial activity of actinomycetes isolated from waste dump soil?

Question 2: Which actinomycete isolate metabolites can synthesize antibacterial silver nanoparticles?

Question 3: What is the identity of the actinomycetes isolates that synthesize antibacterial silver nanoparticles?

1.5. Objectives

1.5.1. General objective

To identify actinomycetes producing bioactive metabolite capable of synthesizing antibacterial silver nanoparticle isolated from Thika waste dump soil

1.5.2. Specific objectives

1. To determine antibacterial activity of metabolites produced by actinomycetes isolated from Thika waste dump soil
2. To synthesize and evaluate antibacterial activity of actinomycete metabolite mediated silver nanoparticles
3. To identify actinomycete isolates that produce antibacterial metabolite capable of antibacterial silver nanoparticles synthesis

1.6. Significance of the study

Selective isolation and bioassay guided screening of antibacterial producing local actinomycete isolates are important for further commercialization of products against resistant bacteria. This helps to reduce the challenges of human health due to different antibiotic resistant pathogens frequently occurring in the world in general and in East

Africa in particular. It will also add the scientific knowledge in microbial biotechnology, and medical sciences.

Syntheses of antibacterial silver nanoparticles using actinomycete bioactive metabolite reduce economical cost and environmental concerns. It will give direction how a biological method contributes in antibacterial nano-drug synthesis.

This study also identified the potential local isolates based on different nucleotide sequence databases using as reference. Thus, it will be guided and used as a base line to investigate other new and potential actinomycetes from other undiscovered different habitats.

1.7. Scope, assumptions and limitation of the study

The test bacteria pathogens that were used in this study were mainly *S. typhi*, *E. coli*, *S. boydii* and *V. cholerae*. Soil sample collection used for this study was from waste disposal/dump areas in Thika, Kenya. This study targeted on actinomycetes producing antibacterial metabolites and capable of synthesizing metabolite mediated antibacterial silver nanoparticle. The antibacterial activity test was done using direct challenge (streak plate) method and well diffusion assay. The crude metabolites produced by actinomycete isolates were tested for antibacterial activity and synthesis of antibacterial silver nanoparticles. In the present study, the crude bioactive metabolites were not further analysed for purification, metabolite profiling and chemical structure identification.

More emphasis was given on 16s rRNA gene sequence and phylogenetic tree-based analysis for identification of the actinomycetes using reference sequences retrieved from NCBI-BLASTn and EzTaxon-e database. However, detail phenotypic analysis and characterization of the potential actinomycetes were not done. This method of

characterization of the actinomycetes is less effective and not cost effective when compared to molecular methods and molecular phylogenetic analysis.

CHAPTER TWO: LITERATURE REVIEW

2.1. Antibacterial resistance bacteria and its impact

Infections are common and adversely affect public health and global economies. They are caused by a variety of infectious agents (such as bacteria, and their toxins) transmitted from an infected to susceptible host (Barreto, Teixeira, & Carmo, 2006). The diseases caused by bacteria can be managed, prevented and treated via antibacterial agents. Antibacterial agents are antibiotics which are derived from microorganisms that inhibit the growth or kill other bacteria. However, bacteria can be either intrinsically or acquired resistant to antibacterial agents. Resistance bacteria is the ability of bacteria to resist the effects of an antibacterial agent to which they were once sensitive. It is a major concern of improper use (misuse, overuse and underuse) of antibacterial agents for the treatment of infectious disease (Hawkey, 2008).

Resistance bacteria has become one of the major public health problems worldwide and it has been spread faster than the development of new antibacterial agents (A. S. Chaudhary, 2016; Spellberg et al., 2008). This has brought difficulties in the treatment and management of infectious diseases caused by resistance bacteria (Friedman, Temkin, & Carmeli, 2016).

Treatment failure is the main contributor to increasing costs of treatment, additional side-effects, longer hospital stay, and longer time off work that affect quality of life of the patient among others. It also affects the success of most modern medicine like the success of cancer chemotherapy, organ transplantation and surgery (Spellberg et al., 2008). These lead to long duration of illness, high health care cost and greater risk of disability that bring a huge clinical and economic burden globally (Giske et al., 2008). It has an economic impact on patients, health-care administrators, pharmaceutical producers, and

the public at large (Mcgowan, 2001). These significantly increase human mortality and morbidity (Kaye & Pogue, 2015).

2.1.1. The mechanism of resistance in bacteria

The resistant in bacteria is a biological phenomenon due to the presence of either antibiotics resistant genes or the occurrence of mutation during replication of pathogenic bacteria. Improper use (overuse, misuse and underuse) of antibiotics, poor infection control and prevention practices give further spread of antibacterial resistance. Additionally, improper use of antibacterial agents in animal husbandry and agriculture were another cause for the incidence of antibacterial resistance. Accordingly, intrinsic (by innate or inherent ability of bacteria) and acquired (by horizontal gene transfer or chromosomal gene mutation) are strategies of antibacterial resistance (Blair et al., 2014; Mary et al., 2011; Sabtu et al., 2015).

The intrinsic resistance of bacterial species to antibiotic is the ability to resist the antibiotic action because of inherent structural (such as presence of extra outer membrane, difference structure composition) or functional characteristics (such as active efflux). Whereas acquired resistance to an antibacterial agent is as a result of either mutations in chromosomal genes or horizontal resistance gene transfer via conjugation, transformation and transduction (Blair et al., 2014; Sherpa, Reese, & Aliabadi, 2015). Conjugative plasmids, integron systems and transposable elements play a central role for acquisition of resistance genes from bacteria to bacteria (Bennett, 2008).

The strategies by which bacteria are either intrinsically or acquire resistance to antibiotics lead to decreases the entry of the drug, changes the drug targets (enzymes, receptors sites) and metabolic inactivation of antibiotics (Blair et al., 2014; MacGowan & Macnaughton,

2017). These are due to resistance-conferring enzyme production, swarming and inter-population interactions (Meredith, Srimani, Lee, Lopatkin, & You, 2015).

Aminoglycoside antibiotics (such as streptomycin, neomycin and kanamycin) resistant bacteria produce enzymes that add functional groups such as adenyl, acetyl or phosphate group to the antibiotic. This modifies the antibiotic that leads to its inactivation hence protecting the bacteria from lethal effect of antibiotics. Erythromycin-resistant bacteria produce an enzyme that helps to add methyl group on the ribosomal RNA and then a ribosome is insensitive to the antibiotics. A tetracycline-resistance bacteria pumps the tetracycline out of the cells by coupling tetracycline flow with proton import (Sugiyama, 2015).

Cephalosporins such as Ceftriaxone and penicillins such as ampicillin and penicillin antibiotics resistant bacteria produce β-lactamase enzymes. These enzymes can break the β-lactam ring of these antibiotics by hydrolysis making antibiotics unable to inhibit the cell wall synthesis of the pathogens. Ceftriaxone or Penicillin resistant bacteria can tolerate and multiply without any problem by such mechanisms (Ugboko & De, 2014).

2.1.2. The status and challenges of antibacterial resistant bacteria

Infections caused by bacterial pathogens are among the top killing infectious diseases in the world. Globally, antibiotic resistant bacteria are frequently occurring. This causes difficulty in treating infections caused by these pathogens. Treatment failures to one or more than two standard antibacterials have been reported. *Escherichia coli* and *Kellebsela pneumonia* are the most frequently occurring antibiotic resistant gram-negative bacteria. Infections caused by antibiotic resistant bacteria such as *Escherichia coli*, *Salmonella enterica*, *Vibrio cholerae* are becoming difficult for effective treatment of patients

(Andersen et al., 2015). They are non-sporulating, rod shaped and gram-negative bacteria belonging to family Enterobacteriaceae. They are causative agents for diarrheal (frequent passing of watery stool) and dysentery (diarrheal with mucus or blood in the feces) disease.

Escherichia coli is a versatile bacterium. It can be either commensal, pathogenic or lab workhorse bacteria. The pathogenic *E. coli* strains cause diverse intestinal and extra-intestinal diseases (Kaper, Nataro, & Mobley, 2004) including gastroenteritis, cystitis, meningitis, peritonitis, and septicemia (Alizade, 2018; Vila et al., 2016; Yassin et al., 2017; Zaman et al., 2017). Intestinal disease (diarrhea) can be caused by either enteropathogenic, enterotoxinogenic or enterohaemorragic *E. coli* (Bélanger et al., 2011). Hundreds of millions of people affected annually by these diseases (Croxen & Finlay, 2010) that represent a major cause of morbidity and mortality worldwide. The treatments of these diseases are now complicated by the emergence of antibacterial resistance. A proficient pathogen should be virulent, resistant to antibiotics, and epidemic (da Silva & Mendonça, 2012). *Escherichia coli* showed resistant against amoxicillin, trimethoprim-sulfamethoxazole, tetracycline, nalidixic acid, ceftriaxone, ciprofloxacin and ofloxacin (Dakal, Kumar, Majumdar, & Yadav, 2016; ME et al., 2012). Another report also confirmed that Shiga toxin-producing *E. coli* isolates were resistant to tetracycline and amoxicillin (Jafari et al., 2009).

Salmonella typhi, the causative agent for typhoid fever, remains unsolved public health problem in developing nations. Typhoid fever is an acute illness that affects approximately 13.5 million people and 190,000 deaths globally in 2010 (Buckle, Walker, & Black, 2012). Abdominal pain, malaise and high fever are symptoms of the disease. Typhoid fever occur where poor sanitation and lack of clean water specially in developing nations (Yan et al.,

2016). Antibacterial therapy is the mainstay for the treatment of typhoid fever and its associated complications. However, *S. typhi* showed resistance to fluoroquinolone (Dutta et al., 2014; Lin et al., 2015), ampicillin, trimethoprim/sulfamethoxazole, streptomycin, chloramphenicol and tetracycline (Dakal et al., 2016; Frye & Jackson, 2013; Yan et al., 2016); and ceftriaxone, ciprofloxacin and azithromycin (Lin et al., 2015). In addition to this, *Salmonella sp* isolates also showed resistance against cephalexin and cephradine (Nawas et al., 2012). The mechanisms of antibiotic resistance in *S. typhi* include inactivation of the drug, active efflux and alteration of drug target sites.

Shigella spp remain important pathogens that are responsible for 5-10% of diarrheal diseases and dysentery called shigellosis occurring worldwide (Kahsay & Muthupandian, 2016; Rezaee, Abdinia, Abri, & Kafil, 2014) and accounts for approximately 40, 000 deaths annually (Williams & Berkley, 2018). It is an important disease particularly in developing nations (Kahsay & Muthupandian, 2016; Rezaee et al., 2014). Chloramphenicol, tetracycline, ampicillin, nalidixic acid, trimethoprim-sulfamethoxazole, azithromycin, ciprofloxacin, and ceftriaxone are antibacterial agents use in the treatment of shigellosis (Klontz & Singh, 2015). However, antibacteria resistance is problem in *Shigella* species that reduce effective treatment of the disease. Most *Shigella spp* isolated from children in hospital were shown resistant to tetracycline and trimethoprim-sulfamethoxazole (Jafari et al., 2009).

Vibrio cholerae is a causative agent of secretory acute diarrheal disease called cholera. Cholera is a serious public health problem that can lead to severe dehydration and death especially in developing nations worldwide (Kitaoka, Miyata, Unterweger, & Pukatzki, 2011). It is an endemic disease in developing countries and its spread can be enhanced by improper food hygiene and poor sanitation. Ampicillin, nalidixic acid, sulphamethoxazole-

trimethropim (SXT), chloramphenicol, tetracycline, nitrofunrantoin, cotrimoxazole, azithromycin and doxycycline antibiotics are commonly administered antibacterial agents for the treatment of this disease. However, recently most of these antibiotics (Dengo-Baloi et al., 2017), fluoroquinolones and tetracycline (Dakal et al., 2016) failed for effective treatment of the disease due to drug resistance in *V. cholerea*. Spontaneous chromosomal mutation, efflux pumps, SXT elements, conjugative plasmids and integrons are the main strategies in antibiotic resistance mechanisms of *V. cholerea* (Kitaoka et al., 2011).

2.2. The status and approaches of antibacterial discovery

The use of chemicals to improve or maintain public health is long history. The discovery of chemicals from microbial products to kill or inhibit pathogenic bacteria to save millions of human lives is one of the achievements in 20th century. The use of penicillin for the treatment of infection in 1942 revolutionize treatment of bacterial infection. As a result, 1950s and 1960s, called antibiotic 'Golden age', research effort produced one-half of antibiotics groups (such as cephalosporins, aminoglycosides, tetracyclines and macrolides) used today. However, after the golden age, the number of registered classes of antibiotics has declined (Takahashi & Nakashima, 2018).

Plant, fungi, bacteria and actinomycetes are the sources of antibacterial agents. However, most of the antibiotics are from actinomycetes particularly from genus *Streptomyces* (Barka et al., 2016; Takahashi & Nakashima, 2018).

Streptomycin in 1944, Chloramphenicol in 1947, tetracycline in 1948, erythromycin in 1952, vancomycin in 1956 are a list of few antibiotics produced from *Streptomyces griseus*, *S. venezuelae*, *S. rimosus*, *Saccharopolyspora erythraea*, *Saccharopolyspora orientales* respectively in the 'golden age' time (Takahashi & Nakashima, 2018).

However, the new antibiotic registry result showed that the rate of searching of antibiotics from biological source is growing very slowly worldwide compared to the rate of emerging antibiotic resistance bacteria.

The search for novel antibacterial producers and their identification continues to be key objective in the discovery of novel bioactive compounds (Adegboye & Babalola, 2016). *In vitro* test result showed that actinomycetes isolated from different countries is a potential source of bioactive compounds against bacteria pathogens such *E. coli, S. typhi, S. boydii, V. cholerea*. The *Streptomyces* species isolated from Ethiopia and Kenya soil showed antibacterial activity against *E. coli* (Bizuye et al., 2017, 2013; Kibret et al., 2018; Rotich et al., 2017).

The *Streptomyces* species isolated from Ethiopia soil (Kibret et al., 2018) and Iran rhizosphere soil, virgin soil and river sediments (Tabrizi et al., 2013) produce anti- *S. typhi* metabolites. Moreover, the *Streptomyces* species isolated from Ethiopia soil also showed antibacterial activity against *S. bodii* (Kibret et al., 2018).

Soil microorganism such as actinomycetes are excellent source of antibacterial compounds. Actinomycetes are found everywhere with other microorganisms (fungi, gram negative bacteria and other gram-positive bacteria) in both aquatic and terrestrial environments. Previous studies have shown that actinomycetes in municipal waste dump soil three times greater in number when compared to other microorganisms (Shirokikh, Solov, & Ashikhmina, 2014).

2.2.1. Isolation of actinomycetes from soil sample

Different techniques and methods are used to isolate actinomycetes for exploitation of their bioactive metabolites for biomedical application. Isolation of potential actinomycetes

is one of the essential steps for searching of antimicrobial compound. It requires a combination of techniques, optimal condition that involves soil sample pretreatments, serial dilution of the sample, spread of the samples on selective growth media and incubate at optimum condition for growth (Bizuye et al., 2013; V. Singh et al., 2016; Zainal Abidin et al., 2016) .

Soil sample collected from natural environment can be air dried and then pretreated by physical and chemical methods. Soil sample pretreatment using physical methods (such as heat) followed by chemical methods (such as phenol, calcium carbonate) reduce contaminants and favors for the growth of different genera of actinomycetes (V. Kumar, Singh, Mohan, Kumar, & Hadi, 2017; Zainal Abidin et al., 2016). Serial dilution of pretreated soil sample using sterile water or saline water help to reduce crowdedness of actinomycetes and facilitate to get a colony of single actinomycete isolate (Bizuye et al., 2013; Zainal Abidin et al., 2016). Selective isolation media supplemented with antibacterial (such as penicillin, streptomycin, ampicillin) and antifungal (such as cyclohexamide, nystatin) antibiotics is very important to prevent the growth of unwanted bacteria and fungi, respectively, and incubation of culture media at optimum growth temperature (28 -37 ^{o}C) for growth of actinomycetes (Bizuye et al., 2013; Zainal Abidin et al., 2016).

2.2.2. Bioassay methods for screening of antibacterial producing actinomycetes

Today several traditional methods are used to screen and assess the *in vitro* activity of antibacterial agents against bacteria pathogens. They can be categorized as diffusion assay (such as streak plate technique, spot/cup diffusion, well diffusion and disc diffusion methods) and dilution assay such as agar dilution and broth micro-dilution methods) (Alagumaruthanayagam, Pavankumar, Vasanthamallika, & Sankaran, 2009; Bonev,

Hooper, & Parisot, 2008). Each bioassay methods have advantages and some limitations based on a variety of conditions to assess the success or failure of antibacterial agents (Mayrhofer et al., 2008). They are sensitive to variations in acidity and content of growth medium, temperature and time of incubation and size of inoculums. Standardization of the methods are essential for all kinds of susceptibility test to evaluate the failure or success of antibacterial agents against pathogens (Mayrhofer et al., 2008).

However, the type bioassay method used for *in vitro* test depend on the bioassay guided screening and testing level. Antibacterial activity screening of selectively isolated actinomycetes (primary screening) and extracted metabolites from actinomycetes against bacterial pathogens (secondary screening) can be done by basic bioassay methods (H. S. Chaudhary, Soni, Shrivastava, & Shrivastava, 2013; V. Singh et al., 2016). Streak plate method can be used for primary antibacterial activity screening whereas well diffusion assay can be used for secondary screening (Balouiri, Sadiki, & Ibnsouda, 2016).

The main aim of primary screening is to select actinomycetes with activity against bacterial pathogens. To evaluate the antibacterial activity of isolated actinomycetes against bacterial pathogens can be done by perpendicular streak plat bioassay method (Adegboye & Babalola, 2016). Streak plate technique sometimes called direct challenge method is easy, cost effective method and the level of exposing contamination is relatively low. On the other hand, the target of secondary screening is done to assess the consistency and the strength of antibacterial activity of bioactive metabolite produced by actinomycetes. It can be done by either well diffusion or disc diffusion assay (Valgas, Souza, Smania, & Jr, 2007).

2.3. Principles and mechanisms for antibacterial silver nanoparticle synthesis

The application of nanotechnology, in various fields such as environment, energy and medicine, is rapidly increasing. Nanotechnology is an emerging, multidisciplinary and significant field of modern research dealing with design, production, characterization and application of nanomaterials (1–100 nm size) (Iravani, Korbekandi, Mirmohammadi, & Zolfaghari, 2016; Ochekpe, Olorunfemi, & Ngwuluka, 2009; Pitkethly, 2004). Nanomaterials such as drugs, devices or systems are made by manipulating the size and shape of individual atoms or molecules, or bulk materials of interest (Ochekpe et al., 2009).

With increasing drug resistant pathogens against bulk antimicrobial agent, nano-medicine has attracted attention (Prabhu & Poulose, 2012). There are various categories of metallic nanoparticles synthesized for medical applications. These includes gold, alloy, silver, and others (Singh et al., 2014). Silver nanoparticles has large surface atoms, large surface energy and spatial confinement when compared to bulk material that affects the pathogens normal physiology (Bhosale, Hajare, Mulay, Mujumdar, & Kothawade, 2015).

The methods used for synthesis of the nanomaterials are generally grouped under either top-down approach or bottom-up approach (Ochekpe et al., 2009; Zhang et al., 2016). The top down approach involves synthesis of nanomaterials by size reduction of bulk material of interest via mechanical **(**milling, grinding or crushing) process (Mohammadlou, Maghsoudi, & Jafarizadeh-Malmiri, 2016). Top-down fabrications of nanomaterials usually comprise mechanical-energy, high energy lasers, thermal and lithographic methods (Ochekpe et al., 2009; Siddiqi, Husen, & Rao, 2018). The limitation of this approach is surface structure imperfection and, it is not easy to produce smaller particle even with high energy consumption. It can also cause significant crystallographic damage to the processed

patterns. These affect the physical property and chemical structure of the nanomaterials (Siddiqi et al., 2018).

The second nanofabrication approach, bottom-up or building-up approach (self-assembly technique), involves synthesis of nanostructures starting from atoms, molecules or small particles or monomers (Mohammadlou et al., 2016). The nanostructures are synthesized onto the substrate by stacking atoms on to each other to form crystal planes, and crystal planes further stack on to each other to form a nanostructure called nonmaterial (Siddiqi et al., 2018; Zewde, Ambaye, Stubbs, & Raghavan, 2016). This approach is the best and easiest method to fabricate and generate high yield silver nanoparticles with a uniform size, shape and distribution. Fabrication of silver nanoparticles are an emerging part of metal nanotechnology that takes the huge significant contribution in nano-medicine. This is due to the characteristics of silver used as both antibacterial activity and drug delivery.

Bottom up approach for fabrication of silver nanoparticles comprises conventional (physical and chemical) and biological methods. The chemical method is fast method and produce high yield of nanoparticles when compared to physical methods. However, chemical methods use toxic chemicals for stabilizing/capping of AgNPs and the products are not environmental friendly whereas the physical methods are expensive and require complex experimental instrument to produce AgNPs (Anwar, 2018; Corciova & Ivanescu, 2018; Zhang et al., 2016).

2.3.1. Biological methods for silver nanoparticles synthesis

Unlike conventional methods, the biological method (green chemistry approach) is an easy, cost effective and environmental friendly method to produce high yield antibacterial silver nanoparticles (Zhang et al., 2016). It requires nontoxic solvent medium, nontoxic reducing and capping/stabilizing agents (Mohammadlou et al., 2016; Shameli et al., 2012;

P. Singh et al., 2016). It uses mostly water (nontoxic solvent) as solvent medium and metabolites from biological systems as reducing and stabilizing/capping agent (Rineesh, Neelakandan, & Thomas, 2018; Tran, Nguyen, & Le, 2013). Biological systems such as bacteria, actinomycetes, fungi and plants are major source of bioactive metabolites capable of synthesizing silver nanoparticle using intracellular and extracellular mechanisms (P. Singh et al., 2016).

Silver nanoparticle formulation using metabolites inside the organism is called intracellular mechanism. However, the product produced by this mechanism is difficult and is not cost effective to scale up the product for downstream process and for further biomedical application. On the other hand, extracellular mechanism involves synthesis of silver nanoparticles using extracellular metabolites produced by the organism. Extracellular mechanisms based synthesis of silver nanoparticles is cost effective, favors large scale production, easily scale up for downstream processing and preferable when compared to intracellular mechanism (Siddiqi et al., 2018; P. Singh et al., 2016).

2.3.2. Synthesis of antibacterial silver nanoparticles using actinomycete metabolites

The biosorption, bioaccumulation, biomineralization and biodetoxification natures of microorganisms makes them potential nanofactories (Prakasham, Kumar, Kumar, & Shankar, 2012). Actinomycetes are rich resource of diverse groups of bioactive metabolites such as antibiotics and it is also known as best nanofactories. They produce bioactive metabolites capable of synthesizing high yield antibacterial silver nanoparticles by extracellularly mechanism (Manivasagan, Venkatesan, Sivakumar, & Kim, 2014). Synthesis of antibacterial silver nanoparticle require silver salt as source of silver, solvent medium, reducing and stabilizing agents (Zhang et al., 2016). The bioactive metabolites that can be harvested from actinomycetes at appropriate growth time and conditions can be

used for reducing and stabilizing or capping agent. Silver nitrate salt is commonly used as a source of silver precursor. Both organic and aqueous solvents can be used as a solvent medium for silver nanoparticle synthesis (Iravani et al., 2016; Zhang et al., 2016).

The formation of silver nanoparticles using actinomycete metabolites, involves dissolution of silver salt, reduction and capping or stabilizing steps. The bioactive metabolite-based reduction of silver salt involves atom nucleation and growth to form silver nanoparticles. The next step is to prevent agglomeration of silver nanoparticles by stabilizing/capping agents (Zhang et al., 2016). Silver nanoparticle synthesized from 72 hr reaction between *S. albidoflavus* bioactive metabolites and silver nitrate solution showed antibacterial activity against bacteria pathogens such as *E. coli* (Prakasham et al., 2012). The 96 hrs reaction between *Streptomyces sp* JAR1 metabolites and silver nitrate solution synthesized antibacterial silver nanoparticle against bacteria such as *E. coli* and *S. typhi* (Chauhan et al., 2013). The three-day reaction result showed that *Streptomyces xinghaiensis* OF1 metabolites was capable of the reduction of silver salt and capping/ stabilizing of silver nanoparticle capable of antibacterial activity against *E. coli* (Wypij et al., 2018).

2.3.3. Characterization of actinomycetes metabolite mediated antibacterial silver nanoparticles

The formation and function of AgNPs synthesized by actinomycete bioactive metabolites can be confirmed by visual observation, using analytical tools and bioassay techniques. The easiest and simplest technique used to confirm the formation of AgNPs is by visual observation of color change and detecting characteristic UV- spectra peak (strong optical absorption) formed between 400-800 nm caused by the collective excitation of metal free electron (Shameli et al., 2012). The functional groups involved for reduction of silver and

capping of AgNPs can be identified by FTIR spectrophotometer (Składanowski et al., 2017). The function (antibacterial activity) of AgNPs can be confirmed by bioassay methods such as well diffusion assay (Prakasham et al., 2012).

The mixture of the silver nitrate solution and cell free metabolites produced by different *Streptomyces* species showed the color change (Karthik, Kumar, Kirthi, Rahuman, & Bhaskara Rao, 2014; Składanowski et al., 2017). Whether the silver ion is reduced or not may be detected by visualization of the color change of the reaction solution after mixing of the bulk solutions of the metabolites and the silver nitrate solution. The synthesis of silver nanoparticles using bioactive metabolites from *Streptomyces rochei* MHM13 (Abd-Elnaby et al., 2016) showed pale yellow color change. On the other study, dark brown color change was observed after synthesis of AgNPs using metabolite from *Streptomyces sp LK3* (Karthik et al., 2014), *S. parvulus* SSNP11 (Prakasham et al., 2014), *Streptomyces sp.* NH21 (Składanowski et al., 2017), *Streptomyces sp*. SS2 (Mohanta & Behera, 2014) and *Streptomyces xinghaiensis* OF1 (Wypij et al., 2018). This is the first qualitative indication that the probabilities of nanoparticles are being formed. However, this product must be further confirmed by other analytical techniques.

Furthermore, UV-visible spectrophotometer is an analytical instrument not only confirmation but also inform the intensity (concentration) of the synthesized AgNPs in the reaction solution (Składanowski et al., 2017). The qualitative and the quantitative measure of the formation of silver nanoparticle is confirmed by observation of characteristic UV-spectra peak within 380-450 nm (Wypij et al., 2018). The synthesis of silver nanoparticles using metabolites from *Streptomyces sp* LK3 (Karthik et al., 2014), *Streptomyces xinghaiensis* OF1 (Wypij et al., 2018) and *Streptomyces sp*. SS2 confirmed a characteristic peak at 420 nm. Another study showed that UV-vis spectra of silver nanoparticles

synthesized by metabolites from *Streptomyces sp.* NH21 and *Streptomyces rochei* MHM13 was observed at 402/ 424 nm (Składanowski et al., 2017) and at 410 nm (Abd-Elnaby et al., 2016), respectively.

The type of functional groups (bio-molecules) involved for synthesis of silver nanoparticles can be confirmed and characterized by FTIR spectrophotometer. FTIR is used to identify the possible functional group involved in reduction of silver salt and capping/stabilizing of silver nanoparticles. FTIR spectra can be scanned between 4000-400 cm^{-1} at 4 cm^{-1} resolution when a commonly pellet called potassium bromide (KBr) pellets are used for analysis of functional groups present in the metabolites and synthesized silver nanoparticles (Wypij et al., 2018).

The FTIR spectra of metabolites and metabolite mediated AgNPs are analyzed and compared to see the band position, band shape and band intensity. Change in band position, shape and intensity of metabolites involved in synthesis of silver nanoparticle when compared to the spectra of the metabolite inform that the functional groups are involved for reduction and stabilizing/ capping in AgNPs synthesis. As reported by (Chauhan et al., 2013), FTIR spectra analysis result showed that amide and hydroxyl functional groups from *Streptomyces sp* JAR1 metabolites were involved to reduce Ag^{+} and cap silver nanoparticle. Additionally, FTIR spectra result confirmed that active functional group O-H (at 3417 cm^{-1}) from *Streptomyces sp* LK3 metabolite (Karthik et al., 2014) from and O-H (at 3384 cm^{-1}) from *Streptomyces aegyptia* NEAE 102 (El-Naggar, Abdelwahed, & Darwesh, 2014) were used to reduce silver salt and cap/stabilize AgNPs.

The functional characterization of synthesized silver nanoparticle against selected bacterial pathogens can be easily tested *in vitro* using different type of bioassay techniques. The

well diffusion assay result showed that silver nanoparticle synthesized using metabolites from *Streptomyces species* showed antibacterial activity against *E. coli* and *S. typhi* (Abd-Elnaby et al., 2016; Chauhan et al., 2013). Disc diffusion method and broth dilution method result revealed that, silver nanoparticle fabricated by metabolite from *Streptomyces sp.* SS2 (Mohanta & Behera, 2014) and *Streptomyces xinghaiensis* OF1 (Wypij et al., 2018) showed antibacterial activity against *E. coli*, respectively. Additionally, well diffusion assay result showed silver nanoparticles synthesized by *S. parvulus* SSNP11 metabolites indicated antibacterial activity against *S. typhi* (Prakasham et al., 2014). However, the well diffusion result indicated that synthesized silver nanoparticle using bioactive metabolites from *Streptomyces sp* JAR1 showed no antibacterial activity against *S. boydii* (Chauhan et al., 2013).

2.4. Approaches for identification of actinomycetes

Actinomycetes are diverse group of gram-positive bacteria with high guanine + cytosine in their DNA. They are comprising of diverse groups with at least more 350 genera known today (Takahashi & Nakashima, 2018). They can be isolated from natural habitats for exploitation in agriculture, biotechnology and medicine particularly in antibiotic production. From these genera, around 95 % of soil actinomycetes are genus *Streptomyces*. Other actinomycete (non-*Streptomyces*) genera are called rare actinomycetes (Barka et al., 2016). Most of antibiotics currently used for treatment of infectious diseases were produced by genus *Streptomyces*. Thus, identification and knowing the taxonomic position of such potential actinomycetes isolated from natural habitat is a tremendously significant step.

Getting enough knowledge about the taxonomic position and the relationship of actinomycetes is also vital for further exploitation of them for industrial and economic

development. Currently, polyphasic (phenotypic, genotypic and phylogenetic) based characterization is used for identification of prokaryotes such as actinomycetes (Adegboye & Babalola, 2012). However, the methods used for collection of data for classification of actinomycetes must be reproducible, able to categorize and differentiate clearly unrelated strains. In addition to these, utility of a typical method assessed depending on the simplicity of use and result interpretation, cost, time and technical difficulty to obtain the results (Olive & Ban, 1999).

2.4.1. Phenotypic based identification of actinomycetes

Phenotypic based characterization is still important features for grouping and identification of actinomycetes. Morphological, biochemical and physiological methods are the major phenotypic characterization methods used for identification of actinomycetes. Phenotype is an observable expression of genotype and determined by environmental conditions. Colony and cell morphology, growth range (such as pH, Temperature, salt concentration, atmospheric conditions) and production of metabolites (such as enzymes, bioactive metabolites) can be applied for taxonomy of actinomycetes (Li, Chen, Jiang, & Jiang, 2016). Based on colony color actinomycetes are grouped under white, black, yellow, grey, orange, green, red color (Zainal Abidin et al., 2016).

The capability of growth in different pH range, they can be grouped under acidophilic, neutrophilic and alkalophilic. Acidophilic actinomycetes grow 3.5 to 6.5 pH range while neutrophilic actinomycetes grow 5 to 9 pH rang. However, majority of soil actinomycetes optimum growth pH is neutrophilic (6 - 9 pH) range (Basilio et al., 2003). Based on the growth capability of salt concentration, actinomycetes can be grouped under different groups. They can also grow in a wide range of temperatures and grouped as mesophilic

and thermophilic (grow between 50 to 60 ^{o}C). However, majority of actinomycetes are mesophilic with optimal growth temperature between 25 and 30 ^{o}C (Barka et al., 2016). Moreover, the majority of actinomycetes are aerobic and capable of producing catalase enzyme. They require macro-nutrients (carbon, nitrogen) and micronutrients (mineral sources) for their growth and production of industrially and pharmaceutically valuable secondary metabolites. The production of these industrially important metabolites depends on the physical and chemical conditions used for growth of actinomycetes. However, the phenotypic result (data) come from morphology, physiology and biochemical characteristic of the actinomycetes can be influenced by different growth conditions (temperature, pH, content of the growth media). The limitations of these methods are time consuming, very tedious and it is also difficult to identify microorganisms at species level (Li et al., 2016).

2.4.2. Genotypic based identification of actinomycetes

The genotypic and molecular phylogenetic based identification of actinomycetes are relatively advanced, influential, reliable, easiest and cost effective techniques (Adegboye & Babalola, 2012). Housekeeping genes such as the small-subunit (16S) rRNA gene having conserved and variable regions are used as a standard molecular taxonomy and phylogeny. The analysis of 16S rRNA gene sequences offers a reproducible, technically easy procedure and scalable. It can drive information and establish large database (Olive & Ban, 1999) for identification. It is the most common housekeeping molecular marker used for several reasons. (i) it present in prokaryotes (ii) it has both conserved and variable regions (iii) it has large enough size (1,500 bp) for informatics (Janda & Abbott, 2007).

Sequence analysis is based on the detection of sequence differences in the hyper-variable regions of the 16S rRNA gene. Broad range PCR primers (such as 27F/1492R, 243F/A3R)

recognize conserved sequences present in bacteria, while amplifying highly variable regions between the primer binding sites (Monciardini, Sosio, Cavaletti, Chiocchini, & Stefano, 2002). The amplified 16s rRNA gene segment is sequenced, analyzed and compared to reference sequences. Some of 16s rRNA gene reference sequence databases require for comparison and identification of prokaryotes are SILVA, RDP, NCBI and EzTaxon-e. The databases and taxonomies assign ranks (Domain, Phylum, Class, order, family, genus, species and strains) to their nodes. However, SILVA and RDP go down up to genus; NCBI go down up to species level whereas EzTaxon-e assign up to strain type level taxonomy. EzTaxon-e is freely available and quality-controlled web based public databases contain peer- reviewed (curated) sequence of type strains. The GenBank database, searched from NCBI, lack peer- reviewed sequence of type strains (Balvočiute & Huson, 2017; M. Kim & Chun, 2014; M. Kim et al., 2013; O. S. Kim et al., 2012).

EzTaxon-e and NCBI are also used to analyze the GC content (%) and the completeness of 16S rRNA gene sequences (Yoon et al., 2017). BLAST nucleotide algorithm is a simple and powerful statistic used to search similar sequences from EzTaxon-e and NCBI for identification and classification of prokaryotes (B. K. Kim et al., 2007). Identification to the genus and species level was defined as a 16S rRNA gene sequence similarity score value of > 97% and >99% with that of the type strain sequence in GenBank, respectively. However, even 100% similarity against known species does not a guarantee for correct identification (Janda & Abbott, 2007). Phylogenetic tree construction is required to confirm the identification by observing the taxonomic position and evolutionary relationships.

2.4.3. Molecular phylogenetics analysis for actinomycetes

A phylogenetic tree is an estimate of the relationship among sequences or taxa and their hypothetical common ancestors. It is a branching diagram composed of nodes and branches (edges) in which species or genes are arranged on branches according to their relationship. The branching pattern of a tree is called the topology of the tree. Branches and nodes can be internal or external (terminal). A branch (edge) represents the time estimate of the evolutionary relationships among the taxonomic units. The terminal nodes at the tips of trees represent operational taxonomic units (OTUs) or leaves correspond to the actual objects such as molecular sequences or taxa (species) being compared. Whereas internal nodes represent the last common ancestor (LCA) or hypothetical taxonomic units (HTUs) to all nodes that arise from that point (Horiike, 2016; Z. Yang & Rannala, 2012).

A phylogenetic tree is important for addressing biological questions such as taxonomic position and relationships among species in systematic and taxonomy. The advancement of nucleotide sequencing technologies has been taken phylogenetic analysis to a new height. Today most phylogenetic tree is constructed based on molecular 16s rRNA gene sequence. The phylogenetic trees are determined based on the nucleotide substitutions that occur during the gene sequence analyzing. The estimation of the number of nucleotide substitution is the important factor in the construction of phylogenetic tree. These can be done by calculating the genetic distance or number of nucleotide substitution (Z. Yang & Rannala, 2012).

Although the nature and scope of phylogenetic studies may vary and require different datasets and computational methods, the basic steps remain the same. It requires four basic steps: (1) Similar sequence search and assemble the datasets (2) align assembled datasets (3) Construction of the phylogenetic tree from those aligned sequences (4) Test and assess

of the tree (Hall, 2013; Horiike, 2016; Jill Harrison & Langdale, 2006; Patwardhan, Ray, & Roy, 2014).

3.4.3.1 Similar sequence search and assemble

The first step in phylogenetic tree is to identify, acquire, download and assemble the homologues sequences from the reference databases. The homologues sequences can be identified, assembled and organized from appropriate web browser or reference sequence databases. There are popular and reliable algorithms to search and get such similar sequence from reference database such as NCBI and EzTaxon-e. Nucleotide algorithm such as BLASTn is one of the most reliable and popular algorithms commonly used to search similar sequences to identify homologous genes from nucleotide sequences (Hall, 2013; Horiike, 2016) .

The BLASTn algorithm find the identical region called hit of the sequence in the nucleotide database to the query nucleotide sequence. The identical region similarity with the query sequence is evaluated by the Expected value (E-value). A lower E-value (near to 0) indicates higher 16s rRNA gene sequence similarity. The E-value considers the length of the query sequence, because shorter sequences have a high probability of occurring in the database by chance. Generally, the threshold of Expected value for nucleotide sequences is les or equal to 10^{-5} and the reference (subject) sequences having less than this E-value to the query sequence are selected and assembled for further phylogenetic analysis (Horiike, 2016).

2.4.3.2. Align assembled sequences

The homology sequences retrieved and assembled are analyzed using multiple sequence alignment analysis using alignment algorithms. It is used to calculate the best match for the

selected sequences, and lines them up so that the identities, similarities, and differences can be seen. This involves arranging a set of sequences in a matrix to identify blocks of conserved residues that reveal homology regions. The quality of multiple sequence alignment is the key to obtain a reliable phylogenetic tree. CLUSTAL W, CLUSTAL X and MUSCLE are some of the programs used to implement multiple sequence alignment (Chen, Jiang, Li, Han, & Jiang, 2017; Horiike, 2016).

Molecular Evolutionary Genetic Analysis (MEGA) offers CLUSTAL and MUSLE alignment algorithms and different tree construction algorithms. CLUSTAL W is one of the most commonly and widely using programs available in MEGA7 and PHYLIP (Phylogeny inferring package). They are large suite of open-access and applicable software packages for phylogenetic inference that estimates trees using statistical methods (Horiike, 2016).

Statistical methods are applied to do multiple sequence alignment analysis, to determine the tree topology and to calculate the branch lengths that best describe the phylogenetic relationships of the aligned sequences in a dataset. The most common computational methods for construction of phylogenetic tree are distance- and character-matrix methods. Molecular phylogenetic tree is constructed from distance- or character-based matrix generated from MSA using CLUSTAL W algorithms (Z. Yang & Rannala, 2012).

2.4.3.3. Phylogenetic tree construction

The most popular and frequently used tree building methods are classified in to distance-based (phenetic) and character-based (cladistic) methods. The distance-based method is rapid (analyze large amount of data in short calculation time) and less computationally intensive when compared to character-based method. In contrast to the distance-matrix methods, the character-based methods utilize all individual substitution among the

sequences to determine the most likely ancestral relationships (Hall, 2013; Horiike, 2016; Patwardhan et al., 2014; Z. Yang & Rannala, 2012).

The distance-based method measures the pair wise distance of two gene sequences and uses evolutionary distance matrix to construct a phylogeny. The distance between each pair of sequences is calculated, a distance matrix is computed, and the phylogeny is constructed based the computed distance matrix. Neighbor-joining (NJ) and Unweighted Pair Group Method with Arithmetic (UPGMA) method are the representative distance-based methods. The UPGMA is the simplest method, and assumes the molecular clock is constant. However, it is known that most evolutionary rate of molecules is not constant. This demerit overcome by NJ method. Neighbor-joining method is a commonly used distance-based method for inferring phylogenetic trees (Horiike, 2016; Z. Yang & Rannala, 2012).

Maximum likelihood (ML) and maximum parsimony (MP) are the popular and representative character- based methods. The Maximum parsimony algorithm deduces for each site the minimum number of character changes required along its branches to explain the observed states at the OTUs. Thus, parsimony uses the data and does not attempt to use any model to estimate the total number of changes. However, it assumes that a common character is derived from a common ancestor and thus underestimates the real divergence between distantly related taxa. This is the disadvantage of the Maximum parsimony. On the other hand, maximum likelihood is a statistical method that estimates the unknown parameters of a probability model and widely used for the construction of phylogenetic trees because of increased computational ability. The topology of the phylogenetic trees constructed using maximum likelihood should yield the highest probability of producing the observed sequences. It requires long calculation time and a substitution model to assess

the probability of mutations (Hall, 2013; Horiike, 2016; Patwardhan et al., 2014; Z. Yang & Rannala, 2012).

2.4.3.4. Phylogenetic tree assessment

Construction of a molecular phylogenetic tree is followed by an assessment of the reliability of the tree. The bootstrap test is a commonly-used method for evaluation of the reliability of specific clades in the tree. Determining the evolutionary distance (branch length of the tree), evaluation of the validity of the tree shape and evaluation of each internal branch of the a tree are the points used to evaluate the constructed molecular phylogenetic tree (Horiike, 2016; Z. Yang & Rannala, 2012).

If an internal branch has high proportion (bootstrap value or bootstrap confidence value), the internal branch is thought to be reliable. One bootstrapping may perform 500-1000 such re-samplings from the original sequences. If the bootstrap value for a given interior branch is 90% or higher, then the tree topology at that branch is considered accurate. Therefore, a bootstrap value of 90 indicated on a branch means that 90 % of the bootstrap trees support the topology at the branch obtained in the original phylogenetic tree (Hall, 2013; Horiike, 2016; Patwardhan et al., 2014).

CHAPTER THREE: MATERIALS AND METHODS

3.1. Soil sample preparation and isolation of actinomycetes

3.1.1. Study period, area and sampling sites

The research study was started 2016 and ended 2018. The study was carried out in industrial and waste dump areas, found in Thika district located in Kiambu County. Thika has many industries so that I chose as a sampling site. Its location has 3°53′ and 1°45′ south latitudes and 36°35′ and 37°25′ east longitudes (Ephantus, Robert, & Paul, 2015). Thika town, is an industrial, 42 km away from northeast of Nairobi, Kenya. In addition to hosting different industries, institution and living houses, it also receives different industrial and municipal waste that comes from a variety of industries, institutions and households found in the town. Wastes from industries were dumped temporally around their industry compound. Kiganjo (Kang'oki) waste dump area receives both the industrial and municipal wastes of the town. This area has been undiscovered site for isolation of antibacterial producing and antibacterial silver nanoparticle synthesizing groups of actinomycetes.

For this study, sampling sites were selected from both industrial compound and Kiganjo waste dump areas. The sampling sites were selected by considering the accessibility and exposure to waste generated from the industries and municipal waste. The soil exposed to these various wastes may create soil environment having variety of micronutrients or minerals, macro-nutrients and metals. These may help to get actinomycetes that have been exposed for such environments and may have been produced diverse groups of metabolites.

The selected sampling sites for this research study were BIDCO Africa Ltd waste disposal site (BAL), BIDCO Africa Ltd waste dump site (BAD), Poly Sack Ltd waste dump site (PLS), Bakex Millers Ltd waste dumping site (BML), Kiganjo waste dump site one (KDO), Kiganjo waste dump site two (KDT), Kiganjo waste dump site three (KGT). Mangu' shrubs rhizosphere site (MRS) was selected as control site. Mangu rhizosphere site is found with in Thika and there was no waste there. The geographical location of different soil sampling sites used for this research study is described in Fig.3.1.

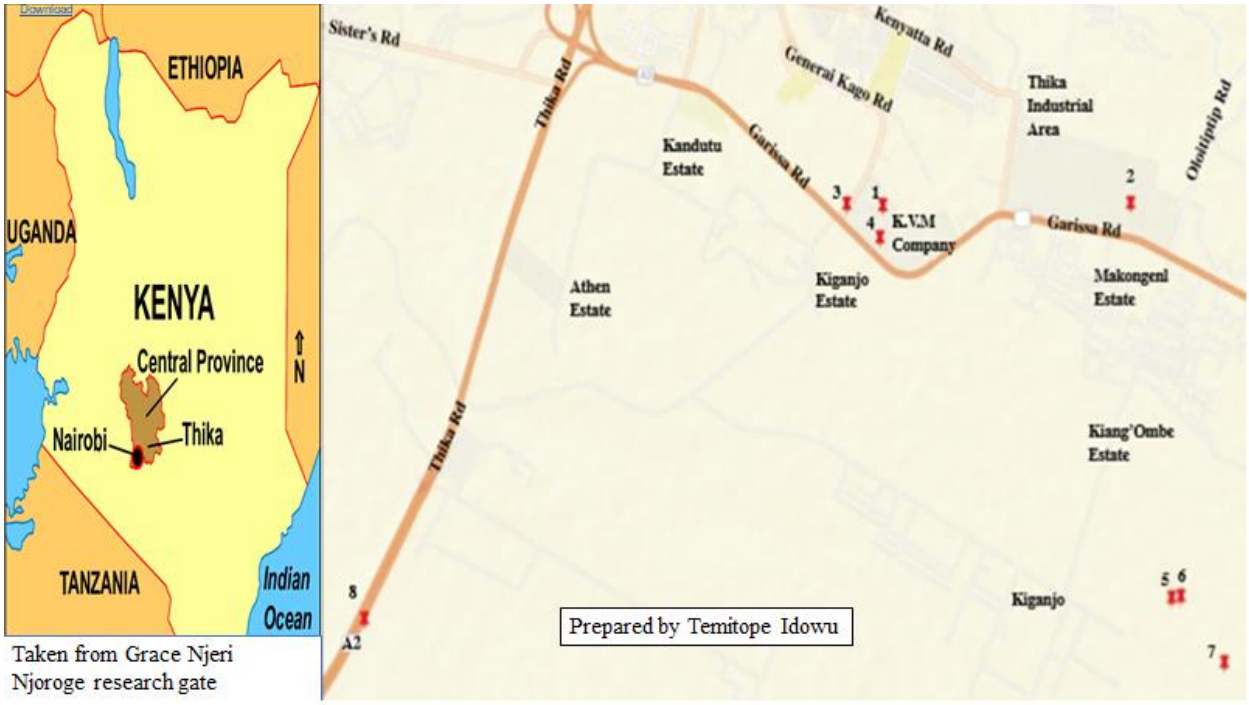

Figure 3.1: Geographic location and representation of soil sample collection sites in Thika, Kenya

The numbers observed on the figure indicates the sites as described 1(BAL), 2(PLS), 3(BAD), 4(BML), 5(KDO), 6(KDT), 7(KGT) and 8(MRS).

3.1.2. Study design, target groups and summery of research work flow

This is cross-sectional laboratory-based study with controls were used as a research design for this study**.** The types of experimental and control groups that was used for this research

study varies based on activities that is described in the procedures below. The study target groups used for this research work was antibacterial metabolite producing and antibacterial silver nanoparticle synthesizing groups of actinomycetes isolated from Thika waste dump sites. The target test pathogens used for this study are obtained from KEMRI and described below from each activity.

The work flow from selective isolation up to identification of potential actinomycetes isolated from waste dump sites is provide description briefly (Fig 3.2).

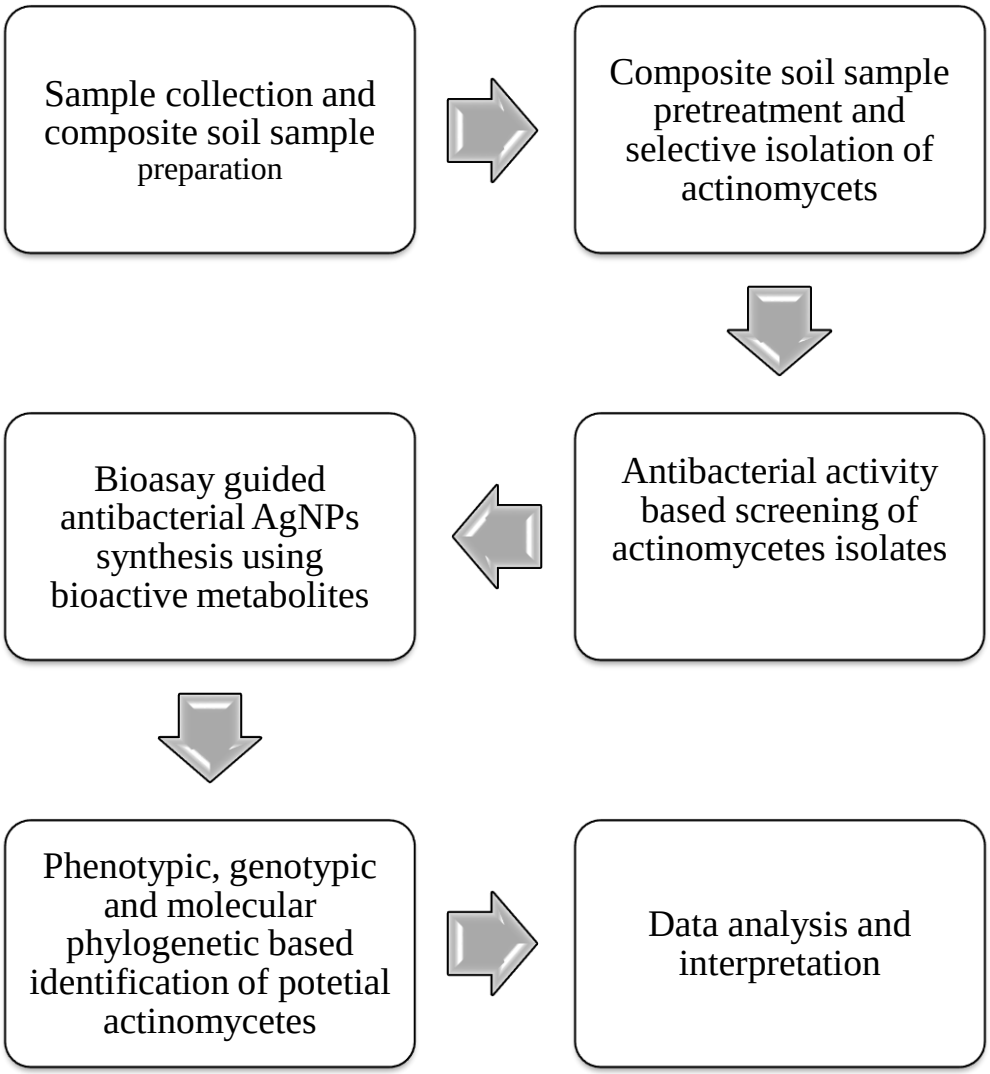

Figure 3.2: Brief diagrammatic description of the research workflow

3.1.3. Soil sample collection and composite soil sample preparation

Seven waste dump sites and a Mangu rhizosphere (control) site were selected. From each site 9 plots (Fig 3.2) were prepared randomly and samples were taken at four different depth at each plot per site to collect unbiased and representative samples (Boone, Grigal, Sollins, Ahrens, & Armstrong, 1999). From these sites, a total of 288 (8 x4x9) soil samples were collected to make a total of 32 composite soil sample based on depth per sampling site to save time and money. Soil sample collection and composite soil sample preparation principles are described below.

The required materials for soil sample collection, packaging and shipping were packed in cool box and transported to waste disposal sites. Ethanol (75%) was used for disinfection of materials used for soil sample collection. Disinfected plastic (kimguard) were put on the land and the required materials for sample collection were put on it. The GPS coordinates for each selected soil sampling sites were recorded using smart phone GPS. Sampling area having 16 m^2 (4 m X 4 m) for each sampling site was prepared. Nine plots were prepared per site in 16 m^2 area using GPS coordinate points (at plot 1) as a starting (reference) point like as described below (Fig 3.2). Soil samples from each plot were collected by disinfected auger from 0-20 cm depth (Xu, Li, & Jiang, 1996) at four different depth levels.

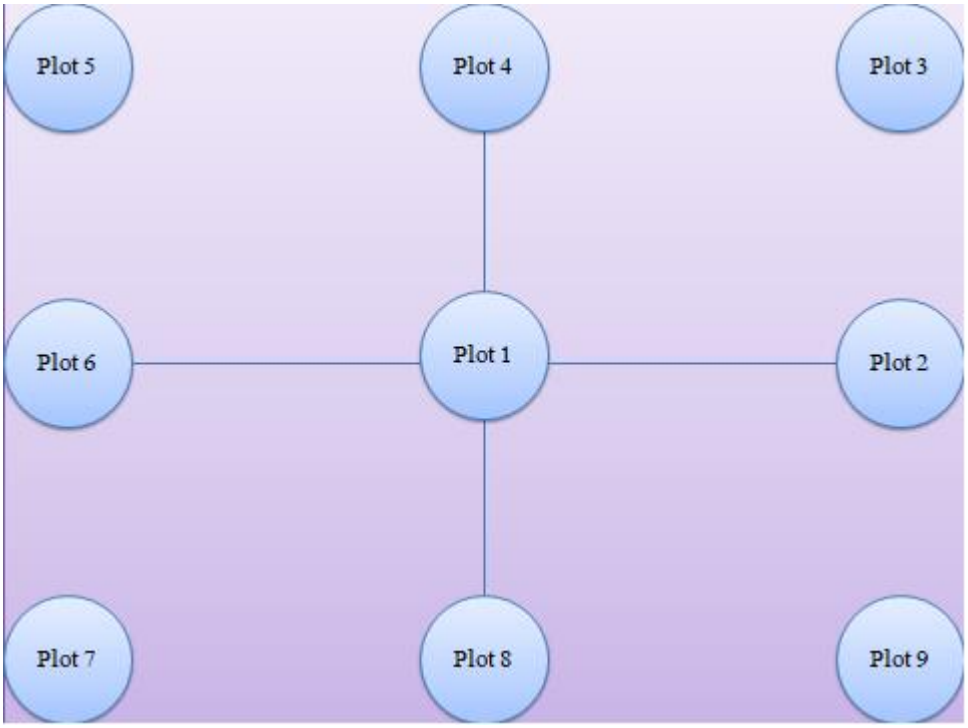

Figure 3.3: Diagrammatic description of soil sample collection plots per sampling site

A plot 1 to plot 9 indicates the points where soil sample collected at 0-5 cm, 5-10, 10-15 and 15-20 cm depth within a sampling site. Plot 1(starting point where the GPS coordinate points were taken)

The four depth levels used for collection of soil samples were 0-5 cm, 5-10 cm, 10-15 cm (Tyagi, Bhatnagar, & Pandey, 2014) and 15-20 cm (Messaoudi, Bendahou, Benamar, & Abdelwouhid, 2015) for preparation of four different composite soil samples per sites as described in the following procedures. Disinfected auger was pushed down at each plot to take soil sample in 0-5 cm depth range interval. Soil samples collected from each 9 plots from 0-5 cm depth level were put on a plastic (kimguard) and were mixed to prepare a composite soil sample per sampling site. A composite soil sample was transferred to polyethylene bag, zip-locked and labeled. The packed and labeled soil samples were put in to the cool box. The holes made during soil sample collection were refilled. The auger used to collect soil sample was re-disinfected meanwhile soil sample collection at each

depth was finished. The same procedure was done for 5-10, 10-15 and 15-20 cm depth levels to make 3 additional different composite soil samples per site.

Generally, a total of four composite soil samples per site were prepared based on the four different depth levels and the prepared composite soil samples were packed using sterile polyethylene bag (Messaoudi et al., 2015; Tyagi et al., 2014; Zainal Abidin et al., 2016). The same procedures were done for the other seven remaining sampling sites. Therefore, from 8 sampling sites a total of 32 composite soil samples were prepared, packed in cool box and transported to Zoology laboratory, Jomo Kenyata University of Agriculture and Technology (JKUAT).

3.1.4. The moisture content and pH analysis for composite soil samples

The moisture content and the pH value of the composite soil sample were analyzed according to (George, George, & Hatha, 2010; Saha & Santra, 2014). The pH meter and the balance were calibrated. Ten gram of composite soil sample was weighed and put in to the beaker. Fifty milliliters of distilled water were measured using graduated cylinder and added in to the beaker containing 10-gram soil and mixed well. The pH meter having both the pH rod and temperature rod was inserted in to the beaker containing the diluted composite soil sample. A triplicate for each composite soil sample was done and the result of the pH of a composite soil sample was recorded. Similar steps were done for each composite soil sample to read and record the pH value of the soil sample.

To determine the moisture content of each composite soil sample, the following procedures were done for each composite soil sample. The power switch for the oven was switched on and it was adjusted at 110 ^{o}C. The weight of Aluminum foil (W_1) and aluminum foil having composite soil sample (W_2) were weighed using calibrated balance.

Aluminum foil containing each composite soil sample were put in the oven and was incubated until moisture content of the composite soil sample was removed. This was confirmed by recording the consistent weight of a composite soil sample at different incubation time interval. Then the weight of dried composite soil sample with aluminum foil (W3) was recorded and the percentage of soil moisture content (% MC) was calculated according to the following formula:

$$\mathbf{MC}\ (\%) = \frac{\mathbf{Weight\ of\ water}}{\mathbf{weight\ of\ moist\ soil}}\mathbf{X100} = \frac{\mathbf{W2 - W3}}{\mathbf{W2 - W1}}\mathbf{X100}$$

A triplicate was done for a composite soil sample to get the average moisture content of the soil sample. Similar steps were done for each composite soil samples to record the moisture content of the soil sample.

3.1.5. Composite soil sample pre-treatment for isolation

The composite soil samples were air dried at room temperature according to (Messaoudi et al., 2015; Zainal Abidin et al., 2016) described as follow. This activity may be used to reduce moisture content dependent bacteria and fungi. The composite soil samples were spread on aluminum foil on the lab bench and they were left for 4-6 days at room temperature to dry. The dryness of a composite soil sample was confirmed by recording the consistent weight of the composite soil sample at different time interval. Air dried composite soil sample was crashed to make fine composite soil sample. It was then packed in sterile polyethylene bag for further analysis.

Air dried composite soil samples were further pretreated for the reduction of temperature (dry heat) and chemical sensitive bacteria and fungi. Air dried composite soil sample was pre-treated first by dry heat method according to (Zainal Abidin et al., 2016) and then chemical treatment using calcium carbonate was done according to (Messaoudi et al.,

2015). Ten grams of air-dried composite soil sample was heated in a hot oven at 120 ^{o}C for 1 hour. The dry heat pretreated composite soil sample was further pretreated by mixing 1% calcium carbonate (for 10 g composite soil sample to 0.1 g $CaCO_3$). The use of a combination of such different pretreatment methods is very important to reduce temperature and chemical sensitive fungi and other bacteria.

3.1.6. Isolation of actinomycetes from pretreated composite soil samples

Preparation of sterile starch casein agar plate media supplemented with antibiotics is described briefly as follow. The components (starch powder 10g, K_2HPO_4 2g, KNO_3 2g, casein 0.3 g, $MgSO_4.7H_2O$ 0.05 g, $CaCO_3$ 0.02 g, $FeSO_4.7H_2O$ 0.01g, agar 18g) were added in the flask containing one litter distilled water and the pH was adjusted to 7.1 by adding a drop of NaOH or HCL solution. The flask containing the mixtures was put in to the autoclave and sterilized for 15 minutes at 121 ^{o}C. The sterile media was cooled down (40 ^{o}C) and it was supplemented with 100 µg /l cyclohexamide and 1 µg /l penicillin. The media was poured on sterile Petri-plate in laminar flow hood and it was left until solidified. The prepared starch casein plate media supplemented with antibiotics was ready to spread sample suspension for selective growth and isolation of actinomycetes.

Serial dilution and spread of soil suspension on starch casein agar plate media was done according to (Bizuye et al., 2013; Sudha Sri Kesavan & Hemalatha, 2015; Zainal Abidin et al., 2016) described briefly as follow. Ten gram of pre-treated composite soil sample was mixed with 90 ml sterilized saline water (0.85%) to make 10^{-1} stock dilution. Serial dilution was done up to 10^{-5}, and 0.1 ml suspension from 10^{-5} was taken and spread using sterile L-glass road (90^{o} bend) on starch casein agar media supplemented antibiotics (experimental group). Experimental group and negative control (media without soil sample) in duplicates were incubated at 28 ^{o}C (D. Singh et al., 2014; Thirumalairaj,

Shanmugasundaram, Sivasankari, Natarajaseenivasan, & Balagurunathan, 2015) for two weeks and the numbers of colonies were recorded. Different colonies per sample from the plates were subcultured in to starch casein slant media for growth and the recovered isolates were temporarily preserved at 4 ^{o}C for bioassay guided (antibacterial activity) screening.

3.2. Screening of actinomycetes isolates for antibacterial activity

3.2.1. Preparation and standardization of bacterial suspension

A total of six test (five gram negative and one gram positive) bacterial pathogens were used to screen the antibacterial activity of recovered isolates. *Escherichia coli ATCC25922*, *Salmonella typhi*, *Shigella boydii*, *Vibrio cholerae*, extended spectrum beta-lactamase (ESBL) producing *E. coli* and Methicillin resistance *Staphylococcus aureus* (MRSA) were the test pathogens used to perform *in vitro* antibacterial susceptibility tests against the recovered isolates. All the clinical and standard bacteria pathogens were obtained from KEMRI.

Test bacterial suspension preparation and standardization was done according to (Ataee, Mehrabi-Tavana, Hosseini, Moridi, & Zadegan, 2012). The test bacterial pathogens were streaked on Muller Hinton agar plate and incubated at 37 ^{o}C for 24 hrs to get pure colonies of a test pathogen. Two to three colonies of a test pathogen were taken using sterile inoculating loop and put in to test tube containing 3 ml sterile water and were mixed well. By adding a colony or adding sterile water, bacterial pathogen suspension turbidity was standardized by using McFarland standard (0.5%) as a reference. The standardized bacterial suspensions were used for both primary and secondary antibacterial activity screening against recovered isolates.

3.2.2. Primary screening for antibacterial activity among actinomycetes

The primary screening was done according to (Bizuye et al., 2013; Zainal Abidin et al., 2016) as described below. The recovered (125) isolates were subcultured in to starch casein broth and incubated for three days at 28 ^{o}C for culture refresh and growth. Each 3 days old culture isolate was streaked on starch casein plate media horizontally using sterile inoculating loop and were incubated at 28 ^{o}C for 8 days with negative control (starch casein plate media).

E. coli ATCC25922, *S. typhi*, *S. boydii* and *V. cholerae* suspensions preparation and turbidity standardization was done according to (Ataee et al., 2012) as described above. The suspension from a test pathogen was taken using sterile inoculating loop and it was streaked perpendicular to the grown actinomycete isolate on starch casein plate media. These were incubated at 37 ^{o}C for 24 hrs for antibacterial activity observation. The antibacterial activities of isolates against test pathogens were observed by visual detection and the inhibition zone (antibacterial activity) was measured using graduated ruler.

3.2.3. Antibacterial activity of actinomycetes isolates against MRSA and ESBL E. coli

Twenty-nine isolates that were showed antibacterial activity against selected test pathogens was also tested against MRSA and ESBL *E. coli* by streak plate method as described in detail above. Each isolate was streaked by sterile inoculating loop on the plate containing starch casein agar and it was incubated for 8 days at 28 ^{o}C (Bizuye et al., 2013; Zainal Abidin et al., 2016).

Both MRSA and ESBL *E. coli* suspension preparation and standardization was done according to (Ataee et al., 2012) as described above. The standardized 18 hrs old suspensions of clinical MRSA and ESBL *E. coli* was streaked perpendicular to each 8 days

old isolates and incubated for 24 hours at 37 ^{o}C. The antibacterial activities of the isolates against test pathogens were recorded by measuring zone of inhibition.

3.2.4. Secondary screening for antibacterial activity among actinomycetes

Secondary screening was done by well diffusion assay (H. S. Chaudhary et al., 2013; V. Singh et al., 2016) using supernatants from starch casein broth cultured isolates that was taken at different day incubation as described below. Isolates (29) showed antibacterial activity during primary screening were selected for secondary screening. Five milliliter of 3 days old seed culture from each active isolate was added in to a flask containing 50 ml sterile starch casein broth and incubated for 13 days at 28 ^{o}C. Two milliliter broth culture from each isolate at different day incubation (up to 13-day old culture) was taken and it was centrifuged at 12000 rpm for 10 minutes to get a supernatant for antibacterial activity screening test.

Nine millimeter diameter wells were prepared on sterile Muller Hinton plate media by using a sterile cork borer (Balouiri et al., 2016). Suspensions were prepared by adding one or more colony of 18 hrs old pathogen (*E. coli ATCC25922, S. typhi, S. boydii* and *V. cholerae*) in a test tube containing 3 ml sterile water. This was standardized by adding a colony or sterile water until the turbidity of the suspension was equivalent to McFarland standard (0.5%) (Ataee et al., 2012). Each standardized pathogen suspension was swabbed using sterile cotton swab on Muller Hinton plate media having 9 mm diameter wells. Eighty micro-liters (Balouiri et al., 2016) supernatant from actinomycete isolates, streptomycin (positive control) and starch casein broth (negative control) was added on each well using micropipette. The triplicates were done and incubated for 24 hrs at 37 ^{o}C. The antibacterial activity of the supernatant and the controls were recorded by measuring the zone of inhibition result in millimeters.

3.3. Synthesis, characterization and evaluation of actinomycete metabolite mediated antibacterial silver nanoparticles

3.3.1. Preparation of metabolites from actinomycete isolates and silver nitrate solution

Supernatant metabolite preparation from isolates and silver nitrate solution preparation from silver nitrate salt was done according to (Składanowski et al., 2017). Locally isolated bioactive metabolite producing isolates were inoculated by streaking using sterile inoculating loop on starch casein plate for three days at 28 ^{o}C. Nine mm diameter was cut using sterile cork borer from the culture media containing cultivated local isolate and transferred to 50 ml sterilized starch casein broth media containing flask and incubated at 28 ^{o}C for 7 days to harvest bioactive secondary metabolites. The 7-day old culture was transferred to sterile centrifuged tube (50 ml size) and was centrifuged at 5000 rpm for 25 minutes to separate the cells from the supernatant containing the secondary bioactive metabolites. The bioactive supernatant was further filtered by 0.22 µm pore size filter paper to make cell free supernatant (metabolite).

On the other hand, 10 mM $AgNO_3$ solution was prepared by adding 1.6987 g $AgNO_3$ in one-liter sterile distilled water. Both cell free supernatants (metabolites) from selected isolates and silver nitrate solution were stored at 4 ^{o}C for AgNPs synthesis.

3.3.2. Synthesis of silver nanoparticle, visual detection and UV-visible spectra analysis

The synthesis of AgNPs was done by the mixture reaction of supernatant metabolites from isolates with $AgNO_3$ solution (silver nitrate in water) according to (El-naggar, Mohamedin, Hamza, & Sherief, 2016; Składanowski et al., 2017). The cell free metabolite solution (50

ml) was mixed with 50 ml of 10 mM $AgNO_3$ solution (1:1 ratio) in sterilized flask and it was incubated at 28 ^oC for seven days with the controls (supernatant only and 10 mM $AgNO_3$ solution only). The color change in the reaction solution at each reaction day interval for both the experimental group and control group was assessed through visual observation.

Meanwhile, the absorption intensity measurement in the reaction solution for both the experimental group and control group was assessed by double beam UV-visible spectrophotometer in absorption mode at every reaction day interval. Two milliliters from the reaction solution (experimental and control group) was taken by micropipette and put in to sterile eppendorf at each reaction day interval. The UV-vis spectrophotometer was switched on and spectra analysis was clicked on to adjust the parameters and to use to spectra analysis. The wave length was adjusted between in 200 nm-800 nm in the absorption mode and other parameters were used as default settings. Two ml distilled water was transferred to quartz cuvette, put in to the UV-spectrophotometer blank holder and the blanking was done first by running the system. Then, two milliliter aliquots from reaction solutions was transferred in to quartz cuvette and put in to UV spectrophotometer sample holder. The absorption intensity of the sample was analyzed, and the result was recorded. The same procedure was done for each reaction groups both experimental and control groups to get the absorption intensity in the adjusted wavelength range for analysis and interpretation (Składanowski et al., 2017).

The reaction solution that showed both color change and characteristic UV spectra peak between 380-500 nm range was recorded as the presence of AgNPs and selected for further analysis. The type of silver nanoparticles synthesized by metabolites from KDT32 and KGT32 isolates were represented as KDT32-AgNP and KGT32-AgNP, respectively.

Absorption intensity of KDT32-AgNP and KGT32-AgNP that showed a characteristic UV peak was measured at 5, 6- and 7-day reaction solutions using double beam Uv-visible spectrophotometer for comparison.

3.3.2. FTIR spectra analysis of bio-molecules used for AgNPs synthesis

The sample preparation for FTIR spectra analysis of AgNPs was done according to (Abd-Elnaby et al., 2016). The synthesized silver nanoparticles using KDT32 and KGT32 metabolites was filtered using 0.22 µm pore size filter paper. Then it was centrifuged at 5000 rpm for 25 minutes, the supernatant was discarded from the pellet and the pellet was washed with sterile distilled water to remove unbound metabolites. This step was repeated three times to remove unbound metabolites from metabolite mediated silver nanoparticles.

The pellets were diluted with sterile distilled water and small amount (2-3 drops) of diluted synthesized AgNPs was taken by capillary tube and was put on potassium bromide (KBr) pellet. The pellets having the suspension were left at room temperature to evaporate the water. Then the pellets were put on sample cell holders and put in calibrated FTIR spectrophotometer (Bruker alpha model, Germany) for FTIR spectra analysis. The FTIR spectra were analyzed and recorded in transmittance mode in the range of 4000-400 cm^{-1} wave numbers at 4 cm^{-1} resolution (P. S. Kumar et al., 2015). The same procedure was also applied for the FTIR spectra analysis of the metabolites only (metabolite solution without treatment of $AgNO_3$). The results of FTIR spectra from both metabolites only (control group) and metabolite mediated AgNPs (experimental group) was recorded for comparison of the band shape, band position and band intensity change between them.

3.3.4. Testing of antibacterial activity of AgNPs using well diffusion assay

The reaction solution containing silver nanoparticles was filtered using 0.22 µm pore size filter paper to reduce/remove residual debris. The filtrate containing metabolite mediated silver nanoparticle was freeze-dried using lyophilizer to make AgNPs powder. The AgNPs powder was collected for antibacterial activity test against bacteria pathogens.

The antibacterial activity of the metabolite mediated AgNPs was evaluated by well diffusion assay according to (Prakasham et al., 2012). The selected pathogens (*E. coli*, *S. typhi* and *S. boydii*) were grown over night on Muller Hinton agar plate. The colonies were taken and added in to test tube containing 5 ml sterile water to make bacterial suspension and the turbidity of the bacterial suspension was standardized by 0.5 McFarland standards (Ataee et al., 2012). The suspensions were taken by sterile cotton swab and it was swabbed on Muller Hinton agar having 9 mm well. The 2 mg/ml of stock solution was prepared from $AgNO_3$, KDT32-AgNPs, KGT32-AgNPs, crude bioactive metabolite extract of KDT32 and KGT32. Streptomycin (0.1 mg/ml) was used as a positive control and water was used as a negative control. From AgNP solution, 80 µl of solution was added on each well. The same procedure was also done for others and the plates were incubated at 37 ^{o}C for 18 hrs. After 18 hrs incubation the inhibition zone result was determined.

3.4. Characterization of potential isolates for identification

The local isolates (KDT32 and KGT32) involved in both productions of antibacterial metabolite and synthesis of metabolite mediated antibacterial silver nanoparticle were selected for identification. Phenotypic characterization (such as colony and cell morphology, growth condition at different pH and salt concentration and catalase test) for such potential local isolates was done. However, the detail characterization was done

based on genotypic and molecular phylogenetic analysis for identification and classification of the potential local isolates. The genomic DNA was extracted, 16s rRNA gene was amplified and the amplified product was sequenced for further analysis. The detail procedures were described as indicated below about genomic DNA extraction, 16s rRNA gene amplification, genotypic based identification and molecular phylogenetic based determination of taxonomic position potential local isolates.

3.4.1. Phenotypic characterization of potential isolates

Starch casein broth (starch powder 10g, K_2HPO_4 2g, KNO_3 2g, casein 0.3 g, $MgSO_4.7H_2O$ 0.05 g, $CaCO_3$ 0.02 g, $FeSO_4.7H_2O$ 0.01g within 1L water) was melted on hotplate and the starch casein broth media was prepared by sterilizing for 15 minutes at 121 ^oC. The sterile starch casein broth media was left in laminar flow hood until it was cooled and ready to use. The potential local isolate was sub-cultured on starch casein broth and was incubated for 3 days at 28 ^oC. A drop of 3 days old culture broth of each local isolate was put on starch casein agar media plate and spread on it using sterile L glass road and it was incubated for one week at 28 ^oC. The colony shape and colony color were assessed.

A drop of sterile water was added on a dry and clean microscope slide. A small sample from a 3-day old colony was scooped by sterile inoculating loop and it was gently stirred with a drop of sterile water on microscope slide to prepare microscope slide smear. The prepared microscope slide smear was heat fixed to fix the smear sample on the slide. The heat fixed microscope slide smear was left on the bench until it was cooled, and it was ready for staining. Drops of crystal violet was added on the heat fixed microscope slide smear to make a reaction between crystal violate and the cell component of the isolate. The slide was left for 1 minute and then it was gently rinsed with water. Drops of grams' iodine solution was added on the slide. It was left for 1 minute and then it was gently rinsed

water. Drops of decolorizing agent (95% acetone) were added and after 10 seconds it was gently rinsed with water. The decolorized sample was counter stained by adding drops of safranin solution and left for 45 minutes. It was rinsed with water and then it was blot dried for microscope use. The slide was put on the stage of light microscope and it was adjusted at 100X magnification power or under oil-immersion to assess the gram reaction and the morphology of the cell (H. S. Chaudhary et al., 2013).

A small sample of 3-day old colony of the local isolate was scooped using sterile inoculating loop and put on a clean and dry microscope slide. A drop of 3 % hydrogen peroxide (3 % H_2O_2) solution using a dropper was added on the sample microscope slide. A drop of hydrogen peroxide solution was added on free slide and used as negative control. Simultaneously, the result of the reaction was assessed by observation and the result was recorded (Li et al., 2016).

The components of starch casein media (starch powder 10g, K_2HPO_4 2g, KNO_3 2g, casein 0.3 g, $MgSO_4.7H_2O$ 0.05 g, $CaCO_3$ 0.02 g, $FeSO_4.7H_2O$ 0.01g, agar 18g) was added in a beaker containing 1000 ml water and the pH was adjusted (4, 5, 6, 7, 8, 9, 10, 11, 12 and 13) by adding a drops of NaOH or HCL acid solutions (Kontro, Lignell, Hirvonen, & Nevalainen, 2005; Li et al., 2016). The media was mixed and melted using magmatic stirrer hot plate. Then it was sterilized at 121 ^oC for 15 minutes. The sterilized media was cooled, and it was poured on sterile Petridis in laminar flow hood. The media was let until it was solidified and ready to use. Three days old colony was scooped using sterile inoculating loop and subcultured on starch casein plate by streaking. It was incubated for one week at 28 ^oC and the growth was assessed at different pH.

The components of starch casein media (starch powder 10g, K_2HPO_4 2g, KNO_3 2g, casein 0.3 g, $MgSO_4.7H_2O$ 0.05 g, $CaCO_3$ 0.02 g, $FeSO_4.7H_2O$ 0.01g, agar 18g) was added in a beaker containing 1000 ml water and the pH was adjusted to 7.1 by adding drops of NaOH or HCL solution. The media was mixed and melted using hot plate having magnetic stirrer. 100 ml melted media was poured in to each flask (250 ml size) and different salt weight (1%, 2%, 3%, 4%, 5% to 20% NaCL salt) (Li et al., 2016) was added in to each flask having 100 ml melted media and mixed well. The media having different salt concentration was sterilized for 15 minutes for 121 ^oC. The sterilized media having different salt concentration was poured to sterile Petri-dish in laminar flow hood and left until it was solidified and was ready to use. Three-day old colony was scooped using sterile inoculating loop and it was streaked on the media having different salt concentration. The inoculated starch casein plate media was incubated at 28 ^oC for one week. The growth of each isolates on starch casein media having different salt concentration was assessed.

3.4.2. Genomic DNA extraction

The genomic DNA from KDT32 and KGT32 isolates were isolated and purified by QIAamp Mini kit done according to manufacturer's instructions (Bowman, Roffey, McNevin, & Gahan, 2016). QIAamp Mini kit is a genomic DNA extraction and purification kit. The pure colony of KDT32 and KGT32 isolate was subcultured in to starch casein broth and incubated for 2 days at room temperature. The 2-day old culture of KDT32 and KGT32 isolates were pelleted by centrifugation (8000 rpm for 10 minutes at room temperature).

The pellet was transferred to sterile 1.5 ml size centrifuge tube and resuspended by adding 300 µl ATL buffer to the sample and incubated at 80 ^oC for 20 minutes. About 20 µl of

Proteinase K was added to the sample, mixed and incubated at 56 ºC for 1 hour. The mixture was mixed by vortex mixer and further incubated at 95 ºC for 15 minutes to inactivate the enzyme Proteinase K followed by pulse vortex mixer. An amount of 200 µl AL buffer was added to the sample, mixed by vortex mixer and incubated at 70 ºC for 10 minutes. Two hundred micro-litter ethanol (99%) was added to the lysate, mixed by vortex mixer and centrifuged (8000 rpm) for 30 seconds. The lysate or sample contents were transferred to a new QIAamp Mini spin column in 2 ml tube and centrifuged at 8000 rpm for 1 minute to remove solution from DNA and the filtrate was discarded. Five hundred micro-litter of AW1 buffer solution was added to the sample QIAamp Mini spin column in 2 ml tube and centrifuged at 8000 rpm for 1 minute. The solution was removed and the wash of the sample with AW1 buffer was repeated once again. The QIAamp Mini spin column was transferred in to 2 ml tube and 500 µl AW2 buffer was added. The mixture was centrifuged at 8000 rpm for 1 minute and the filtrate was removed. Washing the sample by AW2 was repeated three times. The QIAamp Mini spin column containing the pellet was put in to another 2 ml tube and centrifuged at 14000 rpm for 1 minute to remove the WA2 and the filtrate with the tube was removed. The QIAamp Mini spin column with the pellet was put in to 2 ml tube, 100 µl AE was added and centrifuged at 8000 rpm for 1 minute for elution of the DNA. It was incubated at room temperature for five minutes and elution was repeated by adding 100 µl AE and centrifuged at the same revolution per minute. The eluted DNA was stored at -35 ºC for further analysis (Bowman et al., 2016).

3.4.3. Analysis of Genomic DNA

The purity, yield and integrity of extracted genomic DNA extracted from local isolates were confirmed using NanoDrop spectrophotometer (Bowman et al., 2016) and agarose gel electrophoresis. The purity and the concentration of the extracted genomic DNA

estimated and evaluated by NanoDrop spectrophotometer (PCR max Lambda). A drop of AE (DNA elution buffer) was used as a blank to optimize and standardize NanoDrop spectrophotometer. Then a drop of extracted genomic DNA was added on a NanoDrop using Micropipette to analyze purity and the concentration of the genomic DNA. The result was observed and recorded for further analysis.

To see the integrity and the quality of genomic DNA, gel electrophoresis was performed (Chen et al., 2017). Agarose (0.5 g) was added in to a flask containing 50 ml 1X TAE buffer with Syber^{R} Safe DNA gel stain (ivitrogen) and melted using microwave for two minutes. The gel was poured in gel electrophoresis rack with comb and left until it was solidified and ready to use. The solidified gel was put in to 1X ATE buffer containing gel electrophoresis rack. The sample DNA (10 µl) and the Quick-load 1kb DNA ladder (New England, BioLabs) were prepared with orange loading dye (6X) (New England, BioLabs) and 10µl from each was loaded in the gel. The gel electrophoresis was set up and run at 90 volt and 80 mA for 35 minutes. The genomic DNA bands were observed under UV light in gel documentation system.

3.4.4. Amplification of 16s rRNA gene

Polymerase Chain Reaction (PCR) is an enzymatic amplification of a specific gene sequence *in vitro* from genomic DNA extracted from samples. The genomic DNA extracted from KDT32 and KGT32 isolates were used as a temple DNA to amplify the region of 16s rRNA gene using 243F and A3R primers. It involves template DNA denaturation, annealing and elongation of primers to amplify a specific gene. For both mixture components and conditions used for amplification 16s rRNA gene from extracted genomic DNA using 243F (5'- GGATGAGCCCGCGGCCTA -3') and A3R (5'- CCAGCCCCACCTTCGAC -3') primers (Monciardini et al., 2002) was described as

follow. The 4 µl of genomic DNA from KDT32 (3.2 ng) and KGT32 (5.10 ng) was used as template DNA and added in master mix (5µl PCR buffer, 1µl dNTPs, 2.50 µl forward primer, 2.50 µl reverse primer, 0.25 µl Taq polymerase, 10 µl Q-solution, 24.75 µl dH_2O). The initial denaturation at 94 ^oC for 4 minutes, 35 cycles of denaturation (at 94 ^oC for 45 seconds), annealing (at 59 ^oC for 45 seconds) and elongation (72 ^oC for 2 minutes) and with 72 ^oC for 10 minutes for final elongation and second hold at 4 ^oC conditions were used. The amplified 16s rRNA gene products were used for further analysis.

3.4.5. Quality and quantity assessment of amplified 16S rRNA gene product

The quality and integrity of amplified 16s rRNA gene product from the genomic DNA of selected isolates were assessed by gel electrophoresis (Chen et al., 2017). Two percent (2%) agarose was prepared in 50 ml of 1X TAE buffer with 5 µl Syber safe DNA staining dye (Ivitrogen) and melted for 2 minutes in microwave. The melted agarose was poured in gel rack with combs and left until solidified. The solidified gel was put in electrophoresis rack filled with 1X TAE buffer. An amount of 10 µl amplified 16s rRNA gene product from samples were prepared with a drop of gel loading dye on sterile film and loaded in the gel well. The Gelpilot Mid-Range ladder (100 bp) was also prepared and loaded to compare the size of the amplified 16s rRNA gene product. The gel electrophoresis was run at 90 volts with 80 mA for 35 minutes. The quality and size of the amplified 16S rRNA gene product was assessed by observing the bands under UV light in gel documentation system.

Moreover, the amplified 16S rRNA gene product concentration and purity was also assessed by NanoDrop spectrophotometer (Bowman et al., 2016). A drop of amplified 16S rRNA product was added on calibrated NanoDrop spectrophotometer. The concentration (µg/ml) and purity (260/280) of the amplified 16s rRNA gene product from each isolate

was analyzed and assessed. The result of the purity and concentration of the amplified 16s rRNA gene product was recorded. The remaining amplified 16S rRNA gene product for each isolate with forward (243F) and reverse (A3R) primers was sent to Macrogen (1105AZ Amsterdam, Netherlands) for purification and sequencing.

3.4.6. 16S rRNA gene sequence assembly and trimming analysis for gene bank submission

The abl file format of 16S rRNA gene sequences was obtained from the Macrogen Company. The quality of the 16s rRNA gene sequence obtained from Macrogen Company was assessed and trimmed by using a combination of both Bioedit software and MEGA 7 software. The abl file of 16s rRNA gene sequence from KDT32 and KGT32 isolates was opened by Bioedit software. The quality of the sequence was assessed by observation of the correct match between the base and base peak (base calling). The mismatch bases with their corresponding base peak (base calling) were edited manually using MEGA 7 software package (Chen et al., 2017).

To obtain the longest feasible high-quality sequences corresponding to each isolate of 16s rRNA gene sequence was opened and assessed using MEGA7 software with default parameters. The poor quality of both ends of a 16s rRNA gene sequence was trimmed to get high quality consensus 16s rRNA gene sequence from each 16s rRNA gene sequence of isolates. The consensus 16s rRNA gene sequence from each potential isolate was saved as FASTA file format and was submitted in GenBank database to get GenBank accession number. The 16s rRNA gene sequence records were directly entered and submitted electronically at (www.ncbi.nlm.nih.gov/projects/ Sequin/) using Sequin tool/program from NCBI (Benson et al., 2012). The accession numbers of 16s rRNA gene sequence for each isolate was received from GenBank database.

3.4.7. Consensus 16S rRNA gene sequence analysis for identification

The consensus 16s rRNA gene sequence from KDT32 and KGT32 isolates were used for size, GC content and sequences similarity search from public nucleotide databases for identification described according to previous report (Yoon et al., 2017). Both NCBI database (https://blast.ncbi.nlm.nih.gov/) and EzTaxon-e (http://eztaxon-e.ezbiocloud.net/) were used to search and retrieve the closest reference sequences found in the database for each consensus 16s rRNA gene sequence obtained from each local isolates.

The size of the gene sequence and GC content of consensus 16S rRNA gene sequence from each isolate was analyzed by using curated (EzTaxon-e) database according to (Chen et al., 2017; O. S. Kim et al., 2012; Yoon et al., 2017). The EzTaxon-e database was opened at (http://eztaxon-e.ezbiocloud.net/) and user account was created after clicking EzBIOCloid's "Identifying" service. FASTA file of consensus sequence from each isolate was uploaded after clinking "Identify single sequence" service. It was run to analyze the size, GC content (%) and sequence completeness of the consensus 16s rRNA gene sequence obtained from each isolate. The total number of hits, sequence identity, sequence completeness and other related information of the reference sequences from the database was also obtained. The closest reference sequences obtained from the database were downloaded as FASTA file format for sequence similarity and molecular phylogenetic analysis.

In addition to EzTaxon-e database, NCBI-BLASTn (https://blast.ncbi.nlm.nih.gov/) based size, GC content and sequence similarity search for each local isolate was also carried out (Chen et al., 2017). Nucleotide BLAST algorithm was opened from NCBI (https://blast.ncbi.nlm.nih.gov/) and FAST file of 16s rRNA gene sequence obtained from

the isolate was uploaded and BLAST search button was clicked with most default parameters. The size and the GC content of the 16s rRNA gene sequence from the local isolates was recorded. The output containing graphic summary, hit table format and alignment was obtained. The result of top hit taxa and their corresponding identity, coverage and nucleotide difference was recorded for analyses and identification of KDT32 and KGT32 isolates.

3.4.8. Molecular phylogenetic tree reconstruction and evaluation

Both character and distance matrices based molecular phylogenetic tree was constructed according to (Cvrčková, 2016; Hall, 2013; Jill Harrison & Langdale, 2006; S. Kumar, Stecher, & Tamura, 2016; Ryan, Adley, & Pembroke, 2013). To determine the taxonomic position and evolutionary relationships, stepwise character and distance matrices based molecular phylogenetic analysis of 16s rRNA gene sequence among the sequence potential local isolates and their closely related reference sequences were performed as described below. The 16S rRNA gene sequence of KDT32, KGT32 isolates and closest reference sequences of genus *Streptomyces* species retrieved from EzTaxon-e databases were aligned and analyzed by CLUSTAL W program (Kurashima, 2016) using MEGA 7 software package. The aligned sequences were saved as MEGA file to run maximum-likelihood and neighbor joining algorithms using MEGA 7 to generate evolutionary character matrices and distance matrices. Jukes Cantrol model was selected to exclude the gaps and positions with ambiguities. The maximum likelihood and neighbor joining original tree was generated and saved for interpretation.

The reliability of the resultant neighbor joining and maximum likelihood tree topologies were assessed and evaluated by bootstrap analysis based on 1000 re-sampling of the neighbor-joining and maximum likelihood dataset, respectively (Chen et al., 2017; Hall,

2013). Both the original tree and bootstrap tree were compared to see the reliability of the tree. Nucleotide substitution rate per site analyzed by both cluster method and character method-based tree was described as scale bar in ratio. Both the resultant original and bootstrap tree constructed by neighbor joining and maximum likelihood algorithms were exported from MEGA 7 software for further analysis and interpretation of the result.

3.5. Data analysis

Data collected from the experiments of the research study were analyzed using descriptive analysis by excel and SPSS version 20 and the mean $\pm$ standard deviation were calculated. The value of the moisture content, pH, total count of CFU/g of collected soil sample, the distributions of recovered isolates were analyzed using Microsoft excels.

The inhibition zone of antagonistic activity of the actinomycetes isolates and antibacterial activity of the metabolites and metabolite mediated silver nanoparticles was analyzed. The mean $\pm$ standard deviation value of inhibition zone of antibacterial activity against selected bacterial pathogens was compared. These comparisons were performed using one-way ANOVA ranked with Tukey's multiple range tests with descriptive analysis by SPSS version 20. The differences were tested on $p<0.05$ (95% probability level) and all statistical values at $p<0.05$ are statistically significantly different.

The sequence similarity of KDT32 and KGT32 16s rRNA gene sequence with reference sequences were described using percentage. The taxonomic position of the isolates were inferred by construction of both character and distance matrices based molecular phylogenetic tree.

3.6. Ethical consideration

The locations for collection of composite soil samples were waste disposal and damping sites that were not involved any endangered or protected species, so it was not needed strict and specific permission. The topology, land structure and the plant and animal diversity of the places were not affected by using appropriate sample collection procedure. Additionally, the antibacterial activity test was done *in vitro* against bacterial human pathogens available in KEMRI. These were not required any specific and strict permission.

CHAPTER FOUR: RESULTS

4.1. Isolation and antibacterial screening of actinomycetes from Thika waste dump soil

4.1.1. Sampling site description, composite soil sample analysis and colony counting

BIDCO Africa Ltd waste disposal site (BAL) has sandy soil with oiled waste. BIDCO Africa Ltd waste dumping site (BAD) sampling site has sandy soil with sewage sludge waste. Bakex Millers Ltd waste dump site (BML) has loam soil with wheat husk. Poly Sack Ltd waste dump site (PLS) has sandy soil with ashes.

Kiganjo waste dumping site one has dark grey sandy with paper bags, wigs and paper wastes dumped on it. Sandy soils with charcoal and ashes are the description of KDT site. Kiganjo waste dump site three (KGT) has grey sandy soil with oiled sludge, broken glasses, avocado peels dumped on it. On the other hand, Mangu' Rhizosphere Site (MRS) has sandy and sticky soil in the shrubs.

A total of 32 composite soil samples were collected from 8 soil sampling sites. The moisture content, pH and number of CFU/g of composite soil varied among eight sampling sites. The highest moisture content was recorded from KDT site (48.65$\pm$7.26 %). Acidic soil was from both BAD (pH 5.74$\pm$0.37) and BML (pH5.95$\pm$0.29), while alkaline soil was from KDT site (pH9.16$\pm$0.24). The highest average colony count (16.75$\pm$7.32 X 10^6 CFU/g) was recorded from KDO site. However, no growth was observed from BAD site (Table 4.1).

Table 4.1: Sampling site description, soil characteristics and number of CFU/g

Sampling sites	Soil type with major dump wastes	GPS coordinates (º)		MC (%)	pH	Average CFU/g (10^6)
		Latitude	Longitude			28 ºC
BAL	Sandy with oiled sludge	-1.051134	37.086341	23.90±1.88	8.12±0.23	1.38±0.95
PSL	Sandy with ashes	-1.050989	37.105572	16.44±1.88	7.71±0.20	1.88±0.25
BAD	Sandy with sludge	-1.051035	37.083528	15.71±6.17	5.74±0.37	0.00±0.00
BML	Loam with wheat husks	-1.053114	37.086125	14.33±6.89	5.95±0.29	3.00±2.16
KDO	Sandy with wigs, paper bags	-1.075395	37.108762	33.23±3.32	8.16±0.15	16.75±7.32
KDT	Sandy with charcoal	-1.075283	37.109494	48.65±7.26	9.16±0.24	1.63±1.25
KGT	Sandy with sludge	-1.079382	37.112864	26.28±3.06	7.70±0.16	1.25±0.50
MRS	Sandy and sticky	-1.076685	37.046068	22.13±0.51	7.60±0.29	1.50±1.73
Starch casein media (Negative control)						0.00±0.00

Key: CFU/g (Colony forming unit per gram of soil), MC (moisture content), º(degree)

4.1.2. Distribution of recovered isolates with respect to sites

A total of 125 isolates were recovered from 7 sites where the largest number of isolates were recovered from KDO (56 (45%)). Except for BAL site, all other five sites had greater number of recovered isolates when compared to control (MRS) site. From a total of 125, 29 (23.2%) isolates showed antibacterial activity against more than one the studied pathogens. All active isolates were recovered from six (PLS, BML, KDO, KDT, KGT and MRS (control)) sites. The greater number of active isolates were recovered from both PLS (8 (28%)) and KDO (8 (28%)) sites when compared to other sites and control or MRS site (3(10%)). There was no active isolate recovered from BAL site (Fig.4.1).

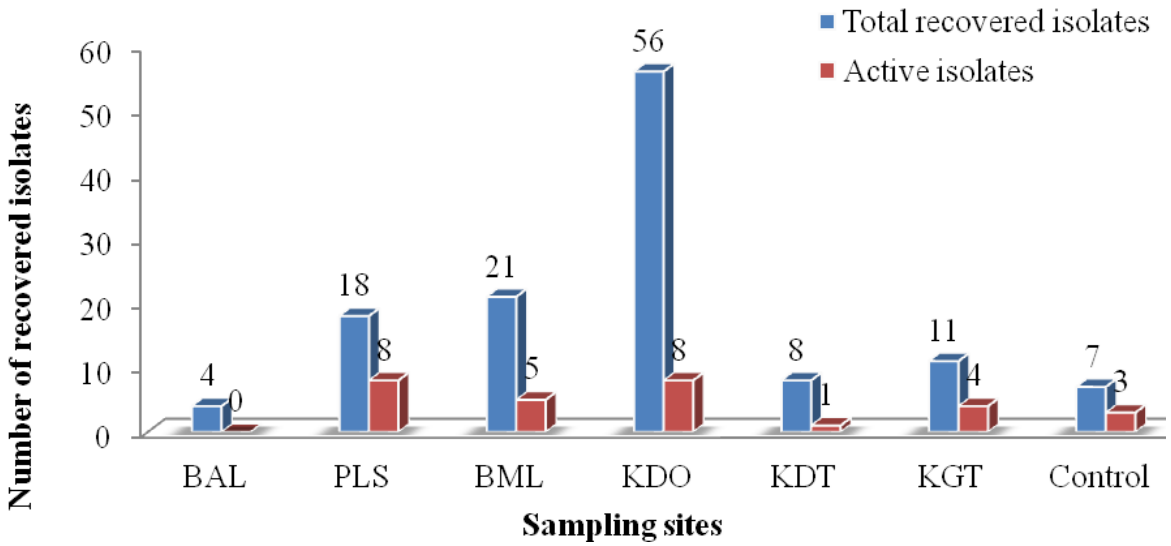

Figure 4.1: Distribution of isolates with respect to sampling site

4.1.3. Distribution of recovered isolates and active isolates with respect to sampling depth

From a total of 125 isolates recovered from 7 sampling sites at different depth, the greater number of isolates (35 (28%)) were recovered from 5-10 cm depth when compared to other depths. According to the result, the active isolates were found in all depth, but the number varied from depth to depth. The greater number of active isolates (9 (31%)) were obtained from a depth of 10-15 cm when compared to other depths (Fig.4.2).

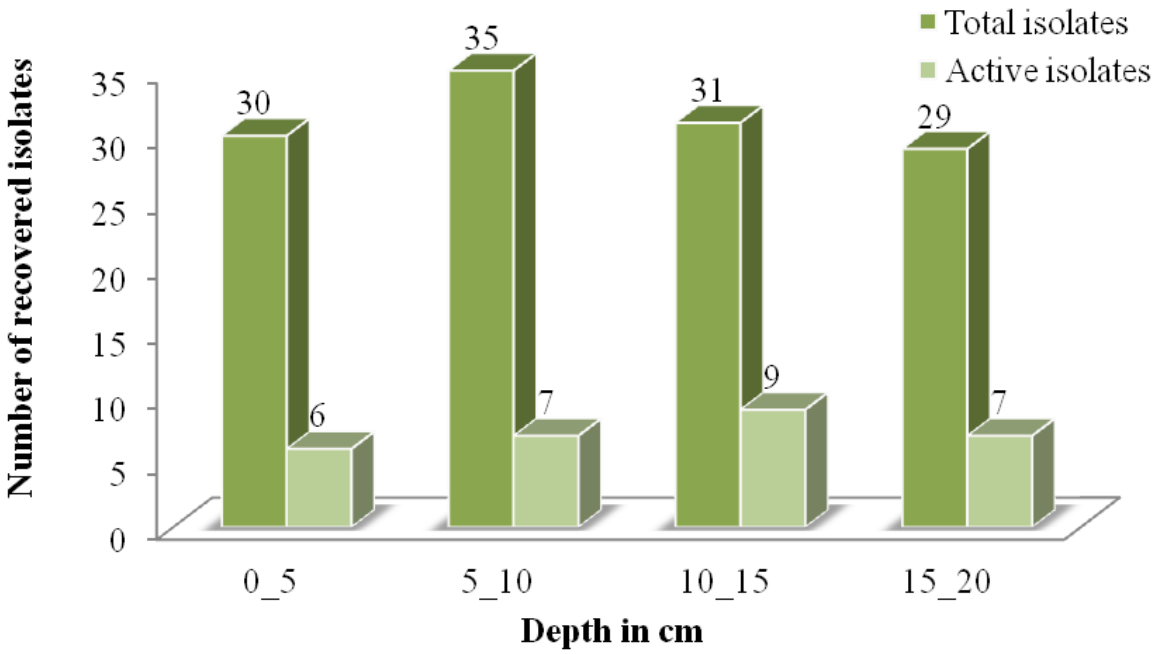

Figure 4.2: Distribution of recovered isolates with respect to depth

4.1.4. Comparison of antibacterial activity of isolates against selected pathogens during primary antibacterial screening

The antibacterial activity of active isolates against selected bacterial pathogens were compared and described using the inhibition zone measured in millimeter. The activity of selected isolates against selected pathogens using streak plate assay were depicted (Fig. 4.3).

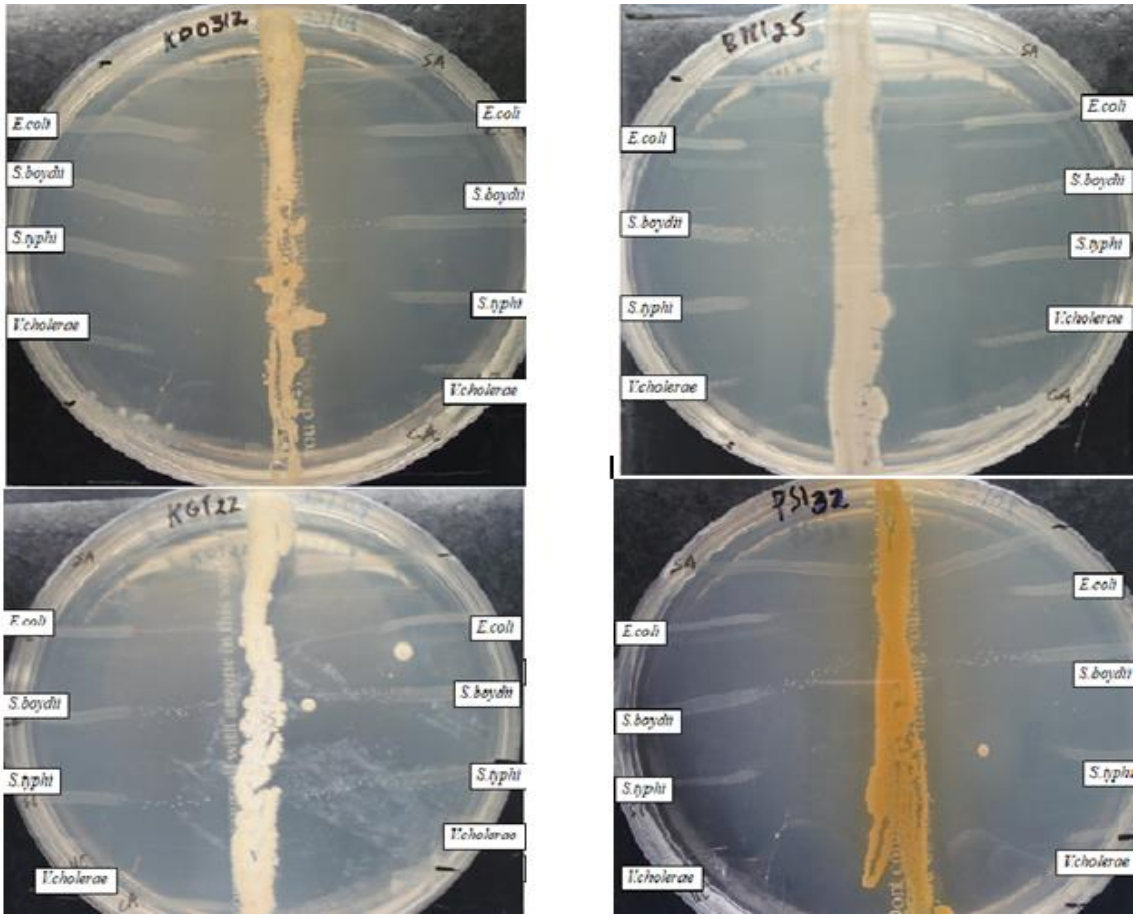

Figure 4.3: Inhibition zone of selected isolates (KDO123, KGT22, BML25 and PLS32) against selected pathogens

The clear distance between the isolate and the pathogen is the inhibition zone

There was a significant difference ($p \leq 0.05$) of inhibition zone among the bioactivity of 29 active isolates against one or more selected bacteria. The highest activity against *E. coli ATCC25922* was recorded for KGT22 (30±0.0 mm) when compared to MRS 44 (2.0±0.0 mm) from control site. In addition, KGT22 active isolate also showed highest anti- *S. typhi* (30.0±0.0 mm) and anti- *V. cholerae* (36.0±1.0 mm) when compared to others. Moreover, *S. boydii* was more inhibited by KGT22 (31.3±0.6 mm) followed by BML44 (26.3±0.6 mm), PLS11 (25.3±0.6 mm) and PLS32 (25.0±0.0mm (Table 4.2).

Table 4.2: The antibacterial activity (mm) of isolates against bacterial pathogens during primary screening

Sites	Active isolates	*ATCC25922*	*S. boydii*	*S. typhi*	*V. cholera*
	PLS11	22.3±0.6^{k}	25.3±0.6^{j}	26.0±0.0^{op}	25.0±0.0^{j}
PLS	PLS13	0.0±0.0^{a}	0.0±0.0^{a}	5.3±0.6^{cde}	10.0±0.0^{c}
	PLS23	16.0±1.0^{ij}	15.7±0.6^{h}	14.7±0.6^{l}	20.0±0.0^{h}
	PLS31	8.3±0.6^{ef}	7.3±0.6^{ef}	7.7±0.6^{fg}	15.3±0.6^{fg}
	PLS32	26.0±1.0^{l}	25.0±0.0^{j}	25.7±0.6^{op}	32.0±0.0^{l}
	PLS34	8.3±0.6^{ef}	5.3±0.6^{cd}	6.7±0.6^{ef}	16.0±1.0^{g}
	PLS41	8.3±0.6^{ef}	5.0±0.0^{c}	7.3±0.6^{f}	19.0±0.0^{h}
	PLS44	9.3±0.6^{fg}	10.3±0.6^{g}	11.0±0.0^{ij}	12.7±0.6^{d}
BML	BML22	10.3±0.6^{g}	10.0±0.0^{g}	11.7±0.6^{jk}	12.3±0.6^{de}
	BML25	22.0±1.0^{k}	21.0±1.0^{i}	20.3±0.6^{m}	22.3±0.6^{i}
	BML26	14.3±0.6^{hi}	0.0±0.0^{a}	15.0±0.0^{l}	14.3±0.6^{f}
	BML44	25.0±0.0^{l}	26.3±0.6^{j}	27.0±0.0^{p}	30.3±0.6^{k}
	BML45	7.3±0.6^{de}	5.3±0.6^{cd}	6.3±0.6^{def}	15.7±0.6^{fg}
KDO	KDO19	6.3±0.6^{cd}	5.0±0.0^{c}	5.7±0.6^{cde}	14.7±0.6^{fg}
	KDO122	5.3±0.6^{c}	7.0±1.0^{de}	4.3±0.6^{c}	10.0±0.0^{c}
	KDO123	13.3±0.6^{h}	20.0±0.0^{i}	20.0±0.0^{m}	30.0±0.0^{k}
	KDO22	16.3±0.6^{j}	20.3±0.6^{i}	21.0±0.0^{mn}	25.3±0.6^{j}
	KDO24	10.3±0.6^{g}	21.0±1.0^{i}	22.0±1.0^{n}	25.3±0.6^{j}
	KDO38	8.3±0.6^{ef}	7.7±0.6^{ef}	9.0±0.0^{gh}	15.3±0.6^{fg}
	KDO310	5.3±0.6^{c}	6.0±0.0^{cde}	12.7±0.6^{k}	20.0±0.0^{h}
	KDO312	16.0±1.0^{ij}	20.0±0.0^{i}	25.0±0.0^{o}	30.0±0.0^{k}
KDT	KDT32	5.3±0.6^{c}	6.3±0.6^{cde}	10.0±0.0^{hi}	11.3±0.6^{cde}
KGT	KGT12	14.3±0.6^{hi}	14.7±0.6^{h}	15.0±0.0^{l}	15.0±0.0^{fg}
	KGT22	30.0±0.0^{m}	31.3±0.6^{k}	30.0±0.0^{q}	36.0±1.0^{m}
	KGT31	10.0±0.0^{fg}	9.0±0.0^{fg}	10.0±0.0^{hi}	11.0±0.0^{cd}
	KGT32	11.0±0.0^{g}	10.3±0.6^{g}	10.3±0.6^{hij}	11.0±1.0^{cd}
MRS	MRS43	5.3±0.6^{c}	6.3±0.6^{cde}	5.0±0.0^{cde}	15.0±0.0^{fg}
(Control)	MRS44	2.0±0.0^{b}	2.3±0.6^{b}	0.0±0.0^{a}	4.0±0.0^{b}
site	MRS45	3.0±0.0^{b}	2.3±0.6^{b}	2.0±0.0^{b}	5.0±0.0^{b}
Negative control		0.0±0.0^{a}	0.0±0.0^{a}	0.0±0.0^{a}	0.0±0.0^{a}

Key: Negative control (Starch casein agar plate and pathogen only), +control (isolate from MRS or control site), 0 (no inhibition zone). Values are means ± standard deviation (SD). The outcomes not sharing a common superscript letter (a<b<c…) in the same column are significantly different at P<0.05.

4.1.5. Antibacterial activity screening of isolates against MRSA and ESBL *E. coli* by streak plate assay

Antibacterial activity of 29 active isolates also tested against clinical MRSA and *E. coli*. From these, only 5 (17.2%) isolates showed antibacterial activity against clinical MRSA and *E. coli* and the bioactivity showed significantly difference (p<0.05) among active isolates. Isolate KDO24 showed highest inhibition zone against MRSA (16.25±0.50 mm) and *E. coli* (26.5±0.58 mm) when compared to others. Isolate KDO24 and KGT12 showed bioactivity against both MRSA and *E. coli* (Table 4.3).

Table 4.3: Bioactivity of isolates against clinical MRSA and *E. coli* using streak plate method

Isolates	MRSA	*ESBL E. coli*
PLS32	14.5 ± 0.58^{cd}	0.0 ± 0.0^{a}
BML25	13.75 ± 1.50^{c}	0.0 ± 0.0^{a}
BML44	8.0 ± 1.83^{b}	0.0 ± 0.0^{a}
KDO24	16.25 ± 0.50^{d}	26.5 ± 0.58^{c}
KGT12	10.5 ± 0.58^{b}	4.0 ± 0.82^{b}
Control	0.0 ± 0.0^{a}	0.0 ± 0.0^{a}

Key: Control (media and clinical pathogen). Values are means± SD. The outcomes not sharing a common superscript letter (a<b<c<…) in the same column are significantly different at P<0.05.

4.1.6. Comparison of number of active isolates in relation to incubation period during secondary screening

The supernatants from 29 isolates were taken at different period of incubation and then tested antibacterial activity against selected bacteria pathogens for further secondary screening. Here only active isolates, susceptible pathogens and the antibacterial producing incubation period were described. From a total of 29 active isolates, supernatants taken from 8-13 days old culture of 11 (37.93%) isolates showed antibacterial activity against one or more selected pathogens. As antibacterial activity of the supernatant taken from 8-day old culture showed the highest number of isolates were active against *E. coli ATCC25922* (11(37.9%)) and *S. typhi* (6 (20.7%)) when compared to others incubation period. However, at 9-day incubation period, the highest number of active isolates against *S. boydii* (6 (20.7%)) were recorded when compared to other incubation periods (Fig 4.4). These results indicate that the number of incubation days influence the production of antibacterial compounds by actinomycete isolates.

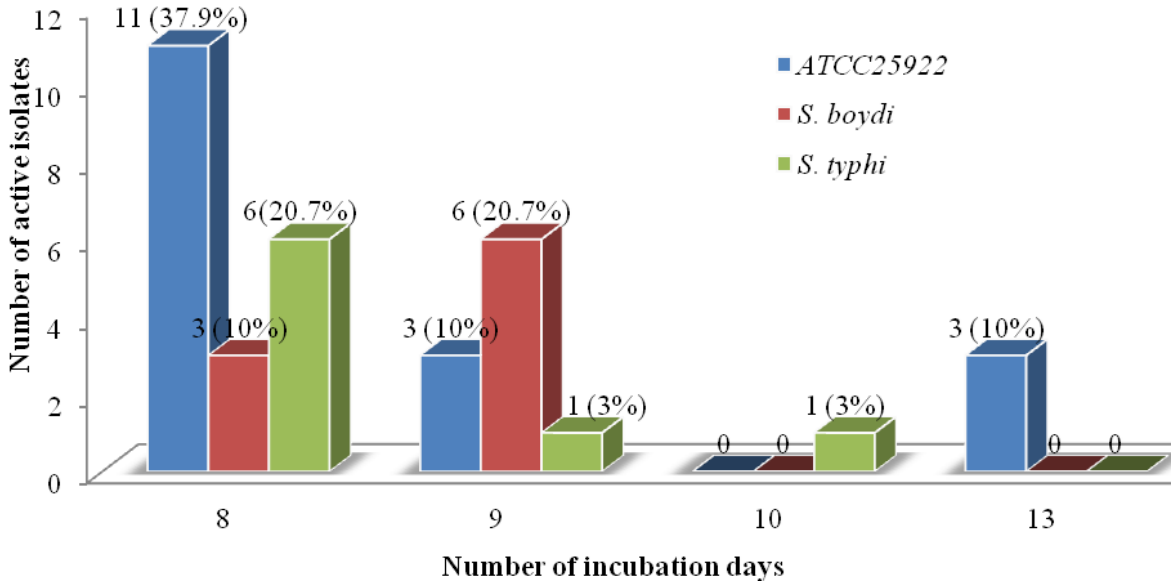

Figure 4.4: Comparison of the number of active isolates against selected pathogens with respect to incubation period

4.1.7. Comparison of antibacterial activity of supernatants with different incubation period of isolates

The antibacterial activities of the supernatant from 29 isolates were tested against selected pathogens by well diffusion assay. The antibacterial active isolates against one or more pathogens and susceptible pathogens are only described on Table 4.4 and Fig.4.5.

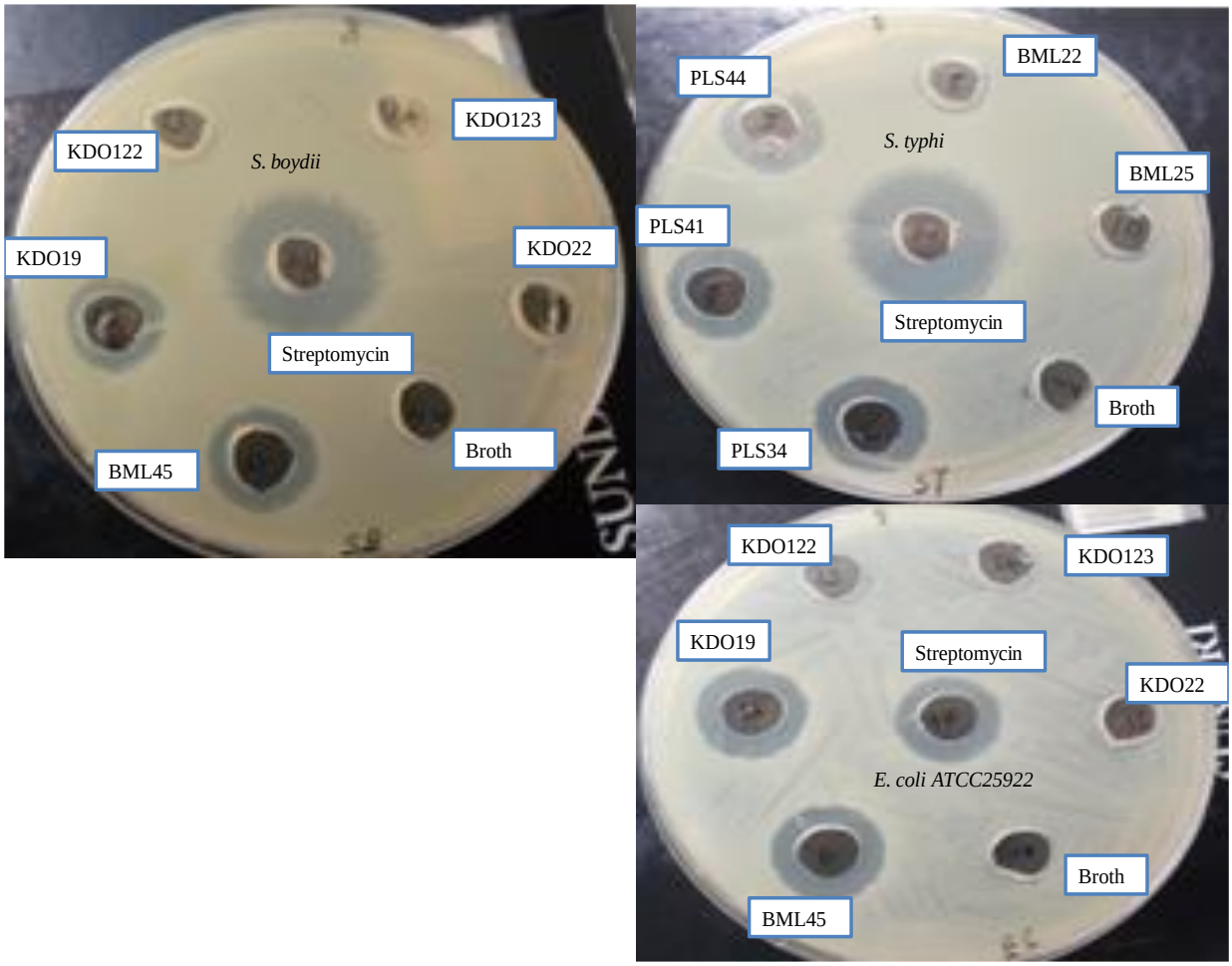

Figure 4.5: Inhibition zone by supernatant from 8-day cultured isolates against selected bacteria pathogens.

The antibacterial activity of the supernatants from 11 (37.93%) isolates were significantly ($p<0.05$) higher from the control. The antibacterial activity of supernatants from isolate BML45 (17±1 mm), KDO19 (17±1 mm) and KDO38 (17±0 mm) showed greater

inhibition against *E. coli ATCC25922* compared to others. Greater inhibition zone against *S. boydii* was recorded by supernatants from both isolate KGT31 (17±1 mm) and KGT32 (17±0 mm) when compared to other supernatant activity. The antibacterial activity of supernatant from isolate PLS34 (17±1 mm) and PLS44 (17±1 mm) showed the highest activity against *S. typhi* when compared to other supernatant activity. However, the activities of the supernatants were lower when compared to streptomycin (24.7±0.6) (Table 4.4).

Table 4.4: Comparison of zone of inhibition of supernatant from selected incubation period

Isolates	***E. coli ATCC25922***	***S. boydii***	***S. typhi***
	At 8 day	At 9 day	At 8 day
PLS13	15 ± 1^{bcd}	0 ± 0^{a}	0 ± 0^{a}
PLS31	16 ± 1^{cd}	0 ± 0^{a}	14 ± 1^{bc}
PLS34	15 ± 1^{bcd}	0 ± 0^{a}	17 ± 1^{d}
PLS41	16 ± 1^{cd}	0 ± 0^{a}	16 ± 1^{cd}
PLS44	14 ± 0^{bc}	0 ± 0^{a}	17 ± 1^{d}
BML45	17 ± 1^{d}	15 ± 0^{b}	0 ± 0^{a}
KDO19	17 ± 1^{d}	16 ± 1^{bc}	0 ± 0^{a}
KDO38	17 ± 0^{d}	15 ± 1^{b}	0 ± 0^{a}
KDT32	15 ± 1^{bcd}	15 ± 0^{b}	0 ± 0^{a}
KGT31	13 ± 1^{b}	17 ± 1^{c}	12 ± 1^{b}
KGT32	15 ± 1^{bcd}	17 ± 0^{c}	13 ± 1^{b}
STP	20.3 ± 0.6^{e}	24 ± 1^{d}	24.7 ± 0.6^{e}
Broth	0 ± 0^{a}	0 ± 0^{a}	0 ± 0^{a}

Key: STP (Streptomycin or positive control), broth (negative control), 0 (no activity observed). Values are means± SD. The outcomes not sharing a common superscript letter (a<b<c<d…) in the same column are significantly different at P<0.05.

4.2. Actinomycetes metabolite mediated synthesis and characterization of antibacterial silver nanoparticles

4.2.1. Visual detection and UV-visible spectra analysis for confirmation of metabolite mediated AgNPs synthesis

According to the result of both visual and UV-vis spectrophotometer detection result confirmed that metabolites from two (18.18%) isolates (KDT32 and KGT32) were successfully synthesized AgNPs. The color change result showed that the visual color change had been started after one-day reaction for both. The mixture reaction between KDT32 metabolite and $AgNO_3$ solution showed a color change from straw solution to dark salmon as shown on figure a (Fig. 4.6a). On the other hand, the mixture reaction between KGT32 metabolite and $AgNO_3$ solution showed a color change from straw to pale golden rod (Fig 4.6b).

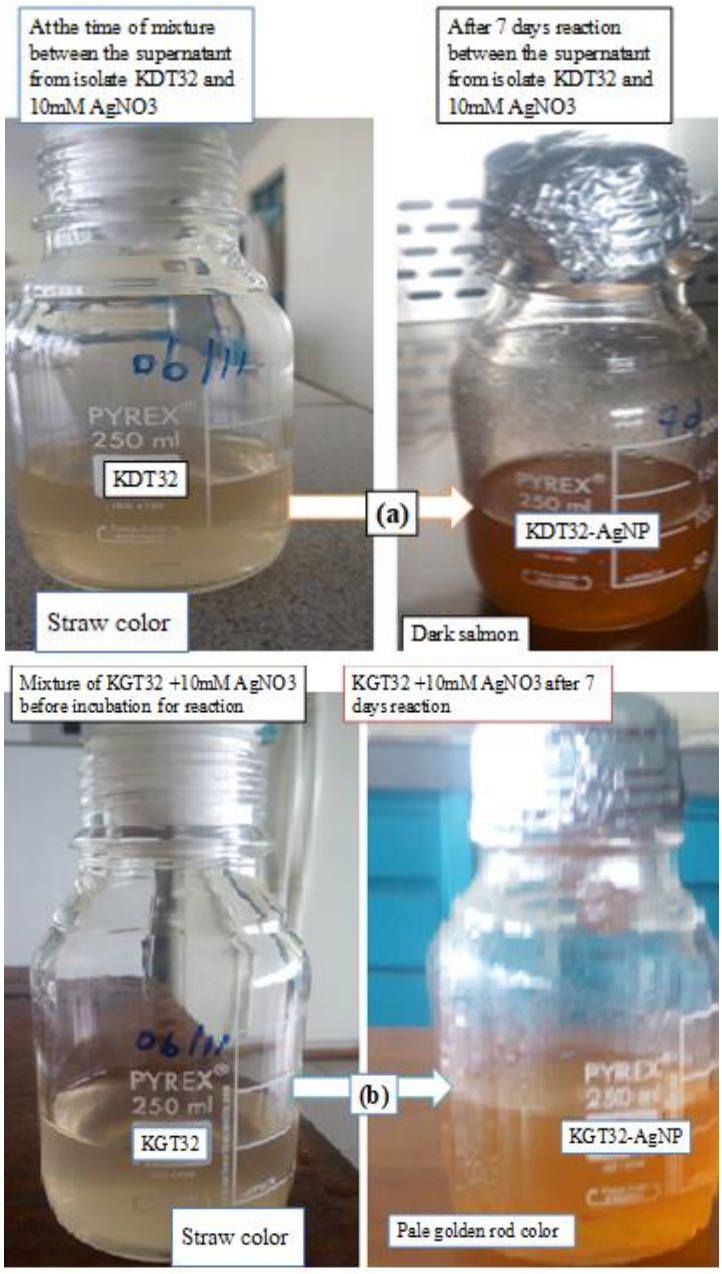

Figure 4.6: Color changes after KDT32-AgNPs (a) and KGT32-AgNPs (b) formation

The KDT32-AgNP and KGT32-AgNP represents a silver nanoparticle formed by KDT32 metabolite (produced by KDT32 isolate) and KGT32 metabolite (produced by KGT32 isolate), respectively.

In addition to visual detection, UV- vis spectrophotometer was used to confirm the presence of characteristic UV-spectra peak between 400-500 nm. As observed from Fig.4.7 and Fig 4.8 there was no any evidence of characteristic absorption peak scanned in

the range of 400-500 nm by the reaction solution at the time of mixing and the controls (metabolite solution and $AgNO_3$ solution). However, the reaction solution of KDT32-$AgNO_3$ and KGT32-$AgNO_3$ after 5-day reaction exhibited a clear excitation or characteristic peak.

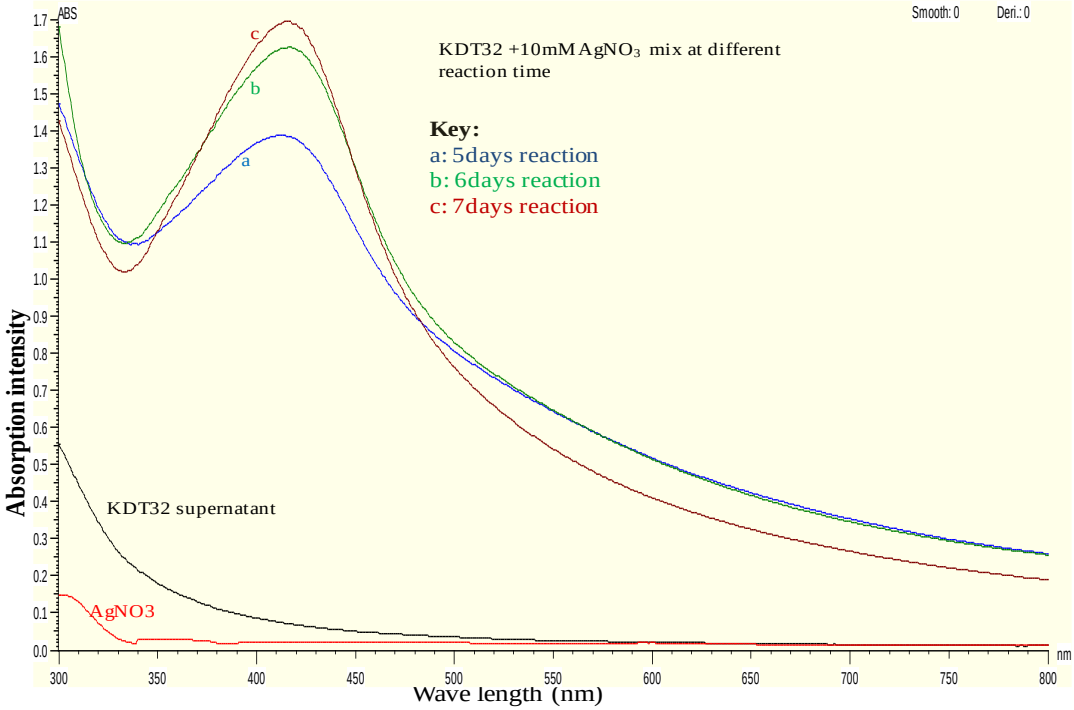

Figure 4.7: Comparison of the KDT32-AgNPs absorption intensity at maximally centered peak wave length at different reaction days

Reaction solution of KDT32-$AgNO_3$ after 5, 6 and 7-day reaction showed a clear characteristic peak centered at 411.5, 416.5 and 415.5 nm, respectively. The formation of KDT32-AgNP was progressively increasing from 1.3872 to 1.6925 of absorption intensity as the reaction time increases from 5 to 7 day, respectively (Fig 4.7). As the result indicate that the highest absorption intensity for KDT32-AgNPs formation (1.6925) was observed at 7-day reaction. These results confirmed that KDT32-AgNPs was formed.

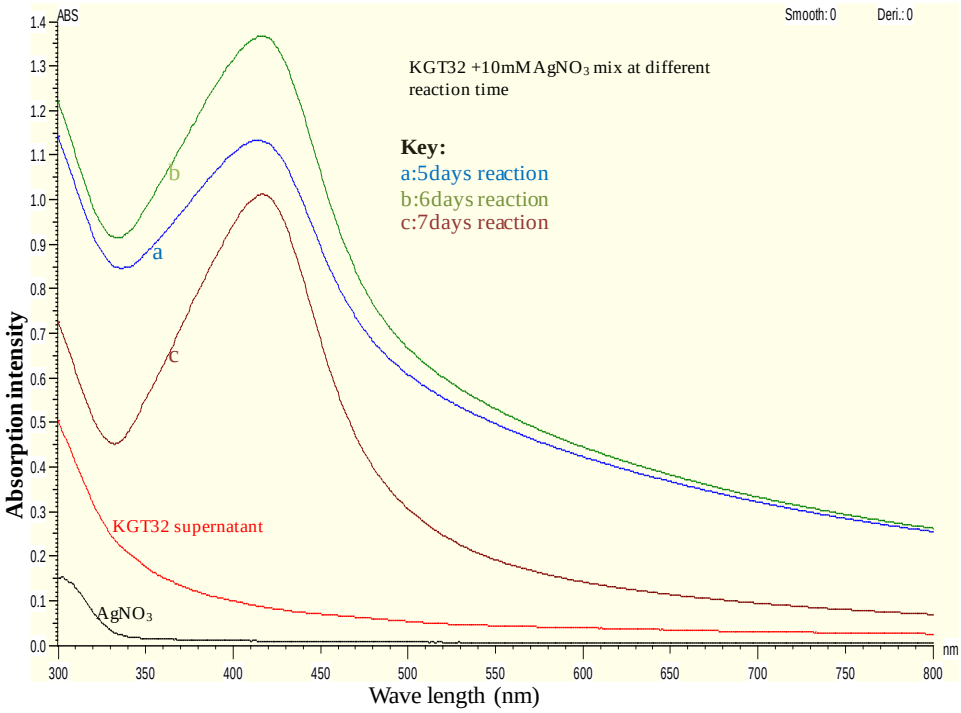

Figure 4.8: Comparison of absorption intensity of KGT32-AgNPs with respect to reaction time

Moreover, as shown on figure 4.3 the KGT32-AgNPs formation also showed an increase in absorption intensity from 1.1331 to 1.3665 and decrease to 1.0114 as the reaction time increases from 5, 6 to 7 days. The position of the maximum spectra peaks also showed with a minor shift center at 413.5 nm, 416 nm to 416.5 nm, respectively (Fig 4.8). Thus, the maximum absorption intensity (1.3665) of KGT32-AgNPs was observed at 6-day reaction centered at 416 nm.

4.2.2. Comparison of the formation of actinomycete metabolite mediated AgNPs

As the result indicate that the highest absorption intensity (concentration) was observed by KDT32-AgNPs when compared to KGT32-AgNPs obtained from reactions of all days. Specifically, as the 7-day reaction result indicated that the highest (1.6925) and lowest (1.0114) absorption intensity was formed by KDT32-AgNPs and KGT32-AgNPs, respectively. Therefore, this result indicates that the synthesis capability of AgNPs using

KDT32 metabolite is better when compared to synthesis of AgNPs using KGT32 metabolite (Fig. 4.9).

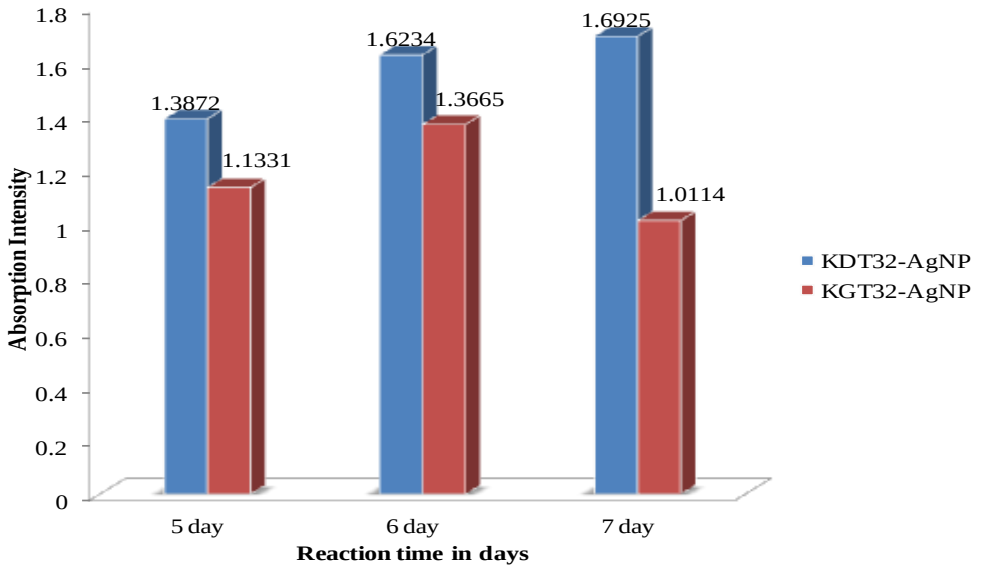

Figure 4.9: The comparison of the absorption intensity of synthesized AgNPs at different reaction time

4.2.3. Identification of bio-molecules used for AgNPs synthesis by FTIR

FTIR analysis was carried out to identify the possible functional groups involved for the reduction of Ag^{+} and capping of AgNPs. The FTIR spectra that have band spectra results of functional groups from metabolites were compared with the FTIR spectra band peaks of synthesized nanoparticles.

FTIR spectra result showed that KDT32 metabolites exhibited the strong and medium absorption bands at different wave number (3774.79, 3386.91, 2090.27, 1638.98, 1396.67, 461.42 cm^{-1}) (Fig 4. 10). The medium and sharp band at 3774.79 cm^{-1} and strong and broad band at 3386.91cm^{-1} corresponds to O-H stretch. The medium band at 2090.27 cm^{-1} and the strong band at 1638.98 cm^{-1} represent –NCS (isothiocyanate) stretch and C=C

(alkenes) stretch, respectively. The medium band at 1396.67 cm^{-1} and strong band at 461.42 cm^{-1} represents organic sulfate stretch and stretching of S-S, respectively.

Furthermore, the FTIR spectra of KDT32-AgNPs showed differences in the position, intensity and shape of bands when compared to the FTIR spectra of KDT32 metabolite. The result suggesting that formation of KDT32-AgNPs was done by the involvement of functional groups or bio-molecules present from KDT32 metabolite. FTIR spectra of KDT32-AgNPs revealed strong band peak at 3391.31, 1640.85 and 445.93 cm^{-1}. The spectra showed strong and broad band at 3391.31 cm^{-1} assigned to the stretching vibration of OH. In addition to this, the strong and sharp band also observed at 1640.85 (stretching of -C=C-) and 445.93 cm^{-1} (stretching of S-S). Thus, the shifting of the band position from 3386.91 to 3391.31 cm^{-1}, 1638.98 to 1640.85 cm^{-1} and 461.42 to 445.93 cm^{-1} may indicate due to the binding of the bio-molecules to the AgNPs (Fig 4.10). These band shift indicated that, OH, C=C and S-S functional groups or bio-molecules from KDT32 metabolite was involved for synthesis of KDT32-AgNPs.

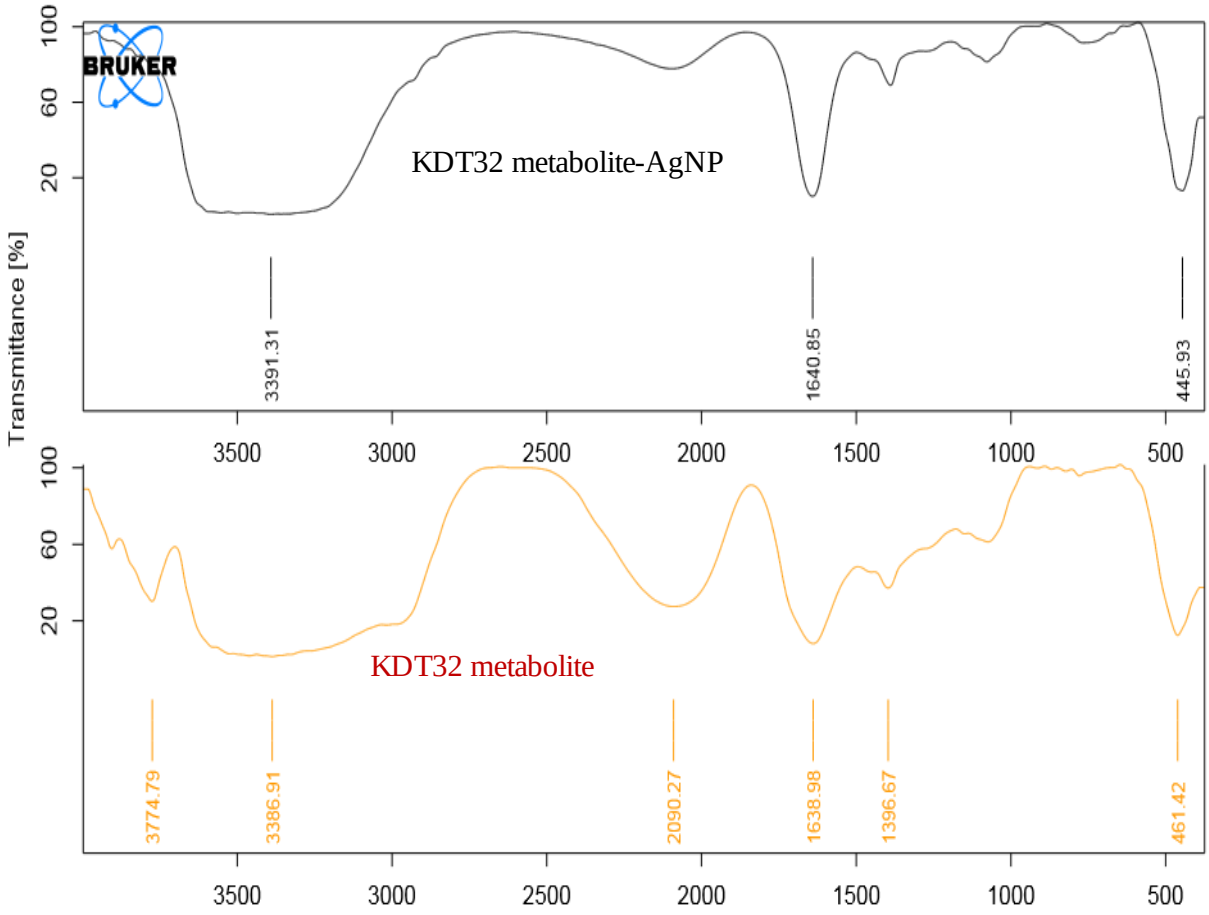

Figure 4.10: FTIR spectra comparison between the KDT32 metabolite and KDT32-AgNPs

The FTIR spectra of KGT32 metabolites showed that there were four strong bands (at 3117.76, 2074.04, 1603.98 and 743.82 cm^{-1}) and one medium band (at1392.90 cm^{-1}) formed. The functional groups assigned for these bands were OH (3117.76 cm^{-1}), -NCS or (isothiocyanate (2074.04 cm^{-1}), C=C (1603.98 cm^{-1}), S-S (1392.90 cm^{-1}) and C-H out plan bending (743.82 cm^{-1}). On the other hand, as FTIR spectra of KGT32-AgNPs indicate that there were three strong bands observed at 3408.99, 1639.15 and 451.60 cm^{-1} that showed shift in band position, shape and intensity as observed on fig.11. The shifting band position from 3117.76 to 3408.99 cm^{-1}, 1603.98 to 1639.15 cm^{-1} and 743.82 to 451.6 cm^{-1} indicate that OH, C=C and C-H functional groups were involved for the reduction of Ag^{+} and capping of KGT32-AgNPs (Fig.4.11).

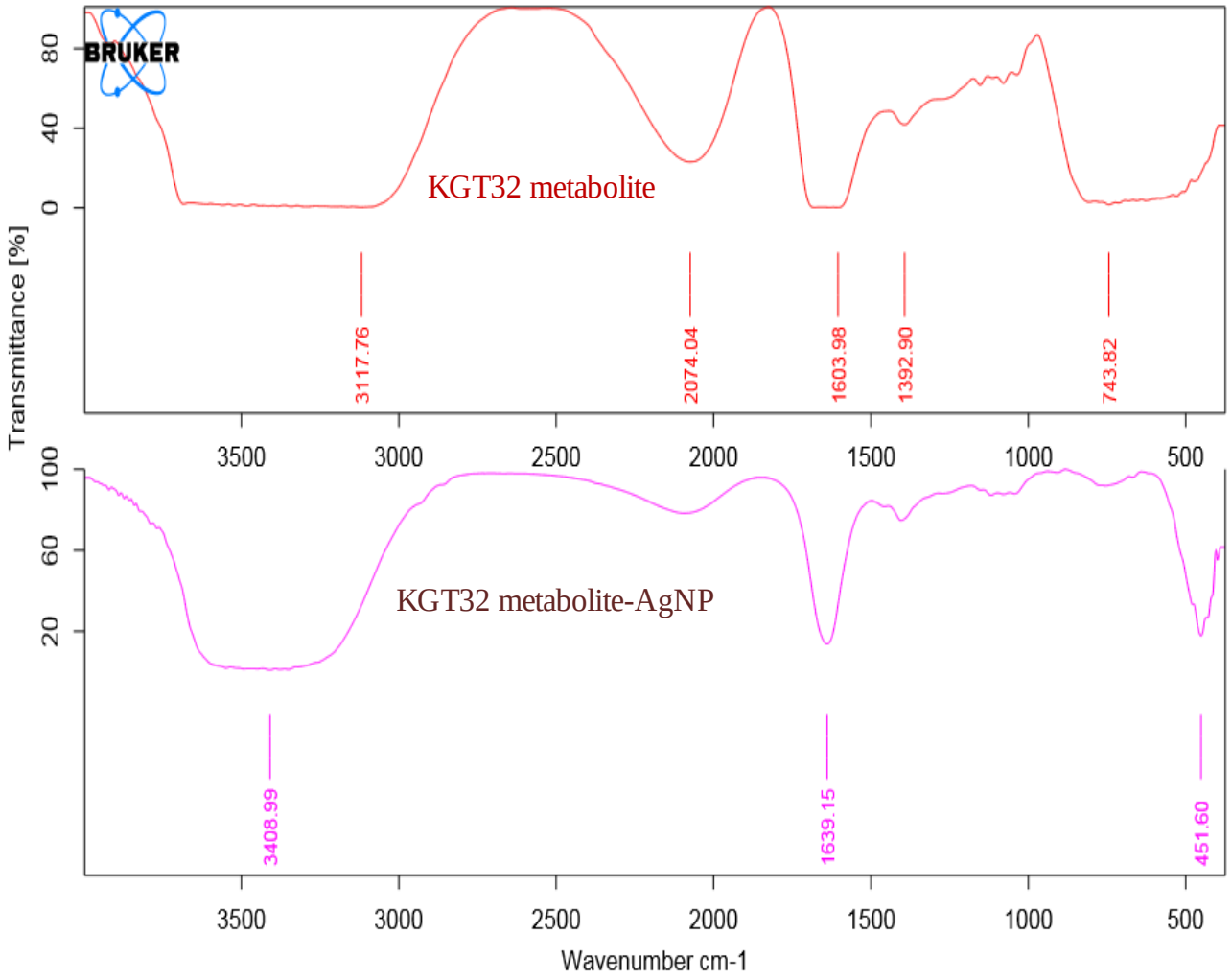

Figure 4.11: The description and comparison of the FTIR spectra of KGT32 metabolite and KGT32-AgNPs

4.2.4. Antibacterial activity evaluation of metabolite mediated AgNPs

The bactericidal activity of KDT32-AgNPs and KGT32-AgNP showed that inhibition zone was greater when compared to their corresponding metabolites and $AgNO_3$. The inhibition zone of KDT32-AgNP and KGT32-AgNPs as well as their corresponding crude extracts showed antibacterial activity against *E. coli* and *S. typhi* (Fig 4.12).

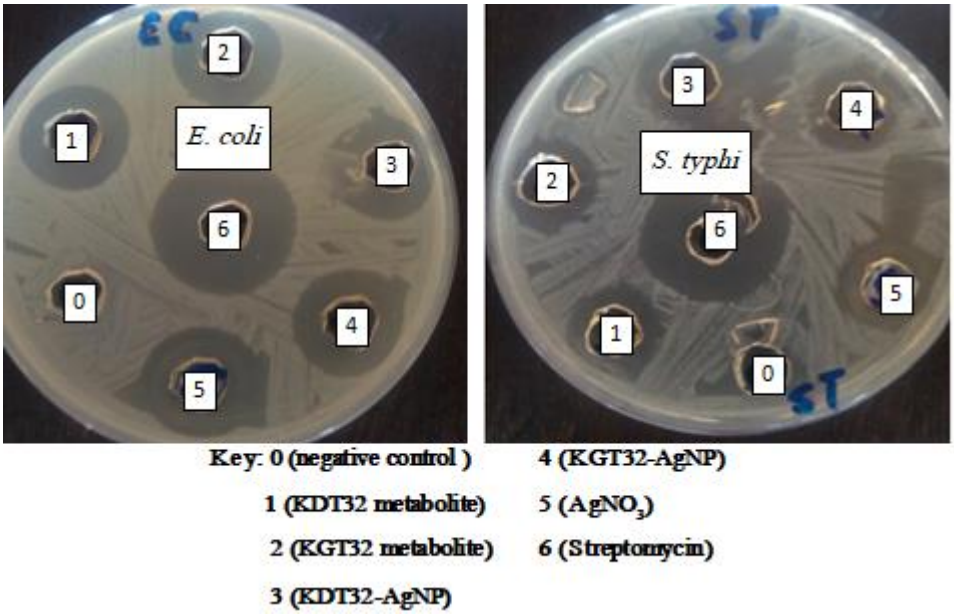

Figure 4.12: Inhibition zone of metabolite mediated silver nanoparticles against *E. coli* and *S. typhi*

However, the crude extract from both isolates and their corresponding synthesized nanoparticle did not show antibacterial activity against *S. boydii*. Particularly, the inhibition zone of KDT32-AgNPs (19.0±1.4 mm) against *S. typhi* was higher that when compared to the antibacterial activity of KDT32 crude extracts (15.0±0.0 mm) (Table 4.5).

Table 4.5: Evaluation of antibacterial activity of actinomycete metabolite mediated AgNPs

Bioactive agents	**Inhibition zone (mm) against bacterial pathogens**		
	E. coli	***S. typhi***	***S. boydii***
KDT32	19.0 ± 1.4^{b}	15.5 ± 0.7^{b}	0 ± 0.0^{a}
KDT32-AgNPs	22.0 ± 1.4^{b}	19.0 ± 1.4^{c}	0 ± 0.0^{a}
KGT32	20.5 ± 0.7^{b}	15.0 ± 0.0^{b}	0 ± 0.0^{a}
KGT32-AgNPs	21.5 ± 0.7^{b}	17.0 ± 0.0^{bc}	0 ± 0.0^{a}
$AgNO_3$	20.5 ± 0.7^{b}	15.5 ± 0.7^{b}	$11.\ 0\pm0.0^{b}$
STP	29.0 ± 1.4^{c}	25.5 ± 0.7^{d}	25.5 ± 0.7^{c}
Negative control	0 ± 0.0^{a}	0 ± 0.0^{a}	0 ± 0.0^{a}

Key: STP (Streptomycin or positive control), sterile water (negative control), 0 (no activity observed). Values are means± SD. The outcomes not sharing a common superscript letter (a<b<c<d…) in the same column are significantly different at P<0.05.

4.3. Identification of isolates KDT32 and KGT32

4.3.1. Phenotypic characterization of isolates KDT32 and KGT32

The color of the colony of KDT32 and KGT32 isolate was light yellow and white, respectively. The shapes and texture of the colony of both isolates were circular and hard to scoop, respectively. The gram reaction result showed that both KDT32 and KGT32 isolates were gram positive bacteria and their cellular shape were filamentous. Catalase test result revealed that both isolates could produce catalase enzyme (Fig 4.13 and Table 4.6).

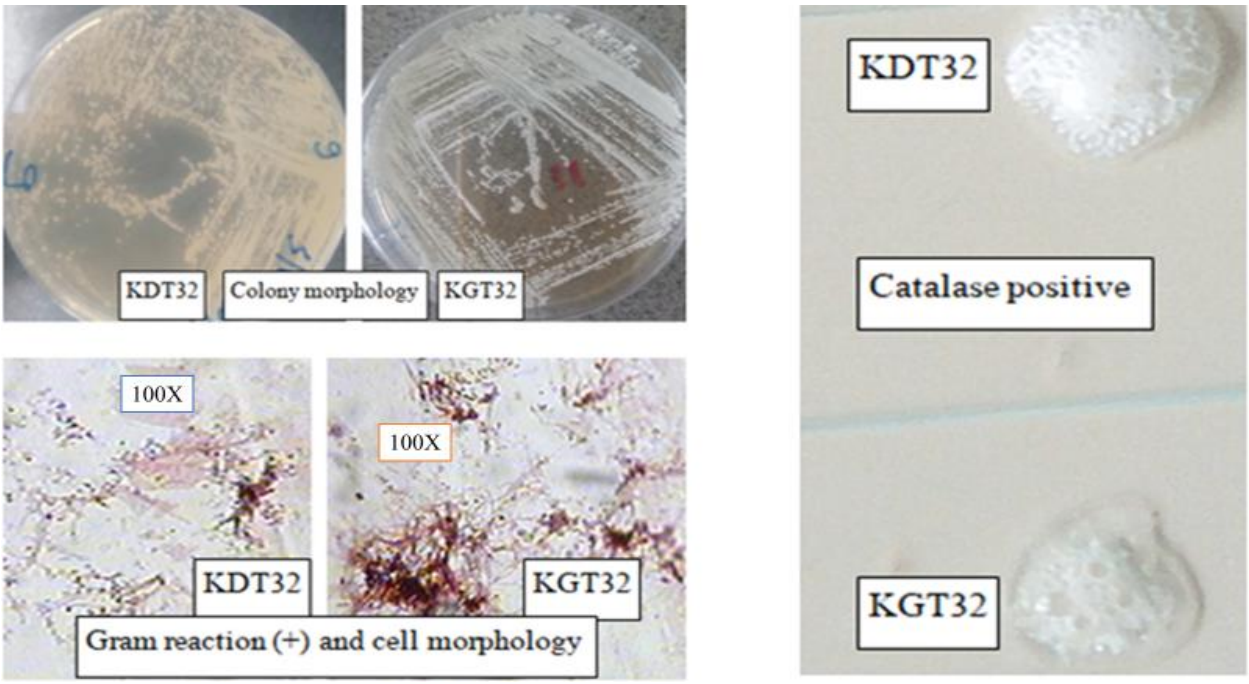

Figure 4.13: Morphology and catalase activity of KDT32 and KGT32 isolates

The colony morphology and cell morphology of the local isolates observed on the figure was three-day old culture on starch casein agar plate and at100X magnification power of the compound light microscope, respectively. The catalase positive result observed on the

figure is a photo taken after few seconds of the reaction between the three-day old local isolates and 3% hydrogen peroxide

As the pH tolerance test result showed that KDT32 and KGT32 isolate could grows in a range of 6-12 and 5-12 pH, respectively. Moreover, as salt tolerance test result showed that KDT32 and KGT32 isolate could grows in a range of 0-7% and 0-9% NaCL salt concentration (Table 4.6).

Table 4.6: Morphological and growth condition-based characterization of KDT32 and KGT32 isolates

Characteristics		**KDT32**	**KGT32**
Colony	Color	Light yellow	White
	Shape (form)	Circular	Circular
	Texture	Hard to scoop	Hard to scoop
Gram reaction		Positive	Positive
Cell shape		Filamentous	Filamentous
Catalase test		Positive	Positive
Growth pH range		6-12	5-12
Growth salt range		0-7%	0-9%

4.3.2. Analysis of amplified 16s rRNA gene product

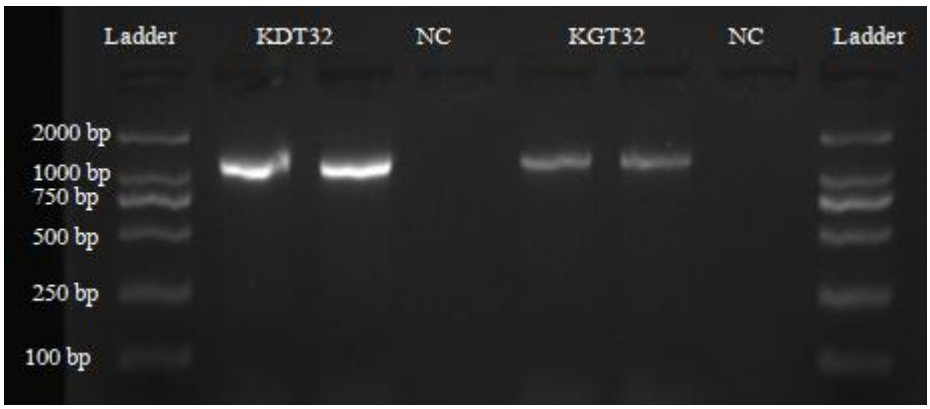

Figure 4.14: Amplified 16s rRNA gene product of KDT32 and KGT 32 isolates

Ladder (Gel pilot mid-range ladder, 100 lanes, six fragments, 100 to 2000 bp, QIAGEN), NC (negative control, master mix)

The quality and purity of the amplified 16s rRNA gene product of KDT32 and KGT32 isolates are described on fig 4.14 and table 4.7. As observed on fig 4.14, the gel result showed that the band of amplified product of KDT32 and KGT32 was between 1000 and 2000 bp size. Moreover, Nanodrop spectrophotometer result analysis showed that the concentration and the purity of the amplified product of KDT32 and KGT32 are described (Table 4.7). The amplified gene products with the primers were sent to Macrogen Company for purification and sequencing of 16S rRNA gene.

Table 4.7: Purity and concentration analysis of the amplified product used for sequencing

Amplified source	**Product**	**Concentration (µg/ml)**	**Purity (260/280)**
KDT32		320.5	1.623
KGT32		428.48	1.889

4.3.3. 16s rDNA sequence analysis for identification of KDT32 and KGT32 isolates

The length of the partial 16s rRNA gene sequence of KDT32 and KGT32 was 986 and 948 bp, respectively. The calculated GC (%) content from KDT32 and KGT32 16s rRNA gene sequence was 58.32% and 59.6%, respectively (Table 4.8).

NCBI-BLASTn search using default settings showed that there were multiple hits to members of Streptomyces species for both KDT32 and KGT32 isolate sequences. From this multiple hits, the first top hit and most closet match for KDT32 16s rRNA gene sequences was Streptomyces sp. MBE174 (AB873097.1). Moreover, KDT32 16s rRNA gene sequence similarity and coverage against Streptomyces sp. MBE174 was 99 % and 100 %, respectively (Table 4.8). The pair wise alignment result showed KDT32 sequence

was almost aligned base to base with Streptomyces sp. MBE174 (AB873097.1) sequence between the subject coordinate of 417 and 1401. However, there was a gap observed at 1378 coordinate (nucleotide position) of Streptomyces sp. MBE174 sequence and T nucleotide was seen at coordinate 961 of the KDT32 sequence (Fig 4.15).

```
Query  1     CTTTCAGCAGGGAAGAAGCGAGAGTGACGGTACCTGCAGAAGAAGCGCCGGCTAACTACG  60
             ||||||||||||||||||||||||||||||||||||||||||||||||||||||||||||
Sbjct  417   CTTTCAGCAGGGAAGAAGCGAGAGTGACGGTACCTGCAGAAGAAGCGCCGGCTAACTACG  476
Query  61    TGCCAGCAGCCGCGGTAATACGTAGGGCGCAAGCGTTGTCCGGAATTATTGGGCGTAAAG  120
             ||||||||||||||||||||||||||||||||||||||||||||||||||||||||||||
Sbjct  477   TGCCAGCAGCCGCGGTAATACGTAGGGCGCAAGCGTTGTCCGGAATTATTGGGCGTAAAG  536
Query  121   AGCTCGTAGGCGGCTTGTCGCGTCGGTTGTGAAAGCCCGGGGCTTAACCCCGGGTCTGCA  180
             ||||||||||||||||||||||||||||||||||||||||||||||||||||||||||||
Sbjct  537   AGCTCGTAGGCGGCTTGTCGCGTCGGTTGTGAAAGCCCGGGGCTTAACCCCGGGTCTGCA  596
Query  181   GTCGATACGGGCAGGCTAGAGTTCGGTAGGGGAGATCGGAATTCCTGGTGTAGCGGTGAA  240
             ||||||||||||||||||||||||||||||||||||||||||||||||||||||||||||
Sbjct  597   GTCGATACGGGCAGGCTAGAGTTCGGTAGGGGAGATCGGAATTCCTGGTGTAGCGGTGAA  656
Query  241   ATGCGCAGATATCAGGAGGAACACCGGTGGCGAAGGCGGATCTCTGGGCCGATACTGACG  300
             ||||||||||||||||||||||||||||||||||||||||||||||||||||||||||||
Sbjct  657   ATGCGCAGATATCAGGAGGAACACCGGTGGCGAAGGCGGATCTCTGGGCCGATACTGACG  716
Query  301   CTGAGGAGCGAAAGCGTGGGGAGCGAACAGGATTAGATACCCTGGTAGTCCACGCCGTAA  360
             ||||||||||||||||||||||||||||||||||||||||||||||||||||||||||||
Sbjct  717   CTGAGGAGCGAAAGCGTGGGGAGCGAACAGGATTAGATACCCTGGTAGTCCACGCCGTAA  776
Query  361   ACGGTGGGCACTAGGTGTGGGCAACATTCCACGTTGTCCGTGCCGCAGCTAACGCATTAA  420
             ||||||||||||||||||||||||||||||||||||||||||||||||||||||||||||
Sbjct  777   ACGGTGGGCACTAGGTGTGGGCAACATTCCACGTTGTCCGTGCCGCAGCTAACGCATTAA  836
Query  421   GTGCCCCGCCTGGGGAGTACGGCCGCAAGGCTAAAACTCAAAGGAATTGACGGGGGCCCG  480
             ||||||||||||||||||||||||||||||||||||||||||||||||||||||||||||
Sbjct  837   GTGCCCCGCCTGGGGAGTACGGCCGCAAGGCTAAAACTCAAAGGAATTGACGGGGGCCCG  896
Query  481   CACAAGCGGCGGAGCATGTGGCTTAATTCGACGCAACGCGAAGAACCTTACCAAGGCTTG  540
             ||||||||||||||||||||||||||||||||||||||||||||||||||||||||||||
Sbjct  897   CACAAGCGGCGGAGCATGTGGCTTAATTCGACGCAACGCGAAGAACCTTACCAAGGCTTG  956
Query  541   ACATACACCGGAAAGCATTAGAGATAGTGCCCCCCTTGTGGTCGGTGTACAGGTGGTGCA  600
             ||||||||||||||||||||||||||||||||||||||||||||||||||||||||||||
Sbjct  957   ACATACACCGGAAAGCATTAGAGATAGTGCCCCCCTTGTGGTCGGTGTACAGGTGGTGCA  1016
Query  601   TGGCTGTCGTCAGCTCGTGTCGTGAGATGTTGGGTTAAGTCCCGCAACGAGCGCAACCCT  660
             ||||||||||||||||||||||||||||||||||||||||||||||||||||||||||||
```

```
Sbjct  1017  TGGCTGTCGTCAGCTCGTGTCGTGAGATGTTGGGTTAAGTCCCGCAACGAGCGCAACCCT  1076
Query  661   TGTCCCGTGTTGCCAGCAGGCCCTTGTGGTGCTGGGGACTCACGGGAGACCGCCGGGGTC  720
              ||||||||||||||||||||||||||||||||||||||||||||||||||||||||||||
Sbjct  1077  TGTCCCGTGTTGCCAGCAGGCCCTTGTGGTGCTGGGGACTCACGGGAGACCGCCGGGGTC  1136
Query  721   AACTCGGAGGAAGGTGGGGACGACGTCAAGTCATCATGCCCCTTATGTCTTGGGCTGCAC  780
              ||||||||||||||||||||||||||||||||||||||||||||||||||||||||||||
Sbjct  1137  AACTCGGAGGAAGGTGGGGACGACGTCAAGTCATCATGCCCCTTATGTCTTGGGCTGCAC  1196
Query  781   ACGTGCTACAATGGCCGGTACAATGAGCTGCGATACCGTGAGGTGGAGCGAATCTCAAAA  840
              ||||||||||||||||||||||||||||||||||||||||||||||||||||||||||||
Sbjct  1197  ACGTGCTACAATGGCCGGTACAATGAGCTGCGATACCGTGAGGTGGAGCGAATCTCAAAA  1256
Query  841   AGCCGGTCTCAGTTCGGATTGGGGTCTGCAACTCGACCCCATGAAGTCGGAGTCGCTAGT  900
              ||||||||||||||||||||||||||||||||||||||||||||||||||||||||||||
Sbjct  1257  AGCCGGTCTCAGTTCGGATTGGGGTCTGCAACTCGACCCCATGAAGTCGGAGTCGCTAGT  1316
Query  901   AATCGCAGATCAGCATTGCTGCGGTGAATACGTTCCCGGGCCTTGTACACACCGCCCGTC  960
              ||||||||||||||||||||||||||||||||||||||||||||||||||||||||||||
Sbjct  1317  AATCGCAGATCAGCATTGCTGCGGTGAATACGTTCCCGGGCCTTGTACACACCGCCCGTC  1376
Query  961   ATCGTCACGAAAGTCGGTAACACCCG  986
              | |||||||||||||||||||||||
Sbjct  1377  A-CGTCACGAAAGTCGGTAACACCCG  1401
```

Figure 4.15: The BLAST analysis between the KDT32 (query) sequence and Streptomyces sp. MBE174 (AB873097.1) (sbjct=subject) sequence from NCBI database The nucleotide with red color indicated in the figure showed the difference between the query (KDT32) and the subject (*Streptomyces sp. MBE174* (AB873097.1)) sequence

After NCBI-BLASTn search of KGT32 isolate sequence against the nucleotide database, 100 hits having 99 % similarity from the genus *Streptomyces* members were recorded. From these, *Streptomyces sp. strain SP4-AB2* (MH013316.1) was the first top closest species for KGT32 isolates when compared to other multiple hits. The KGT32 16s rRNA gene sequence was aligned with in 28-975 nucleotide position (coordinate) of *Streptomyces sp. strain SP4-AB2* sequence. From this, KGT32 16s rRNA gene sequence similarity and coverage against *Streptomyces sp. strain SP4-AB2* 16s rRNA gene sequence

was 99 % (946/948) and 100 %, respectively. The statistics of this alignment indicate that there were 946 nucleotides aligned out of 948 (Table 4.8).

Table 4.8: Closest matched species from the NCBI/GenBank database against 16S rDNA sequences of KDT32 and KGT32 isolates

Isolate	Accession number	Length (bp)*	GC* content	Closest match	Accession number	Identity	Query coverage	E-Value
KDT32	MH301089	986	58.32%	*Streptomyces sp. MBE174*	AB873097.1	99% (985/986)	100%	0.00
KGT32	MH301090	948	59.6%	*Streptomyces sp. strain SP4-AB2*	MH013316.1	99% (946/948)	100%	0.00

Key: **"Isolate"** the code of our strain isolated from Thika waste damped soil **"Length (bp)*"** the total size of the 16s rRNA gene sequence obtained from the isolate; **"GC* content"** the ratio of Guanine and cytosine base pairs from the total sequence of our isolate: **Star (*)** indicates that the results were confirmed from both EzTaxon-e and NCBI-BLASTn databases; **"Closest match"** the most similar species from the database to our isolate **"Accession number"** 16s rRNA gene sequence ID of the most similar species **"Identity"** the similarity of 16s rRNA gene sequence of our isolate and the closet match species sequence **"Query coverage"** the ratio of the sequence from our isolate aligned to the closest species obtained from the database

Thus, there are two nucleotides that make mismatch (2/948) between the 16s rRNA gene sequence KGT32 and *Streptomyces sp. strain SP4-AB2*. The first mismatch was observed between G at coordinate 159 of KGT32 sequence and A at coordinate 186 of *Streptomyces sp. strain SP4-AB2* sequence. The second mismatch was seen between A at coordinate 866 of the KGT32 sequence and G at coordinate 893 of *Streptomyces sp. strain SP4-AB2*

sequence (Fig 4.16). Thus, these differences showed that transition type of mismatch was happened between the sequence of KGT32 and *Streptomyces sp. strain SP4-AB2*.

```
Query  1    GAGGGCGACCGGCCACACTGGGACTGAGACACGGCCCAGACTCCTACGGGAGGCAGCAGT  60
            ||||||||||||||||||||||||||||||||||||||||||||||||||||||||||||
Sbjct  28   GAGGGCGACCGGCCACACTGGGACTGAGACACGGCCCAGACTCCTACGGGAGGCAGCAGT  87
Query  61   GGGGAATATTGCACAATGGGCGAAAGCCTGATGCAGCGACGCCGCGTGAGGGATGACGGC  120
            ||||||||||||||||||||||||||||||||||||||||||||||||||||||||||||
Sbjct  88   GGGGAATATTGCACAATGGGCGAAAGCCTGATGCAGCGACGCCGCGTGAGGGATGACGGC  147
Query  121  CTTCGGGTTGTAAACCTCTTTCAGCAGGGAAGAAGCGAGAGTGACGGTACCTGCAGAAGA  180
            |||||||||||||||||||||||||||||||||||| ||||||||||||||||||||||
Sbjct  148  CTTCGGGTTGTAAACCTCTTTCAGCAGGGAAGAAGCGAAAGTGACGGTACCTGCAGAAGA  207
Query  181  AGCGCCGGCTAACTACGTGCCAGCAGCCGCGGTAATACGTAGGGCGCAAGCGTTGTCCGG  240
            ||||||||||||||||||||||||||||||||||||||||||||||||||||||||||||
Sbjct  208  AGCGCCGGCTAACTACGTGCCAGCAGCCGCGGTAATACGTAGGGCGCAAGCGTTGTCCGG  267
Query  241  AATTATTGGGCGTAAAGAGCTCGTAGGCGGCTTGTCACGTCGGTTGTGAAAGCCCGGGGC  300
            ||||||||||||||||||||||||||||||||||||||||||||||||||||||||||||
Sbjct  268  AATTATTGGGCGTAAAGAGCTCGTAGGCGGCTTGTCACGTCGGTTGTGAAAGCCCGGGGC  327
Query  301  TTAACCCCGGGTCTGCAGTCGATACGGGCAGGCTAGAGTTCGGTAGGGGAGATCGGAATT  360
            ||||||||||||||||||||||||||||||||||||||||||||||||||||||||||||
Sbjct  328  TTAACCCCGGGTCTGCAGTCGATACGGGCAGGCTAGAGTTCGGTAGGGGAGATCGGAATT  387
Query  361  CCTGGTGTAGCGGTGAAATGCGCAGATATCAGGAGGAACACCGGTGGCGAAGGCGGATCT  420
            ||||||||||||||||||||||||||||||||||||||||||||||||||||||||||||
Sbjct  388  CCTGGTGTAGCGGTGAAATGCGCAGATATCAGGAGGAACACCGGTGGCGAAGGCGGATCT  447
Query  421  CTGGGCCGATACTGACGCTGAGGAGCGAAAGCGTGGGGAGCGAACAGGATTAGATACCCT  480
            ||||||||||||||||||||||||||||||||||||||||||||||||||||||||||||
Sbjct  448  CTGGGCCGATACTGACGCTGAGGAGCGAAAGCGTGGGGAGCGAACAGGATTAGATACCCT  507
Query  481  GGTAGTCCACGCCGTAAACGGTGGGCACTAGGTGTGGGCAACATTCCACGTTGTCCGTGC  540
            ||||||||||||||||||||||||||||||||||||||||||||||||||||||||||||
Sbjct  508  GGTAGTCCACGCCGTAAACGGTGGGCACTAGGTGTGGGCAACATTCCACGTTGTCCGTGC  567
Query  541  CGCAGCTAACGCATTAAGTGCCCCGCCTGGGGAGTACGGCCGCAAGGCTAAAACTCAAAG  600
            ||||||||||||||||||||||||||||||||||||||||||||||||||||||||||||
Sbjct  568  CGCAGCTAACGCATTAAGTGCCCCGCCTGGGGAGTACGGCCGCAAGGCTAAAACTCAAAG  627
Query  601  GAATTGACGGGGGCCCGCACAAGCGGCGGAGCATGTGGCTTAATTCGACGCAACGCGAAG  660
            ||||||||||||||||||||||||||||||||||||||||||||||||||||||||||||
Sbjct  628  GAATTGACGGGGGCCCGCACAAGCGGCGGAGCATGTGGCTTAATTCGACGCAACGCGAAG  687
Query  661  AACCTTACCAAGGCTTGACATACACCGGAAACGTCTGGAGACAGGCGCCCCCTTGTGGTC  720
            ||||||||||||||||||||||||||||||||||||||||||||||||||||||||||||
```

```
Sbjct  688  AACCTTACCAAGGCTTGACATACACCGGAAACGTCTGGAGACAGGCGCCCCCTTGTGGTC  747
Query  721  GGTGTACAGGTGGTGCATGGCTGTCGTCAGCTCGTGTCGTGAGATGTTGGGTTAAGTCCC  780
            ||||||||||||||||||||||||||||||||||||||||||||||||||||||||||||
Sbjct  748  GGTGTACAGGTGGTGCATGGCTGTCGTCAGCTCGTGTCGTGAGATGTTGGGTTAAGTCCC  807
Query  781  GCAACGAGCGCAACCCTTGTCCCGTGTTGCCAGCAGGCCCTTGTGGTGCTGGGGACTCAC  840
            ||||||||||||||||||||||||||||||||||||||||||||||||||||||||||||
Sbjct  808  GCAACGAGCGCAACCCTTGTCCCGTGTTGCCAGCAGGCCCTTGTGGTGCTGGGGACTCAC  867
Query  841  GGGAGACCGCCGGGGTCAACTCGGAAGAAGGTGGGGACGACGTCAAGTCATCATGCCCCT  900
            |||||||||||||||||||||||| ||||||||||||||||||||||||||||||||||
Sbjct  868  GGGAGACCGCCGGGGTCAACTCGGAGGAAGGTGGGGACGACGTCAAGTCATCATGCCCCT  927
Query  901  TATGTCTTGGGCTGCACACGTGCTACAATGGGCCGGTACAATGAGCTG  948
            |||||||||||||||||||||||||||||||||||||||||||||||
Sbjct  928  TATGTCTTGGGCTGCACACGTGCTACAATGGGCCGGTACAATGAGCTG  975
```

Figure 4.16: The BLAST analysis between the KGT32 (query) sequence and Streptomyces sp. strain SP4-AB2 (sbjct=subject) sequence from NCBI database

The nucleotide with red color indicates in the figure showed the difference between the query (KGT32) and the subject (*Streptomyces sp. strain SP4-AB2*) sequence

According to EzTaxon-e server search result confirmed that 30 *Streptomyces* species showed between 99.19 % - 99.8 % sequence similarities to KDT32 isolate. Specifically, *Streptomyces lavenduligriseus* strain *NRRL ISP-5487*^{T} is the first top closest hit that showed 99.8% sequence similarity to 16s rRNA gene sequence of KDT32 isolate (Table 4.9). In this case, 985/986 bp of 16s rRNA gene sequence of KDT32 was aligned with in 403-1388 bp range of 16s rRNA gene sequence of *Streptomyces lavenduligriseus* strain NRRL ISP-5487^{T}. The number of mismatch or nucleotide difference between the partial sequence of KDT32 and *Streptomyces lavenduligriseus* strain NRRL ISP-5487^{T} was 2 from a total of 985 aligned base pair.

Similarly, there are 30 *Streptomyces* species obtained from the EzTaxon-e database that showed between 99.26%- 99.79 % sequence similarities to KGT32 isolate. From a total of

30, four strains showed 99.79 % sequence similarity (two nucleotide difference only) to KGT32 16s rRNA gene sequence. However, the first most top closest species to 16s rRNA gene sequence of KGT32 was 16s rRNA gene sequence of *Streptomyces albidoflavus* strain DSM40455^{T} (Table 4.9). From this, 947/948 bp of 16s rRNA gene sequence of KGT32 was aligned with in 264-1211bp range of 16s rRNA gene sequence of *Streptomyces albidoflavus* strain DSM40455^{T}. The number of mismatched nucleotides between KGT32 and *Streptomyces albidoflavus* strain DSM40455^{T} was 2 from a total of 947 aligned nucleotide base pairs. Therefore, it was discovered that isolate KDT32 and isolate KGT32 belonged/affiliated to genus *Streptomyces*. The sequence was deposited in GenBank database as *Streptomyces pausti* KDT32 and *Streptomyces pausti* KGT32 with MH301089 and MH301090 accession number, respectively.

Table 4.9: KDT32 and KGT32 16s rRNA gene sequence analysis for identification using EzTaxon databases

Isolate	Completeness	First Top hit taxon	First top hit strain ^{T}	Accession number	Similarity	Diff/total nt	Top hit taxonomy
KDT32	68%	*Streptomyces lavenduligriseus*	NRRL ISP-5487^{T}	JOBD01000085	99.8%	2/985	Bacteria ^{D} Actinobacteria ^{P} Actinobacteria ^{C} Streptomycetales ^{O} Streptomycetaceae ^{F} Streptomyces ^{G}
KGT32	65.5%	*Streptomyces albidoflavus*	ATCC25422 & DSM40455^{T}	Z76676	99.79%	2/847	Bacteria ^{D} Actinobacteria ^{P} Actinobacteria ^{C} Streptomycetales ^{O} Streptomycetaceae ^{F} Streptomyces ^{G}

Key: "**Completeness"** the ratio of the length of our sequence to the full-length sequence; **"Top hit taxon"** the first closet species in the database; **"First top hit strain ^{T}"** the first top closet strain type**; "Accession"** the ID for the closet species in the database;

"**Similarity"** the sequence similarity between the closet species and our isolate; "**Different/ total nucleotide"** the number of mismatched base pair between the closet species and our isolate from the total number of compared sequences; **"Top hit taxonomy"** taxonomical hierarchy of our isolate based 16s rRNA gene sequence from Domain (Bacteria) to genus (*Streptomyces*){D=Domain, P= Phylum, C=Class, O=order, F=Family, G=Genus}

4.3.4. Molecular phylogenetic analysis of KDT32 and KGT32 isolates

The 16s rRNA gene sequence of KDT32 and KGT32 with sequences for 60 *Streptomyces* type strains retrieved from EzTaxon-e database were analyzed using NJ and ML algorithms to see the taxonomic position of our potential isolates. According to the result of phylogenetic tree showed that, both of our isolates found at different taxonomic position. The result of comparative analysis of 16S rRNA gene sequence and phylogenetic relationship tree confirmed that both KDT32 and KGT32 isolates showed clade with different *Streptomyces* species retrieved from EzTaxon-e database as described below (Fig.4. 17).

The phylogenetic tree result from both NJ and ML analysis confirmed that KDT32 isolate formed monophyletic clade with *Streptomyces nodosus* strain ATCC 14899 (CP009313) which was supported by 54 % and 57 % boot strap value, respectively. Moreover, the 16s rRNA gene sequence of KDT32 and *Streptomyces nodosus* strain ATCC 14899 showed 99.79% sequence similarity (Fig.4. 17).

On the other hand, the result of NJ and ML tree analysis revealed that KGT32 formed a distinct clade with *Streptomyces fabae* T66 (KM229360) and *Streptomyces cinerochromogenes* NBRC13822 (AB184507) which was supported with 34% and 25%

bootstrap value, respectively. KGT32 16s rRNA gene sequence showed 99.68% and 99.58% sequence similarity with *Streptomyces fabae* T66 (KM229360) and *Streptomyces cinerochromogenes* NBRC13822 (AB184507), respectively (Fig.4. 17). Thus, these confirmed that the local isolates that produce bioactive metabolites capable of synthesis of antibacterial silver nanoparticles were grouped under genus *Streptomyces* species.

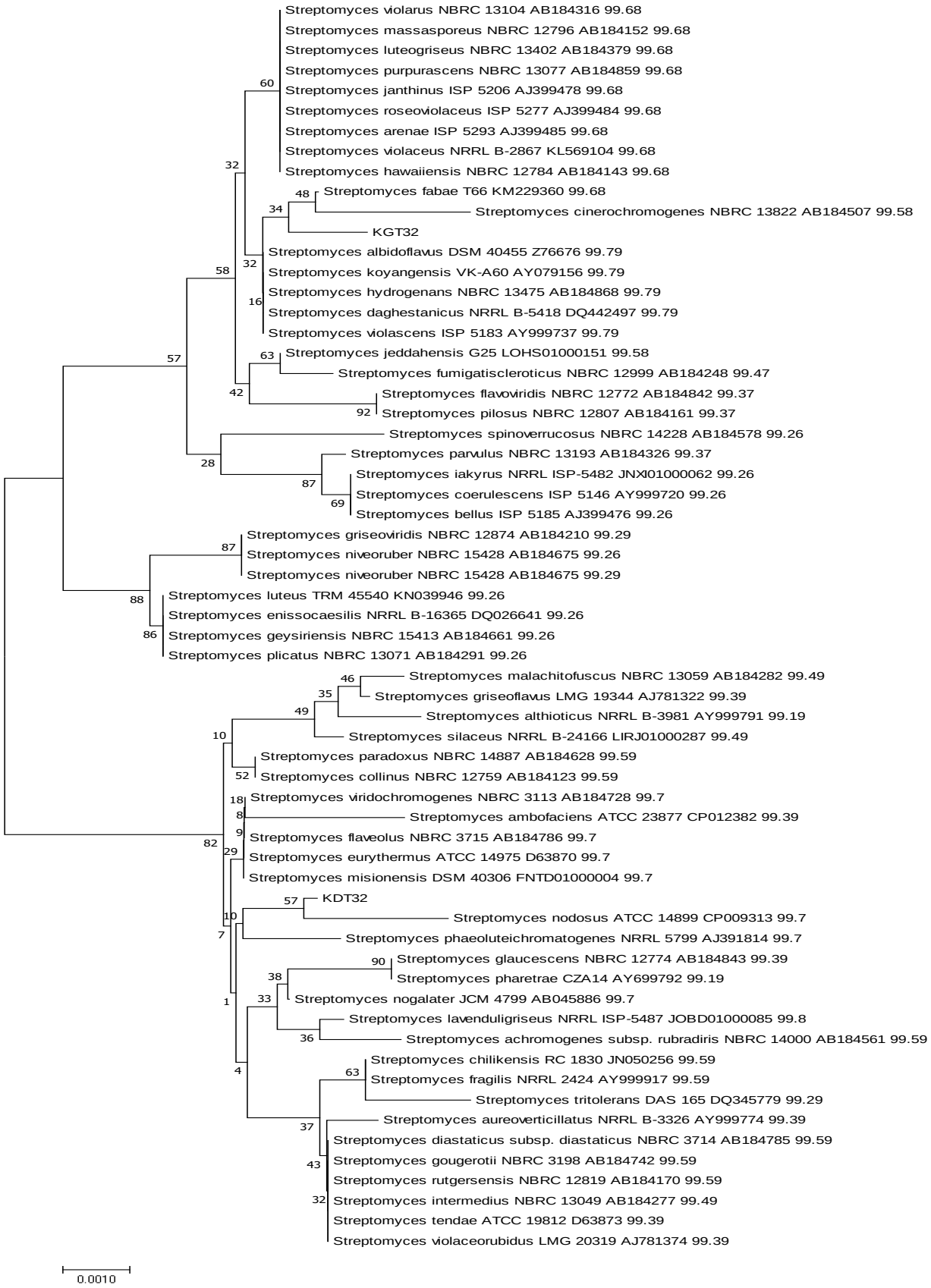
Streptomyces violarus NBRC 13104 AB184316 99.68
Streptomyces massasporeus NBRC 12796 AB184152 99.68
Streptomyces luteogriseus NBRC 13402 AB184379 99.68
Streptomyces purpurascens NBRC 13077 AB184859 99.68
Streptomyces janthinus ISP 5206 AJ399478 99.68
Streptomyces roseoviolaceus ISP 5277 AJ399484 99.68
Streptomyces arenae ISP 5293 AJ399485 99.68
Streptomyces violaceus NRRL B-2867 KL569104 99.68
Streptomyces hawaiiensis NBRC 12784 AB184143 99.68
Streptomyces fabae T66 KM229360 99.68
Streptomyces cinerochromogenes NBRC 13822 AB184507 99.58
KGT32
Streptomyces albidoflavus DSM 40455 Z76676 99.79
Streptomyces koyangensis VK-A60 AY079156 99.79
Streptomyces hydrogenans NBRC 13475 AB184868 99.79
Streptomyces daghestanicus NRRL B-5418 DQ442497 99.79
Streptomyces violascens ISP 5183 AY999737 99.79
Streptomyces jeddahensis G25 LOHS01000151 99.58
Streptomyces fumigatiscleroticus NBRC 12999 AB184248 99.47
Streptomyces flavoviridis NBRC 12772 AB184842 99.37
Streptomyces pilosus NBRC 12807 AB184161 99.37
Streptomyces spinoverrucosus NBRC 14228 AB184578 99.26
Streptomyces parvulus NBRC 13193 AB184326 99.37
Streptomyces iakyrus NRRL ISP-5482 JNXI01000062 99.26
Streptomyces coerulescens ISP 5146 AY999720 99.26
Streptomyces bellus ISP 5185 AJ399476 99.26
Streptomyces griseoviridis NBRC 12874 AB184210 99.29
Streptomyces niveoruber NBRC 15428 AB184675 99.26
Streptomyces niveoruber NBRC 15428 AB184675 99.29
Streptomyces luteus TRM 45540 KN039946 99.26
Streptomyces enissocaesilis NRRL B-16365 DQ026641 99.26
Streptomyces geysiriensis NBRC 15413 AB184661 99.26
Streptomyces plicatus NBRC 13071 AB184291 99.26
Streptomyces malachitofuscus NBRC 13059 AB184282 99.49
Streptomyces griseoflavus LMG 19344 AJ781322 99.39
Streptomyces althioticus NRRL B-3981 AY999791 99.19
Streptomyces silaceus NRRL B-24166 LIRJ01000287 99.49
Streptomyces paradoxus NBRC 14887 AB184628 99.59
Streptomyces collinus NBRC 12759 AB184123 99.59
Streptomyces viridochromogenes NBRC 3113 AB184728 99.7
Streptomyces ambofaciens ATCC 23877 CP012382 99.39
Streptomyces flaveolus NBRC 3715 AB184786 99.7
Streptomyces eurythermus ATCC 14975 D63870 99.7
Streptomyces misionensis DSM 40306 FNTD01000004 99.7
KDT32
Streptomyces nodosus ATCC 14899 CP009313 99.7
Streptomyces phaeoluteichromatogenes NRRL 5799 AJ391814 99.7
Streptomyces glaucescens NBRC 12774 AB184843 99.39
Streptomyces pharetrae CZA14 AY699792 99.19
Streptomyces nogalater JCM 4799 AB045886 99.7
Streptomyces lavenduligriseus NRRL ISP-5487 JOBD01000085 99.8
Streptomyces achromogenes subsp. rubradiris NBRC 14000 AB184561 99.59
Streptomyces chilikensis RC 1830 JN050256 99.59
Streptomyces fragilis NRRL 2424 AY999917 99.59
Streptomyces tritolerans DAS 165 DQ345779 99.29
Streptomyces aureoverticillatus NRRL B-3326 AY999774 99.39
Streptomyces diastaticus subsp. diastaticus NBRC 3714 AB184785 99.59
Streptomyces gougerotii NBRC 3198 AB184742 99.59
Streptomyces rutgersensis NBRC 12819 AB184170 99.59
Streptomyces intermedius NBRC 13049 AB184277 99.49
Streptomyces tendae ATCC 19812 D63873 99.39
Streptomyces violaceorubidus LMG 20319 AJ781374 99.39
0.0010

Figure 4.17: Taxonomic position and evolutionary relationship determination of KDT32 and KGT32 isolates sequences with reference sequences (strains of genus *Streptomyces*) from phylogenetic tree constructed by ML algorithm.

The phylogenetic tree was validated by a bootstrap analysis (1000 replications) with values shown at branch nodes. Bar indicates substitutions per nucleotide position. Evolutionary analyses were conducted in MEGA7. **Key:** *Streptomyces violarus* NBRC 13104 AB184316 99.68 (*Streptomyces violarus* = taxon name; NBRC 13104 =strain type; AB184316=GenBank accession number; 99.68= percent of sequence similarity)

CHAPTER FIVE: DISCUSSION

The emergence of antibacterial resistant bacteria is a cause for concern worldwide. It is the basic challenge for effective treatment of infectious disease throughout the globe including the continent of Africa. *Escherichia coli, Salmonella sp, Shigella sp* and *Vibrio sp* are frequently occurring drug resistant groups of gram negative bacteria in East Africa region (Omulo et al., 2015). Thus, searching of actinomycetes isolates from unexplored soil environments for production of antibacterial metabolites and for synthesis of antibacterial silver nanoparticle is required. Identifying and selecting such soil sampling areas in local districts may lead to pharmaceutically valuable bioactive metabolite producing isolates. The literature search indicated that Thika waste dump sites are unexplored area for searching antibacterial metabolites and bioactive metabolite producing potential actinomycetes for synthesis of antibacterial silver nanoparticles.

The bioassay guided screening result showed that from a total of selectively isolated local isolates, 23.2 % isolates had antibacterial active. This indicated that the frequency of getting antibacterial isolates in the present study area was greater than 16.6 % (Bizuye et al., 2013) and lower than when compared to 36.4% (Rotich et al., 2017) and 55.7 % (Zainal Abidin et al., 2016) finding. This variation occurred may be due to difference in geographical location of the sampling sites and sample pre-treatment methods used. However, from present study 23.2% isolates showed either anti- *E. coli ATCC25922, S. boydii, S. typhi* and or *V. cholerae* activity. This was better activity when compared to none of them showed anti- *E. coli ATCC25922* (Rotich et al., 2017), 12.8% of active isolates showed anti-*E. coli ATCC25922* (Zainal Abidin et al., 2016) and 16.6 % isolates showed anti-*E. coli* and anti- *S. typhi ATCC9289* activity (Bizuye et al., 2013).

The antibacterial activity against *E. coli* (26.5±0.58 mm), *S. boydii* (31.3±0.6), *S. typhi* (30±0 mm), *V.cholerae* (36±1 mm) and MRSA (16.25±0.5 mm) was best results recorded from the present study. As the previous study showed that the highest antibacterial activity was 30±2 mm against *E. coli ATCC25922* and 32±2 mm against *S. typhi* ATCC9289 (Bizuye et al., 2013) and > 30 mm against *E. coli* ATCC25922 (Zainal Abidin et al., 2016) was recorded which was greater than the present finding (26±1.0 mm) against *E. coli* ATCC25922. These differences may be due to diverse types of active isolates isolated from different natural environments or using different types of antibacterial activity test method.

The synthesis and assembly of antibacterial silver nanoparticle using bioactive metabolites from organisms is an emerging and growing field in bio-nanotechnology that has resulted potential candidates with ability to kill resistant bacteria (Barros, Fulaz, Stanisic, & Tasic, 2018). Actinomycetes are the potential sources of diverse groups of bioactive compounds capable synthesizing antibacterial silver nanoparticles (Golinska et al., 2014; Manivasagan et al., 2014). This can be characterized by a combination of ways such as visual detection, UV-visible and FTIR spectrophotometer analysis (Prakasham et al., 2012; Składanowski et al., 2017). Its antibacterial activity was characterized and evaluated by different bioassay methods such as well diffusion assay (Prakasham et al., 2012).

The visual detection of the present study revealed that KDT32 metabolite-$AgNO_3$ and KGT32 metabolite-$AgNO_3$ reaction solution showed dark salmon and pale golden rod color change, respectively. These may indicate bio-reduction of Ag^+ and morphological indicator to detect the synthesis of AgNPs. The synthesis of silver nanoparticles by cell free filtrate from *Streptomyces rochei* MHM13 treated with $AgNO_3$ showed pale yellow color change (Abd-Elnaby et al., 2016). On the other study, AgNPs synthesized by

metabolite from *Streptomyces sp LK3* (Karthik et al., 2014), *S. parvulus* SSNP11 (Prakasham et al., 2014), *Streptomyces sp.* NH21 (Składanowski et al., 2017) and *Streptomyces sp*. SS2 (Mohanta & Behera, 2014) showed dark brown color change. These color change occur due to absorption of visible light and the effect of surface Plasmon resonance on silver. The differences in color change may be due to differences in the type of bio-molecules involved in bio-reduction of Ag^+ and capping of silver nanoparticles. These clearly indicate that KDT32 and KGT32 metabolites have a potential to reduce Ag^+ and form silver nanoparticles.

The absorption intensity result showed that the maximum spectra peak was centered at 415.5 nm and 416 nm for KDT32-AgNP and KGT32-AgNPs, respectively. Previous studies revealed that the typical AgNPs show maximum UV-vis spectra peaks between 400-500 nm and this is a reliable criterion indicating the formation of AgNPs. Silver nanoparticles synthesized by metabolites from *Streptomyces rochei* MHM13 showed a characteristic peak at 410 nm (Abd-Elnaby et al., 2016). Silver nanoparticle synthesized by metabolites from *Streptomyces sp*. SS2 (Mohanta & Behera, 2014) and *Streptomyces sp* LK3 (Karthik et al., 2014) showed a characteristic peak at 420 nm. Another study showed that UV-vis spectra of silver nanoparticles synthesized by metabolites from *Streptomyces sp.* NH21 was observed at 402 and 424 nm (Składanowski et al., 2017).

The functional groups involved for synthesis of nanoparticles were identified by observing the change in FTIR spectra band position, shape and intensity in AgNPs compared to the spectra band of the metabolite only. The band position shifts from 3386.91 to 3391.31 cm^{-1}, 1638.98 to 1640.85 cm^{-1} and 461.42 to 445.93 cm^{-1} indicates that O-H stretch, C=C and S-S from KDT32 metabolites were the major functional groups involved for synthesis of KDT32-AgNPs. Similarly, the shift in band position from 3117.76 to 3408.99 cm^{-1},

1603.98 to 1639.15 cm^{-1} and 743.82 to 451.6 cm^{-1} reveals that O-H, C=C and C-H bio-molecules from KGT32 metabolites were involved for synthesis of KGT32-AgNPs. This band peak shift alteration between the metabolite and the metabolite mediated AgNPs shows the existence of bio-molecules that were involved for the reduction of Ag^{+} and capping of silver nanoparticles. As reported by, antibacterial compounds have active functional groups such as amide and hydroxyl groups to reduce Ag^{+} and cap silver nanoparticle (Chauhan et al., 2013). Another study showed that active functional group O-H (3417 cm^{-1}) (Karthik et al., 2014) was involved for the reduction of Ag^{+} and capping of antibacterial silver nanoparticles. Similarly, earlier studies have reported that -OH (3384 cm^{-1}) is one of the functional groups used to reduce Ag^{+} and capping of AgNPs (El-Naggar et al., 2014). These clearly indicate that KDT32 and KGT32 isolates are the source of metabolites having potential functional groups that reduce Ag^{+} and capping silver nanoparticles.

The bioassay study of the KDT32-AgNP and KGT32-AgNP showed antibacterial activity against *E. coli* and *S. typhi*. The inhibition zone of KDT32-AgNP against *E. coli* and *S. typhi* was 22.0$\pm$1.4 mm and 19.0$\pm$1.4 mm, respectively. Similarly, KGT32-AgNP revealed inhibition zone of 21.5$\pm$0.7 mm and 17.0$\pm$0.0 mm against *E. coli* and *S. typhi*, respectively. However, the present study showed that no antibacterial activity was observed against *S. bodii* and similar result was reported by (Chauhan et al., 2013). Earlier reports showed that silver nanoparticle synthesized by *Streptomyces rochei* MHM13 metabolite showed 16 nm and 18 nm inhibition zone against *E. coli* and *S. typhi* , respectively (Abd-Elnaby et al., 2016). In another study (Mohanta & Behera, 2014), silver nanoparticle synthesized by metabolite from *Streptomyces sp.* SS2 showed 18.25 ± 1.5 mm inhibition zone against *E. coli*. Silver nanoparticles synthesized by *S. parvulus* SSNP11 metabolites showed 26 mm

inhibition zone against *S. typhi* (Prakasham et al., 2014). These clearly indicate that KDT32 and KGT32 metabolites mediated synthesis of antibacterial silver nanoparticles with potential bio-nanotechnology that can be used in biomedical applications.

The present study demonstrated that both KDT32 and KGT32 isolates are gram positive, have filamentous cell shape and produce catalase enzyme, could grow in a 6-12 and 5-12 pH range; and 0-7% and 0-9% NaCl salt concentration, respectively. This is in agreement with studies that antibacterial metabolite producing *Streptomyces* species isolated from soil showed growth between 4-12 pH and 0-7% salt concentration (Ibrahim, Abd-El-Aal, AG, & El-Sayd, 2014; Kontro et al., 2005).

NCBI-BLASTn search result indicate that sequence of KDT32 isolate showed 99% sequence similarity with sequence of *Streptomyces sp.* MBE174 (AB873097.1). The biomedical and pharmaceutical application of *Streptomyces sp.* MBE174 is unknown. Moreover, based on EzTaxon-e database search result, sequence of KDT32 isolate showed 99.8 % sequence similarity with *S. lavenduligriseus* strain NRRL ISP-5487 which has been shown to produce polyene macrolides (pentenomycine II, Pentenomycine III and narangomycine) (J. Yang et al., 2016).

Similarly, the sequences of KGT32 isolate showed 99 % similarity with *Streptomyces sp. strain SP4-AB2* (MH013316.1) where it's medical and industrial role has yet to be determined. EzTaxon-e similarity search indicated that sequence of KGT32 isolate showed 99.79 % similarity with *S. albidoflavus* strain DSM40455, *S. koyangensis* strain VK-A60, *S. hydrogenans strain* NBRC 13475, *S. daghestanicus* strain NRRL B-5418 and *S. violascens* strain ISP 5183. They are known in production of different antimicrobial compounds such as paulomycins A and B (Sarmiento-Vizcaíno et al., 2015), 4-phenyl-3-butenoic acid (Lee, Lee, Jung, & Hwang, 2005), actinomycin D (Kulkarni, Gorthi,

Banerjee, & Chattopadhyay, 2017) and valinomycine (Pimentel-Elardo et al., 2010), respectively. Unlike local isolates KDT32 and KGT32, literature search about the role of these reference *Streptomyces* species in nano-drug synthesis has not been reported.

The phylogenetic tree constructed from KDT32, KGT32 and reference sequences retrieved from EzTaxon-e database revealed that the taxonomic position of both KDT32 and KGT32 isolates formed different clade with species of genus *Streptomyces*. Both NJ and ML tree inferred that KDT32 isolate formed a monophyletic clade with *S. nodosus* strain ATCC 14899 (CP009313) that has 99.7 % sequence similarity. *Streptomyces nodosus* is known in production of antifungal antibiotics (polyene macrolide antibiotic amphotericin B) (Caffrey, Lynch, Flood, Finnan, & Oliynyk, 2001) and other bioactive compounds (polyketides, peptides, siderophores and terpenes) (Sweeney, Murphy, & Caffrey, 2016). On the other hand, KGT32 isolate formed a distinct clade with *S. fabae* strain T66 (KM229360) and *S. cinerochromogenes* strain NBRC13822 (AB184507). *Streptomyces fabae* is known for production of antibacterial and antifungal antibiotics (Nguyen & Kim, 2015) and *S. cinerochromogenes* produce cineromycin B type which a role in anti-adipocyte differentiation (Matsuo, Kondo, Kawasaki, & Imamura, 2015). However, the role of these reference *Streptomyces* species in nano-drug synthesis is unknown. Thus, KDT32 and KGT32 isolates not only produce antibacterial metabolite but also the metabolites are capable of synthesizing antibacterial silver nanoparticles.

CHAPTER SIX: CONCLUSIONS AND RECOMMENDATIONS

6.1. Conclusions

1. Actinomycete isolates from Thika waste dump soil showed antibacterial activity against one or more than one bacteria pathogen (*E. coli* ATCC25922, *S. typhi*, *S. boydii*, *V. cholera*, MRSA and *E. coli*).
2. Bioactive metabolites from KDT32 and KGT32 isolates synthesize antibacterial silver nanoparticle (KDT32-AgNP and KGT32-AgNP) against *E. coli* and *S. typhi* but tot against *S. boydii*.
3. The KDT32 and KGT32 isolates are identified as *Streptomyces* species.

6.2. Recommendations

Based on the above conclusions the following recommendations are forwarded:

1. KDT32 and KGT32 isolates are recommended to use for both production of antibacterial and synthesis of antibacterial AgNPs
2. The antibacterial metabolites produced by KDT32 and KGT32 require further analysis to purify and characterize for identification of the compound and dosage determination.
3. The antibacterial silver nanoparticles synthesized by the metabolites produced by the KDT32 and KGT32 isolates require further analysis to determine the size and shape of the antibacterial silver nanoparticles.

REFERENCES

Abd-Elnaby, H. M., Abo-Elala, G. M., Abdel-Raouf, U. M., & Hamed, M. M. (2016). Antibacterial and anticancer activity of extracellular synthesized silver nanoparticles from marine Streptomyces rochei MHM13. *Egyptian Journal of Aquatic Research*, *42*(3), 301–312. https://doi.org/10.1016/j.ejar.2016.05.004

Adegboye, M. F., & Babalola, O. O. (2012). Taxonomy and ecology of antibiotic producing actinomycetes. *African Journal of Agricultural Reseearch*, *7*(15), 2255–2261. https://doi.org/10.5897/AJARX11.071

Adegboye, M. F., & Babalola, O. O. (2016). Isolation and Identification of Potential Antibiotic Producing Rare Actinomycetes from Rhizospheric Soils. *Journal of Human Ecology*, *56*(1/2), 31–41. https://doi.org/10.1080/09709274.2016.11907035

Alagumaruthanayagam, A., Pavankumar, A. R., Vasanthamallika, T. K., & Sankaran, K. (2009). Evaluation of solid (disc diffusion) - and liquid (turbidity) -phase antibiogram methods for clinical isolates of diarrheagenic E . coli and correlation with efflux. *The Journal of Antibiotics*, *62*, 377–384. https://doi.org/10.1038/ja.2009.45

Alizade, H. (2018). Escherichia coliin Iran: An Overview of Antibiotic Resistance: A Review Article. *Iranian Journal of Public Health*, *47*(1), 1–12. Retrieved from http://www.ncbi.nlm.nih.gov/pubmed/29318111%0Ahttp://www.pubmedcentral.nih.gov/articlerender.fcgi?artid=PMC5756583

Andersen, J. L., He, G. X., Kakarla, P., Kc, R., Kumar, S., Lakra, W. S., … Varela, M. F. (2015). Multidrug Efflux Pumps from Enterobacteriaceae , Vibrio cholerae and Staphylococcus aureus Bacterial Food Pathogens. *International Journal of Environmental Research and Public Health*, *12*, 1487–1547. https://doi.org/10.3390/ijerph120201487

Anwar, S. H. (2018). A Brief Review on Nanoparticles : Types of Platforms , Biological

Synthesis and Applications. *Journal of Material Sciences*, *6*(2), 109–116. https://doi.org/10.4172/2321-6212.1000222

Ataee, R. A., Mehrabi-Tavana, A., Hosseini, S. M. J., Moridi, K., & Zadegan, M. G. (2012). A Method for Antibiotic Susceptibility Testing: Applicable and Accurate. *Jundishapur Journal of Microbiology*, *5*(1), 341–345. https://doi.org/10.5812/kowsar.20083645.2374

Balouiri, M., Sadiki, M., & Ibnsouda, S. K. (2016). Methods for in vitro evaluating antimicrobial activity: A review. *Journal of Pharmaceutical Analysis*, *6*(2), 71–79. https://doi.org/10.1016/j.jpha.2015.11.005

Balvočiute, M., & Huson, D. H. (2017). SILVA, RDP, Greengenes, NCBI and OTT - how do these taxonomies compare? *BMC Genomics*, *18*(Suppl 2), 1–8. https://doi.org/10.1186/s12864-017-3501-4

Barka, E. A., Vatsa, P., Sanchez, L., Gaveau-Vaillant, N., Jacquard, C., Klenk, H.-P., … van Wezel, G. P. (2016). Taxonomy, Physiology, and Natural Products of Actinobacteria. *Microbiology and Molecular Biology Reviews*, *80*(1), 1–43. https://doi.org/10.1128/MMBR.00019-15

Barreto, M. L., Teixeira, M. G., & Carmo, E. H. (2006). Infectious diseases epidemiology. *Journal of Epidemiology and Community Health*, *60*(3), 192–195. https://doi.org/10.1136/jech.2003.011593

Barros, C. H. N., Fulaz, S., Stanisic, D., & Tasic, L. (2018). Biogenic Nanosilver against Multidrug-Resistant. *Antibiotics*, *69*(7), 1–24. https://doi.org/10.3390/antibiotics7030069

Basilio, A., González, I., Vicente, M. F., Gorrochategui, J., Cabello, A., González, A., & Genilloud, O. (2003). Patterns of antimicrobial activities from soil actinomycetes isolated under different conditions of pH and salinity. *Journal of Applied*

Microbiology, *95*(4), 814–823. https://doi.org/10.1046/j.1365-2672.2003.02049.x

Bélanger, L., Garenaux, A., Harel, J., Boulianne, M., Nadeau, E., & Dozois, C. M. (2011). Escherichia colifrom animal reservoirs as a potential source of human extraintestinal pathogenic E. coli. *FEMS Immunology and Medical Microbiology*, *62*(1), 1–10. https://doi.org/10.1111/j.1574-695X.2011.00797.x

Bennett, P. M. (2008). Plasmid encoded antibiotic resistance : acquisition and transfer of antibiotic resistance genes in bacteria. *British Journal of Pharmacology*, *153*, 347–357. https://doi.org/10.1038/sj.bjp.0707607

Benson, D. A., Karsch-Mizrachi, I., Clark, K., Lipman, D. J., Ostell, J., & Sayers, E. W. (2012). GenBank. *Nucleic Acids Research*, *40*(D1), 48–53. https://doi.org/10.1093/nar/gkr1202

Bhosale, R. S., Hajare, K. Y., Mulay, B., Mujumdar, S., & Kothawade, M. (2015). Biosynthesis , Characterization and Study of Antimicrobial Effect of Silver Nanoparticles by Actinomycetes spp. *International Journal of Current Microbiology and Applied Sciences*, *ISSN:2319*-(2), 144–151.

Bizuye, A., Bii, C., Erastus, G., & Maina, N. (2017). Antibacterial metabolite prospecting from Actinomycetes isolated from waste damped soils from Thika, central part of Kenya. *Asian Pacific Journal of Tropical Disease*, *7*(12), 757–764. https://doi.org/10.12980/apjtd.7.2017D7-162

Bizuye, A., Moges, F., & Andualem, B. (2013). Isolation and screening of antibiotic producing actinomycetes from soils in Gondar town, North West Ethiopia. *Asian Pacific Journal of Tropical Disease*, *3*(5), 375–381. https://doi.org/10.1016/S2222-1808(13)60087-0

Blair, J. M. A., Webber, M. A., Baylay, A. J., Ogbolu, D. O., & Piddock, L. J. V. (2014). Molecular mechanisms of antibiotic resistance. *Nature Publishing Group*, *13*(1), 42–

51. https://doi.org/10.1038/nrmicro3380

Bonev, B., Hooper, J., & Parisot, J. (2008). Principles of assessing bacterial susceptibility to antibiotics using the agar diffusion method. *Journal of Antimicrobial Chemotherapy*, *61*, 1295–1301. https://doi.org/10.1093/jac/dkn090

Boone, R. D., Grigal, D. F., Sollins, P., Ahrens, R. J., & Armstrong, D. E. (1999). Siol sampling, preparation, archiving, and quality control. New York: Oxford University Press.

Bowman, S., Roffey, P., McNevin, D., & Gahan, M. E. (2016). Evaluation of commercial DNA extraction methods for biosecurity applications. *Australian Journal of Forensic Sciences*, *48*(4), 407–420. https://doi.org/10.1080/00450618.2015.1106585

Buckle, G. C., Walker, C. L. F., & Black, R. E. (2012). Typhoid fever and paratyphoid fever: Systematic review to estimate global morbidity and mortality for 2010. *Journal of Global Health*, *2*(1), 1–9. https://doi.org/10.7189/jogh.02.010401

Busti, E., Monciardini, P., Cavaletti, L., Bamonte, R., Lazzarini, A., Sosio, M., & Donadio, S. (2006). Antibiotic-producing ability by representatives of a newly discovered lineage of actinomycetes. *Microbiology*, *152*, 675–683. https://doi.org/10.1099/mic.0.28335-0

Caffrey, P., Lynch, S., Flood, E., Finnan, S., & Oliynyk, M. (2001). Amphotericin biosynthesis in Streptomyces nodosus: Deductions from analysis of polyketide synthase and late genes. *Chemistry and Biology*, *8*(7), 713–723. https://doi.org/10.1016/S1074-5521(01)00046-1

Chaudhary, A. S. (2016). A review of global initiatives to fight antibiotic resistance and recent antibiotics′ discovery. *Acta Pharmaceutica Sinica B*, *6*(6), 552–556. https://doi.org/10.1016/j.apsb.2016.06.004

Chaudhary, H. S., Soni, B., Shrivastava, A. R., & Shrivastava, S. (2013). Diversity and

Versatility of Actinomycetes and its Role in Antibiotic Production, *3*. https://doi.org/10.7324/JAPS.2013.38.S14

Chauhan, R., Kumar, A., & Abraham, J. (2013). A biological approach to the synthesis of silver nanoparticles with Streptomyces sp JAR1 and its antimicrobial activity. *Scientia Pharmaceutica*, *81*(2), 607–621. https://doi.org/10.3797/scipharm.1302-02

Chen, X., Jiang, Y., Li, Q., Han, L., & Jiang, C. (2017). Molecular Phylogenetic Identification of Actinobacteria Xiu. In *Actinobacteria - Basics and Biotechnological Applications* (Vol. 56, pp. 141–174). Intech open. https://doi.org/10.5772/711

Corciova, A., & Ivanescu, B. (2018). Biosynthesis, characterisation and therapeutic applications of plant mediated silver nanoparticles. *Journal of the Serbian Chemical Society*, *83*(05), 515–538. https://doi.org/10.2298/JSC170731021C

Croxen, M. A., & Finlay, B. B. (2010). Molecular mechanisms of Escherichia coli pathogenicity. *Nature Reviews Microbiology*, *8*(1), 26–38. https://doi.org/10.1038/nrmicro2265

Cvrčková, F. (2016). A plant biologists' guide to phylogenetic analysis of biological macromolecule sequences. *Biologia Plantarum*, *60*(4), 619–627. https://doi.org/10.1007/s10535-016-0649-8

da Silva, G. J., & Mendonça, N. (2012). Association between antimicrobial resistance and virulence in Escherichia coli. *Virulence*, *3*(1), 18–28. https://doi.org/10.4161/viru.3.1.18382

Dakal, T. C., Kumar, A., Majumdar, R. S., & Yadav, V. (2016). Mechanistic Basis of Antimicrobial Actions of Silver Nanoparticles, *7*(November), 1–17. https://doi.org/10.3389/fmicb.2016.01831

Dengo-Baloi, L. C., Semá-Baltazar, C. A., Manhique, L. V., Chitio, J. E., Inguane, D. L., & Langa, J. P. (2017). Antibiotics resistance in El Tor Vibrio cholerae 01 isolated

during cholera outbreaks in Mozambique from 2012 to 2015. *PLoS ONE, 12*(8), 1–10. https://doi.org/10.1371/journal.pone.0181496

Dhanasekaran, D., Latha, S., Saha, S., Thajuddin, N., & Panneerselvam, A. (2013). Extracellular biosynthesis, characterisation and in-vitro antibacterial potential of silver nanoparticles using Agaricus bisporus. *Journal of Experimental Nanoscience*, *8*(4), 579–588. https://doi.org/10.1080/17458080.2011.577099

Dutta, S., Das, S., Mitra, U., Jain, P., Roy, I., Ganguly, S. S., … Paul, D. K. (2014). Antimicrobial Resistance , Virulence Profiles and Molecular Subtypes of Salmonella enterica Serovars Typhi and Paratyphi A Blood Isolates from Kolkata , India during 2009-2013. *Public Library of Science One*, *9*(8), 1–13. https://doi.org/10.1371/journal.pone.0101347

El-Naggar, N. E. A., Abdelwahed, N. A. M., & Darwesh, O. M. M. (2014). Fabrication of biogenic antimicrobial silver nanoparticles by Streptomyces aegyptia NEAE 102 as eco-friendly nanofactory. *Journal of Microbiology and Biotechnology*, *24*(4), 453–464. https://doi.org/10.4014/jmb.1310.10095

El-naggar, N. E., Mohamedin, A., Hamza, S. S., & Sherief, A. (2016). Antimicrobial Efficacy of Silver Nanoparticles Loaded on Cotton Fabrics Using Newly Isolated Streptomyces sp . SSHH-1E. *Journal of Nanomaterials*, *2016*, 1–17.

Ephantus, M., Robert, K., & Paul, N. (2015). An Analysis of Solid Waste Generation and Characterization in Thika Municipality of Kiambu County, Kenya. *Journal of Environmental Science and Engineering B*, *4*(4), 210–215. https://doi.org/10.17265/2162-5263/2015.04.005

Friedman, N. D., Temkin, E., & Carmeli, Y. (2016). The negative impact of antibiotic resistance. *Clinical Microbiology and Infection*, *22*(5), 416–422. https://doi.org/10.1016/j.cmi.2015.12.002

Frye, J. G., & Jackson, C. R. (2013). Genetic mechanisms of antimicrobial resistance identified in Salmonella enterica , Escherichia coli , and Enteroccocus spp . isolated from U . S . food animals. *Frontiers in Microbiology*, *4*(135), 1–22. https://doi.org/10.3389/fmicb.2013.00135

George, M., George, G., & Hatha, A. A. M. (2010). Diversity and antibacterial activity of actinomycetes from wetland soil. *The South Pacific Journal of Natural and Applied Sciences*, *28*, 52–57.

Giske, C. G., Monnet, D. L., Cars, O., & Carmeli, Y. (2008). Clinical and economic impact of common multidrug-resistant gram-negative bacilli. *Antimicrobial Agents and Chemotherapy*, *52*(3), 813–821. https://doi.org/10.1128/AAC.01169-07

Golinska, P., Wypij, M., Ingle, A. P., Gupta, I., Dahm, H., & Rai, M. (2014). Biogenic synthesis of metal nanoparticles from actinomycetes: biomedical applications and cytotoxicity. *Applied Microbiology and Biotechnology*. https://doi.org/10.1007/s00253-014-5953-7

Hall, B. G. (2013). Building phylogenetic trees from molecular data with MEGA. *Molecular Biology and Evolution*, *30*(5), 1229–1235. https://doi.org/10.1093/molbev/mst012

Hawkey, P. M. (2008). The growing burden of antimicrobial resistance. *The Journal of Antimicrobial Chemotherapy*, *62 Suppl 1*, 1–9. https://doi.org/10.1093/jac/dkn241

Horiike, T. (2016). An Introduction To Molecular Phylogenetic Analysis. *Reviews in Agricultural Science*, *4*(0), 36–45. https://doi.org/10.7831/ras.4.36

Ibrahim, S. A., Abd-El-Aal, S. K., AG, A., & El-Sayd, M. A. (2014). Molecular Identification and Characterization of Some Gluconacetobacter Strains Isolated from Some Egyptian Fruits. *Research Journal of Pharmaceutical, Biological and Chemical Sciences*, *5*(4), 1617–1627. https://doi.org/10.5829/idosi.aejaes.2014.14.10.8641

Iravani, S., Korbekandi, H., Mirmohammadi, S. V, & Zolfaghari, B. (2016). Synthesis of silver nanoparticles : chemical , physical and biological methods. *Res Pharm Sci*, *9*(6), 385–406.

Jafari, F., Hamidian, M., Rezadehbashi, M., Doyle, M., Salmanzadeh-aharabi, S., Derakhshan, F., & Zali, M. R. (2009). Prevalence and antimicrobial resistance of diarrheagenic Escherichia coli and Shigella species associated with acute diarrhea in Tehran , Iran. *Journal of Infectious Disease and Medical Microbiololgy*, *20*(3), 56–62.

Janda, J. M., & Abbott, S. L. (2007). 16S rRNA gene sequencing for bacterial identification in the diagnostic laboratory: Pluses, perils, and pitfalls. *Journal of Clinical Microbiology*. https://doi.org/10.1128/JCM.01228-07

Jill Harrison, C., & Langdale, J. A. (2006). A step by step guide to phylogeny reconstruction. *Plant Journal*, *45*(4), 561–572. https://doi.org/10.1111/j.1365-313X.2005.02611.x

Kahsay, A. G., & Muthupandian, S. (2016). A review on Sero diversity and antimicrobial resistance patterns of Shigella species in Africa, Asia and South America, 2001-2014. *BMC Research Notes*, *9*(1), 1–6. https://doi.org/10.1186/s13104-016-2236-7

Kaper, J. B., Nataro, J. P., & Mobley, H. L. T. (2004). Pathogenic Escherichia coli. *Nature Reviews Microbiology*, *2*(2), 123–140. https://doi.org/10.1038/nrmicro818

Karthik, L., Kumar, G., Kirthi, A. V., Rahuman, A. A., & Bhaskara Rao, K. V. (2014). Streptomyces sp. LK3 mediated synthesis of silver nanoparticles and its biomedical application. *Bioprocess and Biosystems Engineering*, *37*(2), 261–267. https://doi.org/10.1007/s00449-013-0994-3

Kaye, K. S., & Pogue, J. M. (2015). Infections Caused by Resistant Gram-Negative Bacteria: Epidemiology and Management. *Pharmacotherapy*, *35*(10), 949–962.

https://doi.org/10.1002/phar.1636

Kibret, M., Guerrero-Garzón, J. F., Urban, E., Zehl, M., Wronski, V.-K., Rückert, C., … Zotchev, S. B. (2018). Streptomyces spp . From Ethiopia Producing Antimicrobial Compounds : Characterization via Bioassays , Genome Analyses , and Mass Spectrometry. *Frontiers in Microbiology*, *9*(June), 1–13. https://doi.org/10.3389/fmicb.2018.01270

Kim, B. K., Lim, Y.-W., Kim, M., Kim, S., Chun, J., Lee, J.-H., & Jung, Y. (2007). EzTaxon: a web-based tool for the identification of prokaryotes based on 16S ribosomal RNA gene sequences. *International Journal of Systematic and Evolutionary Microbiology*, *57*(10), 2259–2261. https://doi.org/10.1099/ijs.0.64915-0

Kim, M., & Chun, J. (2014). 16S rRNA gene-based identification of bacteria and archaea using the EzTaxon server. *Methods in Microbiology*, *41*, 61–74. https://doi.org/10.1016/bs.mim.2014.08.001

Kim, M., Lee, K.-H., Yoon, S.-W., Kim, B.-S., Chun, J., & Yi, H. (2013). Analytical Tools and Databases for Metagenomics in the Next-Generation Sequencing Era. *Genomics and Informatics*, *11*(3), 102–113.

Kim, O. S., Cho, Y. J., Lee, K., Yoon, S. H., Kim, M., Na, H., … Chun, J. (2012). Introducing EzTaxon-e: A prokaryotic 16s rRNA gene sequence database with phylotypes that represent uncultured species. *International Journal of Systematic and Evolutionary Microbiology*, *62*(PART 3), 716–721. https://doi.org/10.1099/ijs.0.038075-0

Kitaoka, M., Miyata, S. T., Unterweger, D., & Pukatzki, S. (2011). Antibiotic resistance mechanisms of Vibrio cholerae. *Journal of Medical Microbiology*, *60*(4), 397–407. https://doi.org/10.1099/jmm.0.023051-0

Klontz, K. C., & Singh, N. (2015). Treatment of drug-resistant *Shigella* infections. *Expert*

Review of Anti-Infective Therapy, *13*(1), 69–80. https://doi.org/10.1586/14787210.2015.983902

Kontro, M., Lignell, U., Hirvonen, M. R., & Nevalainen, A. (2005). pH effects on 10 Streptomyces spp. growth and sporulation depend on nutrients. *Letters in Applied Microbiology*, *41*(1), 32–38. https://doi.org/10.1111/j.1472-765X.2005.01727.x

Kulkarni, M., Gorthi, S., Banerjee, G., & Chattopadhyay, P. (2017). Production, characterization and optimization of actinomycin D from Streptomyces hydrogenans IB310, an antagonistic bacterium against phytopathogens. *Biocatalysis and Agricultural Biotechnology*, *10*, 69–74. https://doi.org/10.1016/j.bcab.2017.02.009

Kumar, P. S., Balachandran, C., Duraipandiyan, V., Ramasamy, D., Ignacimuthu, S., & Al-dhabi, N. A. (2015). Extracellular biosynthesis of silver nanoparticle using Streptomyces sp . 09 PBT 005 and its antibacterial and cytotoxic properties. *Applied Nanoscience*, *5*, 169–180. https://doi.org/10.1007/s13204-014-0304-7

Kumar, P. S., Duraipandiyan, V., & Ignacimuthu, S. (2014). Isolation, screening and partial purification of antimicrobial antibiotics from soil Streptomyces sp. SCA 7. *Kaohsiung Journal of Medical Sciences*, *30*(9), 435–446. https://doi.org/10.1016/j.kjms.2014.05.006

Kumar, S., Stecher, G., & Tamura, K. (2016). MEGA7: Molecular Evolutionary Genetics Analysis Version 7.0 for Bigger Datasets. *Molecular Biology and Evolution*, *33*(7), 1870–1874. https://doi.org/10.1093/molbev/msw054

Kumar, V., Singh, D. K., Mohan, S., Kumar, R., & Hadi, S. (2017). Journal of Environmental Chemical Engineering Photoinduced green synthesis of silver nanoparticles using aqueous extract of Physalis angulata and its antibacterial and antioxidant activity. *Biochemical Pharmacology*, *5*(1), 744–756. https://doi.org/10.1016/j.jece.2016.12.055

Kurashima, A. (2016). Amaging pathophysiology of tuberculosis. *Japanese Journal of Chest Diseases*, *75*(5), 458–471. https://doi.org/10.5772/711

Lakshmi, V., & Roshmi, D. (2014). Extracellular synthesis of silver nanoparticles by the Bacillus strain CS 11 isolated from industrialized area, *4*, 121–126. https://doi.org/10.1007/s13205-013-0130-8

Lee, J. Y., Lee, J. Y., Jung, H. W., & Hwang, B. K. (2005). Streptomyces koyangensis sp. nov., a novel actinomycete that produces 4-phenyl-3-butenoic acid. *International Journal of Systematic and Evolutionary Microbiology*, *55*(1), 257–262. https://doi.org/10.1099/ijs.0.63168-0

Li, Q., Chen, X., Jiang, Y., & Jiang, C. (2016). Cultural, Physiological, and Biochemical Identification of Actinobacteria. In *Actinobacteria - Basics and Biotechnological Applications* (pp. 87–111). https://doi.org/10.5772/61462

Lin, D., Chen, K., Wai-Chi Chan, E., & Chen, S. (2015). Increasing prevalence of ciprofloxacin-resistant food-borne Salmonella strains harboring multiple PMQR elements but not target gene mutations. *Scientific Reports*, *5*(14754), 1–8. https://doi.org/10.1038/srep14754

MacGowan, A., & Macnaughton, E. (2017). Antibiotic resistance. *Medicine (United Kingdom)*, *45*(10), 622–628. https://doi.org/10.1016/j.mpmed.2017.07.006

Manivasagan, P., Venkatesan, J., Sivakumar, K., & Kim, S. (2014). Actinobacteria mediated synthesis of nanoparticles and their biological properties : A review. *Critical Reviews in Microbiology*, *7828*, 1–13. https://doi.org/10.3109/1040841X.2014.917069

Mary, G., Soares, S., Figueiredo, L. C., Faveri, M., Cortelli, S. C., Duarte, M., & Feres, M. (2011). Mechanisms of action of systemic antibiotics used in periodontal treatment and mechanisms of bacterial resistance to these drugs. *Journal of Applied Oral*

Science, *20*(3), 295–309.

Matsuo, H., Kondo, Y., Kawasaki, T., & Imamura, N. (2015). Cineromycin B isolated from Streptomyces cinerochromogenes inhibits adipocyte differentiation of 3T3-L1 cells via Krüppel-like factors 2 and 3. *Life Sciences*, *135*, 35–42. https://doi.org/10.1016/j.lfs.2015.05.020

Mayrhofer, S., Domig, K. J., Mair, C., Zitz, U., Huys, G., & Kneifel, W. (2008). Comparison of broth microdilution, Etest, and agar disk diffusion methods for antimicrobial susceptibility testing of Lactobacillus acidophilus group members. *Applied and Environmental Microbiology*, *74*(12), 3745–3748. https://doi.org/10.1128/AEM.02849-07

Mcgowan, J. E. (2001). Economic Impact of Antimicrobial Resistance. *Emerging Infectious Diseases*, *7*(2), 286–292.

ME, I., NE, B., & ME, H. (2012). Increased multi-drug resistant Escherichia coli from hospitals in Khartoum state , Sudan. *African Health Sciences*, *12*(3), 368–375.

Meredith, H. R., Srimani, J. K., Lee, A. J., Lopatkin, A. J., & You, L. (2015). dynamics and intervention. *Nature Chemical Biology*, *11*, 182–188. https://doi.org/10.1038/nchembio.1754

Messaoudi, O., Bendahou, M., Benamar, I., & Abdelwouhid, D. E. (2015). Identification and preliminary characterization of non-polyene antibiotics secreted by new strain of actinomycete isolated from sebkha of Kenadsa, Algeria. *Asian Pacific Journal of Tropical Biomedicine*, *5*(6), 438–445. https://doi.org/10.1016/j.apjtb.2015.04.002

Mohammadlou, M., Maghsoudi, H., & Jafarizadeh-Malmiri, H. (2016). A review on green silver nanoparticles based on plants: Synthesis, potential applications and eco-friendly approach. *International Food Research Journal*.

Mohanta, Y. K., & Behera, S. K. (2014). Biosynthesis, characterization and antimicrobial

activity of silver nanoparticles by Streptomyces sp. SS2. *Bioprocess and Biosystems Engineering*, *37*(11), 2263–2269. https://doi.org/10.1007/s00449-014-1205-6

Monciardini, P., Sosio, M., Cavaletti, L., Chiocchini, C., & Stefano, D. (2002). New PCR primers for the selective amplication of 16S rDNA from di¡erent groups of actinomycetes. *FEMS Microbiology Ecology*, *42*, 419–429. https://doi.org/10.1111/j.1574-6941.2002.tb01031.x

Nawas, T., Mazumdar, R. M., Das, S., Nipa, M. N., Islam, S., Bhuiyan, H. R., & Ahmad, I. (2012). Microbiological Quality and Antibiogram of E . coli , Salmonella and Vibrio of Salad and Water from Restaurants of Chittagong. *Journal of Environmental Science and Natural Resources*, *5*(1), 159–166.

Nguyen, T. M., & Kim, J. (2015). Description of Streptomyces fabae sp . nov ., a producer of antibiotics against microbial pathogens , isolated from soybean (Glycine max) rhizosphere soil. *International Journal of Systematic and Evolutionary Microbiology (2015)*, *65*, 4151–4156. https://doi.org/10.1099/ijsem.0.000551

Ochekpe, N. A., Olorunfemi, P. O., & Ngwuluka, N. C. (2009). Nanotechnology and drug delivery part 1: Background and applications. *Tropical Journal of Pharmaceutical Research*, *8*(3), 265–274. https://doi.org/10.4314/tjpr.v8i3.44546

Olive, D. M., & Ban, P. (1999). Principles and Applications of Methods for DNA-Based Typing of Microbial Organisms. *Journal of Clinical Microbiology*, *37*(6), 1661–1669.

Omulo, S., Thumbi, S. M., Njenga, M. K., & Call, D. R. (2015). A review of 40 years of enteric antimicrobial resistance research in Eastern Africa : what can be done better ? *Antimicrobial Resistance and Infection Control*, *4*(1), 1–13. https://doi.org/10.1186/s13756-014-0041-4

Patwardhan, A., Ray, S., & Roy, A. (2014). Molecular Markers in Phylogenetic Studies-A Review. *Journal of Phylogenetics & Evolutionary Biology*, *2*(2), 1–9.

https://doi.org/10.4172/2329-9002.1000131

Pimentel-Elardo, S. M., Kozytska, S., Bugni, T. S., Ireland, C. M., Moll, H., & Hentschel, U. (2010). Anti-parasitic compounds from Streptomyces sp. strains isolated from Mediterranean sponges. *Marine Drugs*, *8*(2), 373–380. https://doi.org/10.3390/md8020373

Pitkethly, M. J. (2004). Nanomaterials – the driving force. *Materials Today*, *7*(12), 20–29. https://doi.org/10.1016/S1369-7021(04)00627-3

Prabhu, S., & Poulose, E. K. (2012). Silver nanoparticles : mechanism of antimicrobial action , synthesis , medical applications , and toxicity effects. *International Nano Letters*, *2*(32), 1–10.

Prakasham, R. S., Kumar, B. S., Kumar, Y. S., & Kumar, K. P. (2014). Production and Characterization of Protein Encapsulated Silver Nanoparticles by Marine Isolate Streptomyces parvulus SSNP11. *Indian Journal of Microbiology*, *54*(3), 329–336. https://doi.org/10.1007/s12088-014-0452-1

Prakasham, R. S., Kumar, B. S., Kumar, Y. S., & Shankar, G. G. (2012). Characterization of silver nanoparticles synthesized by using marine isolate Streptomyces albidoflavus. *Journal of Microbiology and Biotechnology*, *22*(5), 614–621. https://doi.org/10.4014/jmb.1107.07013

Rezaee, M. A., Abdinia, B., Abri, R., & Kafil, H. S. (2014). Comparison of the antibiotic resistance patterns among Shigella species isolated from pediatric hospital between 1995-1999 and 2009-2013 in North-West of Iran. *Journal of Analytical Research in Clinical Medicine*, *2*(3), 118–122. https://doi.org/10.5681/jarcm.2014.020

Rineesh, N., Neelakandan, M., & Thomas, S. (2018). Applications of Silver Nanoparticles for Medicinal Purpose. *JSM Nanotechnol Nanomedicine*, *6*(1), 1–7.

Rotich, M. C., Magiri, E., Bii, C., & Maina, N. (2017). Bio-Prospecting for Broad

Spectrum Antibiotic Producing Actinomycetes Isolated from Virgin Soils in Kericho County , Kenya. *Advances in Microbiology*, *7*, 56–70. https://doi.org/10.4236/aim.2017.71005

Ryan, M. P., Adley, C. C., & Pembroke, J. T. (2013). The use of MEGA as an educational tool for examining the phylogeny of Antibiotic Resistance Genes, 736–743.

Sabtu, N., Enoch, D. A., & Brown, N. M. (2015). Antibiotic resistance: What, why, where, when and how? *British Medical Bulletin*, *116*(1), 105–113. https://doi.org/10.1093/bmb/ldv041

Saha, A., & Santra, S. C. (2014). Isolation and Characterization of Bacteria Isolated from Municipal Solid Waste for Production of Industrial Enzymes and Waste Degradation. *Journal of Microbiology & Experimentation*, *1*(1), 1–8. https://doi.org/10.15406/jmen.2014.01.00003

Sarmiento-Vizcaíno, A., Braña, A. F., González, V., Nava, H., Molina, A., Llera, E., … Blanco, G. (2015). Atmospheric Dispersal of Bioactive Streptomyces albidoflavus Strains Among Terrestrial and Marine Environments. *Microbial Ecology*, *71*(2), 375–386. https://doi.org/10.1007/s00248-015-0654-z

Shameli, K., Ahmad, M. Bin, Zamanian, A., Sangpour, P., Shabanzadeh, P., Abdollahi, Y., & Zargar, M. (2012). Green biosynthesis of silver nanoparticles using Curcuma longa tuber powder. *International Journal of Nanomedicine*, *7*, 5603–5610. https://doi.org/10.2147/IJN.S36786

Sharma, M. (2014). Original Research Article Actinomycetes : Source , Identification , and Their Applications. *International Journal of Current Microbiology and Applied Sciences*, *3*(2), 801–832.

Sherpa, R. T., Reese, C. J., & Aliabadi, H. M. (2015). Application of iChip to grow “uncultivable” microorganisms and its impact on antibiotic discovery. *Journal of*

Pharmacy and Pharmaceutical Sciences, *18*(3), 303–315. https://doi.org/10.18433/J30894

Shirokikh, I. G., Solov, E. S., & Ashikhmina, T. Y. (2014). Actinomycete Complexes in Soils of Industrial and Residential Zones. *Eurasian Soil Science*, *47*(2), 203–209. https://doi.org/10.1134/S1064229313100062

Siddiqi, K. S., Husen, A., & Rao, R. A. K. (2018). A review on biosynthesis of silver nanoparticles and their biocidal properties. *Journal of Nanobiotechnology*, *16*(1). https://doi.org/10.1186/s12951-018-0334-5

Singh, D., Rathod, V., Fatima, L., Kausar, A., Anjum, N., & Priyanka, B. (2014). Biologically Reduced Silver Nanopartic les from Streptomyces sp . VDP-5 and its Antibacterial Efficacy. *International Journal of Pharmacy and Pharaceutical Science Research*, *4*(2), 31–36.

Singh, P., Kim, Y. J., Zhang, D., & Yang, D. C. (2016). Biological Synthesis of Nanoparticles from Plants and Microorganisms. *Trends in Biotechnology*, *34*(7), 588–599. https://doi.org/10.1016/j.tibtech.2016.02.006

Singh, V., Haque, S., Singh, H., Verma, J., Vibha, K., Singh, R., … Tripathi, C. K. M. (2016). Isolation, screening, and identification of novel isolates of actinomycetes from India for antimicrobial applications. *Frontiers in Microbiology*, *7*(1–9). https://doi.org/10.3389/fmicb.2016.01921

Składanowski, M., Wypij, M., Laskowski, D., Golińska, P., Dahm, H., & Rai, M. (2017). Silver and gold nanoparticles synthesized from Streptomyces sp. isolated from acid forest soil with special reference to its antibacterial activity against pathogens. *Journal of Cluster Science*, *28*(1), 59–79. https://doi.org/10.1007/s10876-016-1043-6

Spellberg, B., Guidos, R., Gilbert, D., Bradley, J., Boucher, H. W., Scheld, W. M., … Edwards, J. (2008). The Epidemic of Antibiotic-Resistant Infections: A Call to Action

for the Medical Community from the Infectious Diseases Society of America. *Clinical Infectious Diseases*, *46*(2), 155–164. https://doi.org/10.1086/524891

Sudha Sri Kesavan, S., & Hemalatha, R. (2015). Isolation and screening of antibiotic producing actinomycetes from garden soil of sathyabama university, Chennai. *Asian Journal of Pharmaceutical and Clinical Research*, *8*(6), 110–114.

Sugiyama, M. (2015). Structural biological study of self-resistance determinants in antibiotic-producing actinomycetes. *Journal of Antibiotics*. Nature Publishing Group. https://doi.org/10.1038/ja.2015.32

Sweeney, P., Murphy, C. D., & Caffrey, P. (2016). Exploiting the genome sequence of Streptomyces nodosus for enhanced antibiotic production. *Applied Microbiology and Biotechnology*, *100*(3), 1285–1295. https://doi.org/10.1007/s00253-015-7060-9

Tabrizi, S. G., Hamedi, J., & Mohammadipanah, F. (2013). Screening of soil actinomyectes against Salmonella serovar Typhi NCTC 5761 and characterization of the prominent active strains. *Iranian Journal of Microbiology*, *5*(4), 356–365. https://doi.org/10.1128/AEM.02161-07

Takahashi, Y., & Nakashima, T. (2018). Actinomycetes, an Inexhaustible Source of Naturally Occurring Antibiotics. *Antibiotics*, *7*(2), 45. https://doi.org/10.3390/antibiotics7020045

Thirumalairaj, J., Shanmugasundaram, T., Sivasankari, K., Natarajaseenivasan, K., & Balagurunathan, R. (2015). Isolation, screening and characterization of potent marine Streptomyces SP . PM105 against antibiotic resistant pathogens. *Asian Pacific Journal of Pharmaceutical and Clinical Research*, *8*(2), 439–443.

Tran, Q. H., Nguyen, V. Q., & Le, A. T. (2013). Silver nanoparticles: Synthesis, properties, toxicology, applications and perspectives. *Advances in Natural Sciences: Nanoscience and Nanotechnology*, *4*(3). https://doi.org/10.1088/2043-

6262/4/3/033001

Tyagi, J., Bhatnagar, T., & Pandey, F. K. (2014). Isolation and Characterization of Actinomycetes from Soil and Screening their Antibacterial Activities against different Microbial Isolates. *International Journal of Life Sciences Research*, *2*(4), 101–105.

Ugboko, H., & De, N. (2014). Review article Mechanisms of quinolone resistance in Salmonella. *International Journal of Current Microbiology and Applied Sciences*, *3*(12), 461–476.

Valgas, C., Souza, S., Smania, E., & Jr, S. (2007). Screening Methods to Determine Antibacterial Activity of NAtural Products. *Brazilian Journal of Micrboiology Universidade Do Sul de Santa Catarina*, 369–380.

Vila, J., Sáez-López, E., Johnson, J. R., Römling, U., Dobrindt, U., Cantón, R., … Soto, S. M. (2016). Escherichia coli: An old friend with new tidings. *FEMS Microbiology Reviews*, *40*(4), 437–463. https://doi.org/10.1093/femsre/fuw005

Williams, P. C. M., & Berkley, J. A. (2018). Guidelines for the treatment of dysentery (shigellosis): a systematic review of the evidence. *Paediatrics and International Child Health*, *38*, S50–S65. https://doi.org/10.1080/20469047.2017.1409454

Wypij, M., Czarnecka, J., Świecimska, M., Dahm, H., Rai, M., & Golinska, P. (2018). Synthesis, characterization and evaluation of antimicrobial and cytotoxic activities of biogenic silver nanoparticles synthesized from Streptomyces xinghaiensis OF1 strain. *World Journal of Microbiology and Biotechnology*, *34*(2), 1–13. https://doi.org/10.1007/s11274-017-2406-3

Xu, L. H., Li, Q. R., & Jiang, C. L. (1996). Diversity of soil actinomycetes in Yunnan, China. *Applied and Environmental Microbiology*, *62*(1), 244–248.

Yan, M., Li, X., Liao, Q., Li, F., Zhang, J., & Kan, B. (2016). The emergence and outbreak of multidrug-resistant typhoid fever in China. *Emerging Microbes & Infections*, *5*(6),

1–6. https://doi.org/10.1038/emi.2016.62

Yang, J., Yang, Z., Yin, Y., Rao, M., Liang, Y., & Ge, M. (2016). Three novel polyene macrolides isolated from cultures of Streptomyces lavenduligriseus. *Journal of Antibiotics*, *69*(1), 62–65. https://doi.org/10.1038/ja.2015.76

Yang, Z., & Rannala, B. (2012). Molecular phylogenetics: principles and practice. *Nature Reviews Genetics*, *13*(5), 303–314. https://doi.org/10.1038/nrg3186

Yassin, A. K., Gong, J., Kelly, P., Lu, G., Guardabassi, L., Wei, L., … Wang, C. (2017). Antimicrobial resistance in clinical Escherichia coli isolates from poultry and livestock, China. *PLoS ONE*, *12*(9), 1–8. https://doi.org/10.1371/journal.pone.0185326

Yoon, S. H., Ha, S. M., Kwon, S., Lim, J., Kim, Y., Seo, H., & Chun, J. (2017). Introducing EzBioCloud: A taxonomically united database of 16S rRNA gene sequences and whole-genome assemblies. *International Journal of Systematic and Evolutionary Microbiology*, *67*(5), 1613–1617. https://doi.org/10.1099/ijsem.0.001755

Zainal Abidin, Z. A., Abdul Malek, N., Zainuddin, Z., & Chowdhury, A. J. K. (2016). Selective isolation and antagonistic activity of actinomycetes from mangrove forest of Pahang, Malaysia. *Frontiers in Life Science*, *9*(1), 24–31. https://doi.org/10.1080/21553769.2015.1051244

Zaman, S. Bin, Hussain, M. A., Nye, R., Mehta, V., Mamun, K. T., & Hossain, N. (2017). A Review on Antibiotic Resistance: Alarm Bells are Ringing. *Cureus*, *9*(6), 1–9. https://doi.org/10.7759/cureus.1403

Zewde, B., Ambaye, A., Stubbs, J., & Raghavan, D. (2016). A Review of Stabilized Silver Nanoparticles – Synthesis, Biological Properties, Characterization, and Potential Areas of Applications. *JSM Nanotechnol Nanomed*, *4*(2), 1.14. Retrieved from

http://www.doiserbia.nb.rs/Article.aspx?ID=0352-51391800021C

Zhang, X., Liu, Z., Shen, W., & Gurunathan, S. (2016). Silver Nanoparticles: Synthesis, Characterization, Properties, Applications, and Therapeutic Approaches. *International Journal of Molecular Sciences*, *17*(9), 1534. https://doi.org/10.3390/ijms17091534

APPENDICES

Appendix 1: Photographic representation of soil sampling sites

Appendix 2: The collected, dried, crushed and packed soil samples

Appendix 3: The prepared plate, slant and broth starch casein media for selective growth, sub culturing and for metabolite production

Starch casein Plate media for selective growth

Starch casein Test tube media for sub-culture

Starch casein Plate media for streak plate assay

Starch casein broth media for metabolite production

Appendix 4: Selectively grown colony on the plate and sub-culture on slant starch casein media

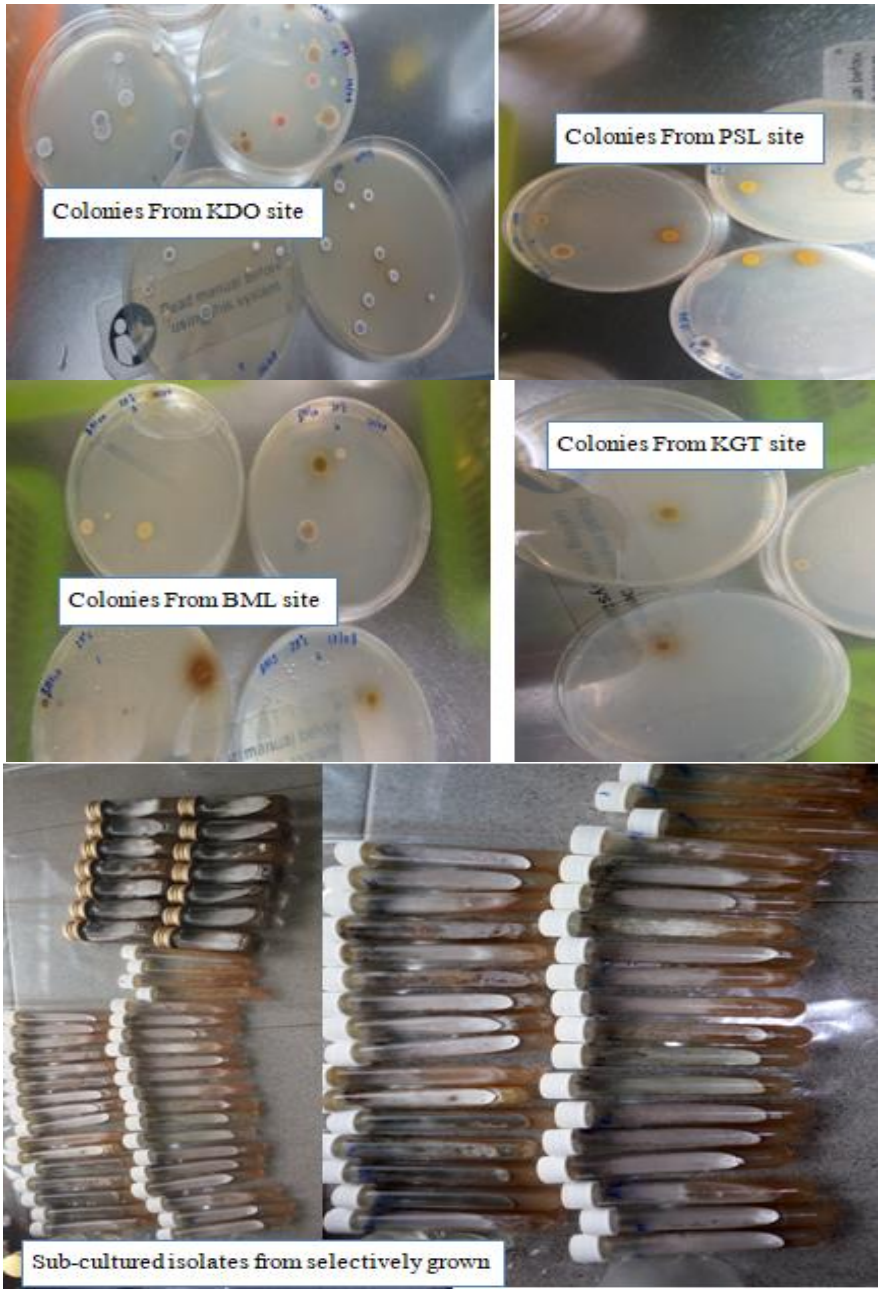

Appendix 5: Antibacterial activity of selected isolates during primary screening (streak plate method) and secondary screening (well diffusion assay)

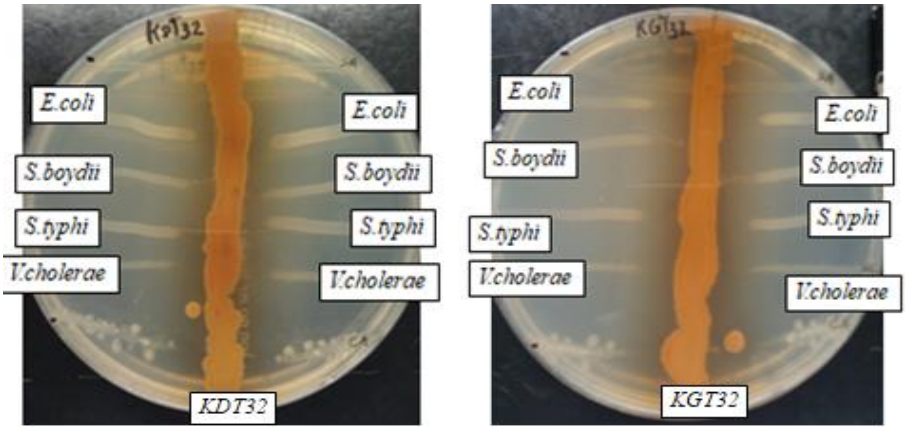

a) Antibacterial activity of KDT32 and KGT32 during primary antibacterial screening

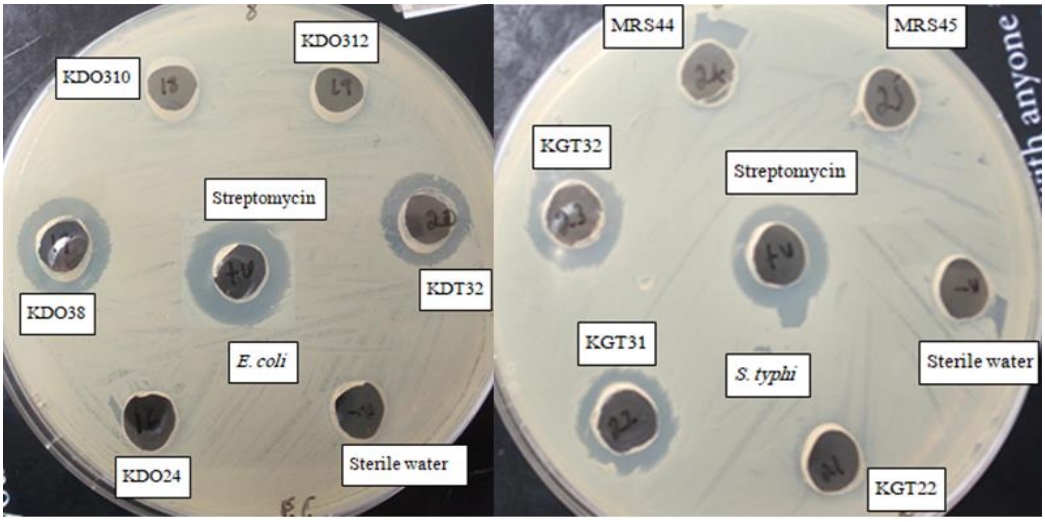

b) Antibacterial activity isolates during secondary screening

Appendix 6: The absorption intensity (UV- spectra) at the time of mixing of metabolites from isolates and silver nitrate solution

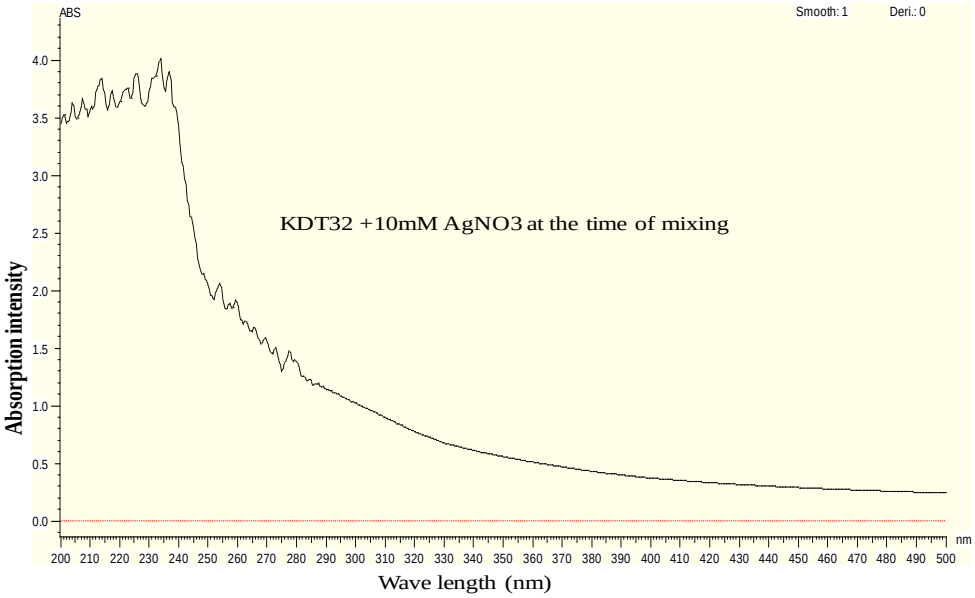

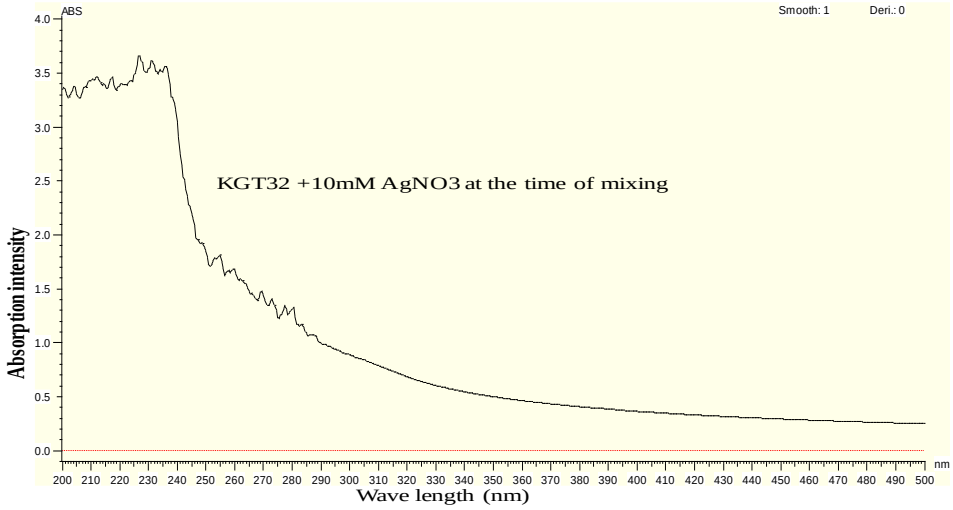

Appendix 7: The gel result for detection of quality genomic DNA of KDT32 and KGT32

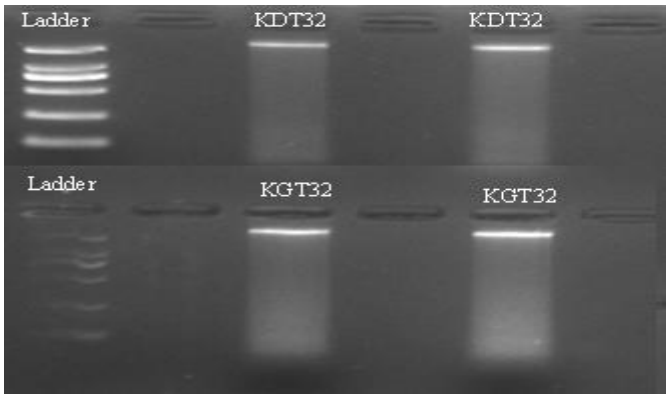

Appendix 8: The purity and concertation of genomic DNA analyzed by Nanodrop

Isolate number	**Isolate code**	**Concentration (µg/ml)**	**Purity (260/280)**
9	KDT32	40.343	1.779
11	KGT32	63.748	1.756

Appendix 9: 16s RNA gene sequences of KDT32 and KGT32

>KDT32 (MH301089)

CTTTCAGCAGGGAAGAAGCGAGAGTGACGGTACCTGCAGAAGAAGCGCCGGC
TAACTACGTGCCAGCAGCCGCGGTAATACGTAGGGCGCAAGCGTTGTCCGGAA
TTATTGGGCGTAAAGAGCTCGTAGGCGGCTTGTCGCGTCGGTTGTGAAAGCCC
GGGGCTTAACCCCGGGTCTGCAGTCGATACGGGCAGGCTAGAGTTCGGTAGGG
GAGATCGGAATTCCTGGTGTAGCGGTGAAATGCGCAGATATCAGGAGGAACA
CCGGTGGCGAAGGCGGATCTCTGGGCCGATACTGACGCTGAGGAGCGAAAGC
GTGGGGAGCGAACAGGATTAGATACCCTGGTAGTCCACGCCGTAAACGGTGG
GCACTAGGTGTGGGCAACATTCCACGTTGTCCGTGCCGCAGCTAACGCATTAA
GTGCCCCGCCTGGGGAGTACGGCCGCAAGGCTAAAACTCAAAGGAATTGACG
GGGGCCCGCACAAGCGGCGGAGCATGTGGCTTAATTCGACGCAACGCGAAGA
ACCTTACCAAGGCTTGACATACACCGGAAAGCATTAGAGATAGTGCCCCCCTT
GTGGTCGGTGTACAGGTGGTGCATGGCTGTCGTCAGCTCGTGTCGTGAGATGT
TGGGTTAAGTCCCGCAACGAGCGCAACCCTTGTCCCGTGTTGCCAGCAGGCCC
TTGTGGTGCTGGGGACTCACGGGAGACCGCCGGGGTCAACTCGGAGGAAGGT
GGGGACGACGTCAAGTCATCATGCCCCTTATGTCTTGGGCTGCACACGTGCTA
CAATGGCCGGTACAATGAGCTGCGATACCGTGAGGTGGAGCGAATCTCAAAA

AGCCGGTCTCAGTTCGGATTGGGGTCTGCAACTCGACCCCATGAAGTCGGAGT
CGCTAGTAATCGCAGATCAGCATTGCTGCGGTGAATACGTTCCCGGGCCTTGT
ACACACCGCCCGTCATCGTCACGAAAGTCGGTAACACCCG

>KGT32 (MH301090)

GAGGGCGACCGGCCACACTGGGACTGAGACACGGCCCAGACTCCTACGGGAG
GCAGCAGTGGGGAATATTGCACAATGGGCGAAAGCCTGATGCAGCGACGCCG
CGTGAGGGATGACGGCCTTCGGGTTGTAAACCTCTTTCAGCAGGGAAGAAGCG
AGAGTGACGGTACCTGCAGAAGAAGCGCCGGCTAACTACGTGCCAGCAGCCG
CGGTAATACGTAGGGCGCAAGCGTTGTCCGGAATTATTGGGCGTAAAGAGCTC
GTAGGCGGCTTGTCACGTCGGTTGTGAAAGCCCGGGGCTTAACCCCGGGTCTG
CAGTCGATACGGGCAGGCTAGAGTTCGGTAGGGGAGATCGGAATTCCTGGTGT
AGCGGTGAAATGCGCAGATATCAGGAGGAACACCGGTGGCGAAGGCGGATCT
CTGGGCCGATACTGACGCTGAGGAGCGAAAGCGTGGGGAGCGAACAGGATTA
GATACCCTGGTAGTCCACGCCGTAAACGGTGGGCACTAGGTGTGGGCAACATT
CCACGTTGTCCGTGCCGCAGCTAACGCATTAAGTGCCCCGCCTGGGGAGTACG
GCCGCAAGGCTAAAACTCAAAGGAATTGACGGGGGCCCGCACAAGCGGCGGA
GCATGTGGCTTAATTCGACGCAACGCGAAGAACCTTACCAAGGCTTGACATAC
ACCGGAAACGTCTGGAGACAGGCGCCCCCTTGTGGTCGGTGTACAGGTGGTGC
ATGGCTGTCGTCAGCTCGTGTCGTGAGATGTTGGGTTAAGTCCCGCAACGAGC
GCAACCCTTGTCCCGTGTTGCCAGCAGGCCCTTGTGGTGCTGGGGACTCACGG
GAGACCGCCGGGGTCAACTCGGAAGAAGGTGGGGACGACGTCAAGTCATCAT
GCCCCTTATGTCTTGGGCTGCACACGTGCTACAATGGGCCGGTACAATGAGCT
G

Appendix 10: NCBI-BLASTn result for KDT32 16s rRNA gene sequence

Sequences producing significant alignments:

Select: All None Selected:0

Alignments Download GenBank Graphics Distance tree of results

Description	Max score	Total score	Query cover	E value	Ident	Accession
Streptomyces sp. MBE174 gene for 16S ribosomal RNA, partial sequence	1771	1771	100%	0.0	99%	AB873097.1
Streptomyces misionensis strain NIIST A2 16S ribosomal RNA gene, partial sequence	1771	1771	100%	0.0	99%	KU686376.1
Streptomyces sp. MemCl6 16S ribosomal RNA gene, partial sequence	1771	1771	100%	0.0	99%	KR080498.1
Streptomyces hygroscopicus strain FoRh26 16S ribosomal RNA gene, partial sequence	1771	1771	100%	0.0	99%	KM370043.1
Streptomyces sp. R20-5 gene for 16S ribosomal RNA, partial sequence	1771	1771	100%	0.0	99%	AB841057.1
Streptomyces sp. R14-5 gene for 16S ribosomal RNA, partial sequence	1771	1771	100%	0.0	99%	AB841042.1
Streptomyces sp. R9-4 gene for 16S ribosomal RNA, partial sequence	1771	1771	100%	0.0	99%	AB841027.1
Streptomyces sp. TP-A0875 gene for 16S ribosomal RNA, partial sequence	1771	1771	100%	0.0	99%	AB451554.1
Streptomyces sp. S096 16S ribosomal RNA gene, partial sequence	1771	1771	100%	0.0	99%	EF577242.1
Streptomyces hygroscopicus subsp. hygroscopicus gene for 16S rRNA, partial sequence, strain: NBRC 3401	1771	1771	100%	0.0	99%	AB184760.1
Actinomycetales bacterium HPA160 16S ribosomal RNA gene, partial sequence	1768	1768	100%	0.0	99%	DQ144220.1
Streptomyces misionensis strain AMA49 16S ribosomal RNA gene, partial sequence	1766	1766	100%	0.0	99%	KX129898.1
Streptomyces sp. R4-2 gene for 16S ribosomal RNA, partial sequence	1766	1766	100%	0.0	99%	AB841004.3
Streptomyces sp. 151KO065 16S ribosomal RNA gene, partial sequence	1766	1766	100%	0.0	99%	KX078377.1
Streptomyces misionensis strain OsiRt-1 16S ribosomal RNA gene, partial sequence	1766	1766	100%	0.0	99%	KU321340.1
Streptomyces sp. XSRh38 16S ribosomal RNA gene, partial sequence	1766	1766	100%	0.0	99%	KP900805.1

Appendix 11: NCBI-BLAST result for KGT32 16s rRNA gene sequence

Sequences producing significant alignments:

Select: All None Selected:0

Alignments Download GenBank Graphics Distance tree of results

Description	Max score	Total score	Query cover	E value	Ident	Accession
Streptomyces sp. strain SP4-AB2 16S ribosomal RNA gene, partial sequence	1701	1701	100%	0.0	99%	MH013316.1
Streptomyces sp. strain SP1-V4 16S ribosomal RNA gene, partial sequence	1698	1698	100%	0.0	99%	MH013308.1
Streptomyces sp. strain W2 16S ribosomal RNA gene, partial sequence	1698	1698	100%	0.0	99%	KY402227.1
Streptomyces sp. strain 49D 16S ribosomal RNA gene, partial sequence	1698	1698	100%	0.0	99%	KY214200.1
Streptomyces sp. strain Y355 16S ribosomal RNA gene, partial sequence	1698	1698	100%	0.0	99%	KX426373.1
Streptomyces sp. strain 544F 16S ribosomal RNA gene, partial sequence	1698	1698	100%	0.0	99%	KX426362.1
Streptomyces sp. strain 563F 16S ribosomal RNA gene, partial sequence	1698	1698	100%	0.0	99%	KX426360.1
Streptomyces sp. strain 562F 16S ribosomal RNA gene, partial sequence	1698	1698	100%	0.0	99%	KX426359.1
Streptomyces sp. strain 541F 16S ribosomal RNA gene, partial sequence	1698	1698	100%	0.0	99%	KX426356.1
Streptomyces sp. strain 528F 16S ribosomal RNA gene, partial sequence	1698	1698	100%	0.0	99%	KX426355.1
Streptomyces sp. strain 525F 16S ribosomal RNA gene, partial sequence	1698	1698	100%	0.0	99%	KX426354.1
Streptomyces sp. strain 10147b 16S ribosomal RNA gene, partial sequence	1698	1698	100%	0.0	99%	KX573711.1
Streptomyces sp. strain IB2015P60-2 16S ribosomal RNA gene, partial sequence	1698	1698	100%	0.0	99%	KX539269.1
Streptomyces sp. JSM 147799 16S ribosomal RNA gene, partial sequence	1698	1698	100%	0.0	99%	KR817749.1
Streptomyces sp. JSM 147823 16S ribosomal RNA gene, partial sequence	1698	1698	100%	0.0	99%	KR817748.1
Streptomyces sp. JSM 147779 16S ribosomal RNA gene, partial sequence	1698	1698	100%	0.0	99%	KR817747.1

Appendix 12: EzTaxon-e BLAST result for the top hit for KDT32 (9-A3R-986) and KGT32 (11-243F-948) 16s rRNA gene sequence and their completeness

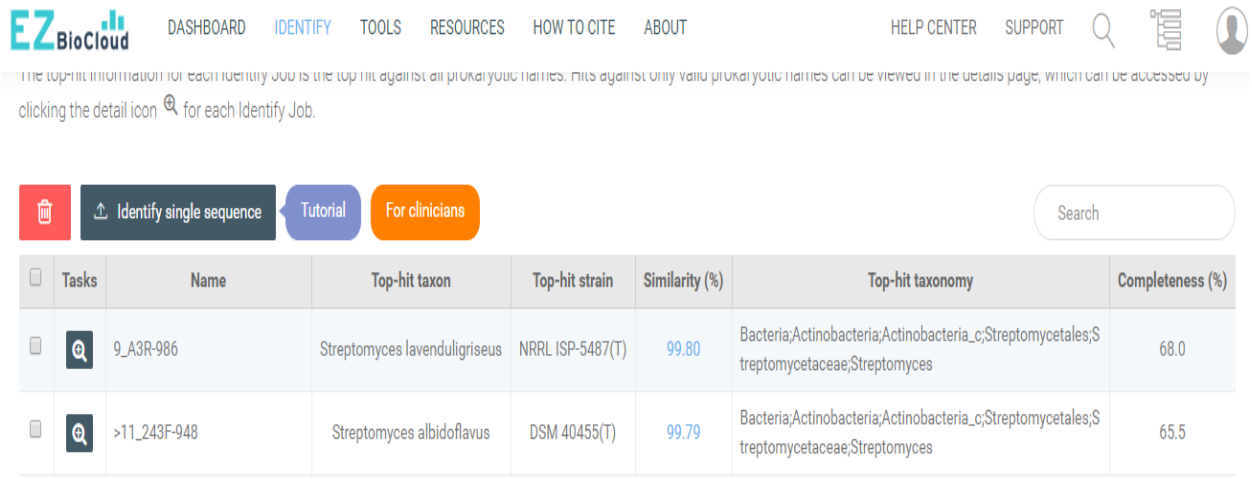

Tasks	Name	Top-hit taxon	Top-hit strain	Similarity (%)	Top-hit taxonomy	Completeness (%)
	9_A3R-986	Streptomyces lavenduligriseus	NRRL ISP-5487(T)	99.80	Bacteria;Actinobacteria;Actinobacteria_c;Streptomycetales;Streptomycetaceae;Streptomyces	68.0
	>11_243F-948	Streptomyces albidoflavus	DSM 40455(T)	99.79	Bacteria;Actinobacteria;Actinobacteria_c;Streptomycetales;Streptomycetaceae;Streptomyces	65.5

Appendix 13: EzTaxon BLAST result for KDT32 16s rRNA gene sequence

Tasks	Hit taxon name	Hit strain name	Accession	Similarity	Diff/Total nt	Hit taxonomy	Completeness (%)
	Streptomyces lavenduligriseus	NRRL ISP-5487(T)	JOBD01000085	99.80	2/985	Bacteria;Actinobacteria;Actinobacteria_c;Streptomycetales;Streptomycetaceae;Streptomyces	100.0
	Streptomyces misionensis	DSM 40306(T)	FNTD01000004	99.70	3/985	Bacteria;Actinobacteria;Actinobacteria_c;Streptomycetales;Streptomycetaceae;Streptomyces	100.0
	Streptomyces eurythermus	ATCC 14975(T)	D63870	99.70	3/985	Bacteria;Actinobacteria;Actinobacteria_c;Streptomycetales;Streptomycetaceae;Streptomyces	100.0
	Streptomyces phaeoluteichromatogenes	NRRL 5799(T)	AJ391814	99.70	3/985	Bacteria;Actinobacteria;Actinobacteria_c;Streptomycetales;Streptomycetaceae;Streptomyces	98.7
	Streptomyces flaveolus	NBRC 3715(T)	AB184786	99.70	3/985	Bacteria;Actinobacteria;Actinobacteria_c;Streptomycetales;Streptomycetaceae;Streptomyces	99.9
	Streptomyces viridochromogenes	NBRC 3113(T)	AB184728	99.70	3/985	Bacteria;Actinobacteria;Actinobacteria_c;Streptomycetales;Streptomycetaceae;Streptomyces	99.9
	Streptomyces nogalater	JCM 4799(T)	AB045886	99.70	3/985	Bacteria;Actinobacteria;Actinobacteria_c;Streptomycetales;Streptomycetaceae;Streptomyces	100.0

Appendix 14: Sequences for query (KDT32) and top 30 hit sequences from EzTaxon-e database

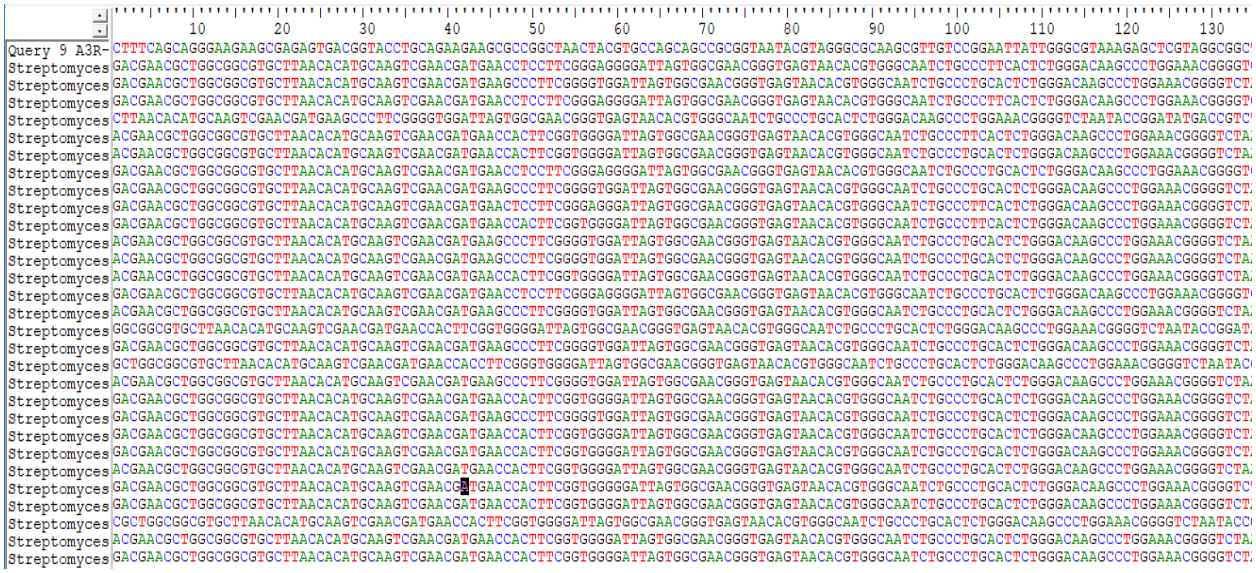

Appendix 15: Alignment details of KDT32 16s rRNA gene sequence and the first top hit sequence from EzTaxon-e database

Alignment details

Query name	9_A3R-986
Hit name	Streptomyces lavenduligriseus NRRL ISP-5487(T)
Similarity	99.80 %
No. of compared	985
No. of mismatched	2

Aligned sequences

Query sequence	AAGCGTTGTCCGGAATTATTGGGCGTAAAGAGCTCGTAGGCGGCTTGTCGCGTCGGTTGTGAAAGCCCGGGGCTTAACCCCGGGTCTGCAGTCGATAC
Hit sequence	AAGCGTTGTCCGGAATTATTGGGCGTAAAGAGCTCGTAGGCGGCTTGTCACGTCGGTTGTGAAAGCCCGGGGCTTAACCCCGGGTCTGCAGTCGATAC

Appendix 16: EzTaxon BLAST result for KGT32 16s rRNA gene sequence

Tasks	Hit taxon name	Hit strain name	Accession	Similarity	Diff/Total nt	Hit taxonomy	Completeness (%)
⇄ ○	Streptomyces albidoflavus	DSM 40455(T)	Z76676	99.79	2/947	Bacteria;Actinobacteria;Actinobacteria_c;Streptomycetales;Streptomycetaceae;Streptomyces	99.7
⇄ ○	Streptomyces koyangensis	VK-A60(T)	AY079156	99.79	2/947	Bacteria;Actinobacteria;Actinobacteria_c;Streptomycetales;Streptomycetaceae;Streptomyces	100.0
⇄ ○	Streptomyces hydrogenans	NBRC 13475(T)	AB184868	99.79	2/947	Bacteria;Actinobacteria;Actinobacteria_c;Streptomycetales;Streptomycetaceae;Streptomyces	100.0
⇄ ○	Streptomyces daghestanicus	NRRL B-5418(T)	DQ442497	99.79	2/946	Bacteria;Actinobacteria;Actinobacteria_c;Streptomycetales;Streptomycetaceae;Streptomyces	99.9
⇄ ○	Streptomyces violascens	ISP 5183(T)	AY999737	99.79	2/945	Bacteria;Actinobacteria;Actinobacteria_c;Streptomycetales;Streptomycetaceae;Streptomyces	97.9
⇄ ○	Streptomyces fabae	T66(T)	KM229360	99.68	3/947	Bacteria;Actinobacteria;Actinobacteria_c;Streptomycetales;Streptomycetaceae;Streptomyces	100.0

Appendix 17: Part of the sequences for query (KGT32) and top 30 hit sequences from EzTaxon-e database

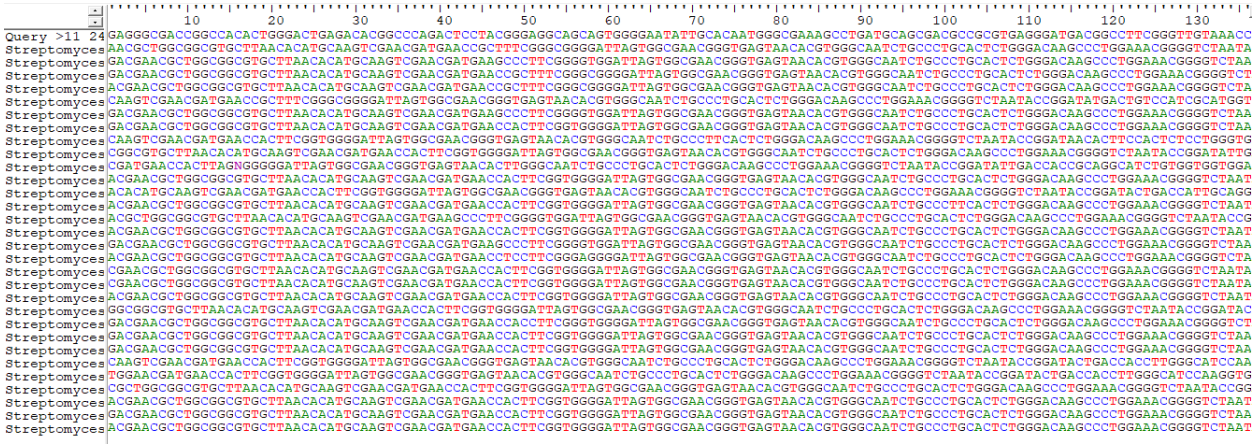

Appendix 18: Alignment details of KGT32 16s rRNA gene sequence (11-243F-948) and the top hit sequence from EzTaxon-e database

Alignment details

Query name	>11_243F-948
Hit name	Streptomyces albidoflavus DSM 40455(T)
Similarity	99.79 %
No. of compared	947
No. of mismatched	2

Aligned sequences

Query sequence	GCGTGAGGGATGACGGCCTTCGGGTTGTAAACCTCTTTCAGCAGGGAAGAAGCGAGAGTGACGGTACCTGCAGAAGAAGCGCCGGCTAACTACGTGCCAG
Hit sequence	GCGTGAGGGATGACGGCCTTCGGGTTGTAAACCTCTTTCAGCAGGGAAGAAGCGAAAGTGACGGTACCTGCAGAAGAAGCGCCGGCTAACTACGTGCCAG

Appendix 19: Published manuscript on Asian Pacific Journal of Tropical Disease

Asian Pacific Journal of Tropical Disease

journal homepage: http://www.apjtcm.com

Original article https://doi.org/10.12980/apjtd.7.2017D7-162

Antibacterial metabolite prospecting from Actinomycetes isolated from waste damped soils from Thika, central part of Kenya

Abebe Bizuye[1,2*], Christine Bii[3], Gatebe Erastus[4], Naomi Maina[2,5]

[1]*Department of Biology, College of Natural and computational Sciences, University of Gondar, Gondar, Ethiopia*

[2]*Molecular and Biotechnology, Pan African University Institute of Basic Sciences, Innovation and Technology, Jomo Kenyatta University of Agriculture and Technology, Nairobi, Kenya*

[3]*Centre for Microbiology Research, Kenya Medical Research Institute, Nairobi, Kenya*

[4]*Kenya Industrial Research Development and Innovation, Nairobi, Kenya*

[5]*Department of Biochemistry, College of Health Sciences, Jomo Kenyatta University of Agriculture and Technology, Nairobi, Kenya*

ARTICLE INFO

Article history:
Received 10 Jul 2017
Received in revised form 9 Nov 2017
Accepted 16 Nov 2017
Available online 29 Nov 2017

Keywords:
Bioactive isolates
Antibacterial activity screening
Bacteria pathogens
Thika
Waste damped soil

ABSTRACT

Objective: To evaluate antibacterial activity of the metabolites produced by actinomycetes isolates isolated from waste damped soil in Thika.

Methods: Soil samples were collected randomly from selected waste damping sites and composite soil samples were prepared. Composite soil samples were pre-treated with dry heat and $CaCO_3$. 0.1 mL of soil suspension from 10^{-5} serial diluted composite soil sample spread on selective media for selective growth and isolation. The primary and secondary screenings and evaluation of antibacterial active isolates were done by streak plate and well diffusion assay, respectively.

Results: 29 (23.2%) isolates showed antibacterial activity during primary screening. From these, isolate KGT22 showed 30 ± 0 mm, 31.3 ± 0.6 mm, 30 ± 0 mm and 36 ± 1 mm inhibition zone against *E. coli* ATCC 25922, *S. boydii*, *S. typhi* and *V. cholerea*, respectively. Isolate KDO24 showed antibacterial activity against both MRSA (16.25 ± 0.50 mm) and *E. coli* (26.5 ± 0.58 mm). Supernatants from 11 (37.93%) isolates showed antibacterial activity during secondary screening. Supernatant from BML45, KGT31 and PLS 34 showed better inhibition

Appendix 20: Submitted manuscript on Journal of Microbiology Open-Wiley

MicrobiologyOpen
Open Access

Molecular based identification of local actinomycete isolates that produce bioactive metabolites capable of synthesizing antibacterial silver nanoparticles

Journal:	*MicrobiologyOpen*
Manuscript ID	Draft
Wiley - Manuscript type:	Original Article
Date Submitted by the Author:	n/a
Complete List of Authors:	Bizuye, Abebe; University of Gondar College of Natural and Computational Sciences, Biology; Jomo Kenyatta University of Agriculture and Technology, Molecular biology and Biotechnology Gedamu, Lashitew ; University of Calgary Cumming School of Medicine, Department of Biological Sciences Bii, Christine; Kenya Medical Research Institute, Center for Microbiology Research Erastus , Gatebe ; Kenya Industrial Research Development and Innovation, Chemistry Maina , Naomi ; Jomo Kenyatta University of Agriculture and Technology, Department of Biochemistry
Search Terms:	Streptomyces, E. coli, Salmonella, secondary metabolites
Abstract:	Abstract Aims: To identify local actinomycetes that produce bioactive metabolites capable of synthesizing antibacterial silver nanoparticles. Methods and results: The synthesis of nanoparticle was confirmed by visual detection and UV-vis spectrophotometer whereas functional groups involved in the synthesis were identified by FTIR spectrophotometer. The antibacterial activity was tested by well diffusion assay. Identification of isolates was done based on 16s rRNA gene sequence analysis. The visual detection showed that dark salmon and pale golden rod color change was observed due to the formation of KDT32-AgNP and KGT32-AgNP, respectively. The synthesis was confirmed by a characteristic UV-spectra peak at 415.5 nm for KDT32-AgNP and 416 nm for KGT32-AgNP. The FTIR spectra revealed that OH, C=C and S-S functional groups were involved for the synthesis of KDT32-AgNP whereas OH, C=C and C-H were involved for the formation of KGT32-AgNP. The inhibition zone results revealed that KDT32-AgNP showed 22.0+1.4 mm and 19.0+1.4 mm against E. coli